This is to certify that the

dissertation entitled

FRAMEWORK FOR INCORPORATING RUTTING PREDICTION MODEL IN THE RELIABILITY-BASED DESIGN OF FLEXIBLE PAVEMENTS

presented by

Hyung Bae Kim

has been accepted towards fulfillment
of the requirements for

Ph.D. degree in Civil Engineering

Major professor

Date 4/5/99

FRAMEWORK FOR INCORPORATING RUTTING PREDICTION MODEL IN THE RELIABILITY-BASED DESIGN OF FLEXIBLE PAVEMENTS

By

Hyung Bae Kim

A DISSERTATION

Submitted to
Michigan State University
in partial fulfillment of the requirements
for the degree of

DOCTER OF PHILOSOPHY

Department of Civil and Environmental Engineering

1999

FRAMEWOR
RE

Most st

procedures fo

AASHTO gui

mechanistic-em

transfer functio

and control o

variations in m

model bias

This stu

prediction mod

element analysi

flexible paveme

flexible paveme

The new

the combination

factors such as

components Th

ABSTRACT

FRAMEWORK FOR INCORPORATING RUTTING PREDICTION MODEL IN THE RELIABILITY-BASED DESIGN OF FLEXIBLE PAVEMENTS

By

Hyung Bae Kim

Most state highway agencies (SHA's) are being encouraged to change their design procedures for flexible pavements from an empirical-based procedure such as the AASHTO guide to mechanistic-based approaches. A successful implementation of mechanistic-empirical (M-E) pavement design requires i) the development of robust transfer functions to accurately predict pavement performance, and ii) the characterization and control of the uncertainties associated with M-E design procedures, including variations in material and cross-sectional properties, inaccuracy of traffic estimation, and model bias.

This study presents the procedure and results of calibrating the existing rutting prediction model in MICHPAVE, a computer program for linear and non-linear finite element analysis of the pavement structure, using field data from thirty-nine in-service flexible pavement sections in Michigan, and a framework for a reliability-based M-E flexible pavement design approach using the calibrated rutting prediction model.

The new rutting prediction model has a nonlinear form developed by considering the combination of mechanistic factors such as primary pavement responses and empirical factors such as pavement material and cross-sectional properties and environmental components. The model is validated using data from eleven in-service flexible pavements

and the data fr

Performance (I

In the r

the reliability

engineering p

procedure are

variation, impr

error The firs

into uncertaint

Based

pavement per

procedures ar

Resistance Fac

the design proc

first order co

parameters and

the overall saf

professional fa

use an iterative

converges to ze

and the data from twenty four general pavement sections from the Long Term Pavement Performance (LTPP-GPS) database.

In the reliability analysis of pavement performance, a model to accurately evaluate the reliability of flexible pavement structure is introduced by incorporating practical engineering probabilistic techniques. The uncertainties associated with the design procedure are categorized into four parts based on the sources of uncertainty: spatial variation, imprecision in quantifying site conditions and traffic, model bias, and statistical error. The first two are integrated into uncertainties of design parameters; the latter two into uncertainties that stem from systematic errors.

Based on the probabilistic techniques introduced in the reliability analysis of pavement performance, two practical reliability-based M-E flexible pavement design procedures are introduced; Reliability Factor Design (RFD) approach and Load and Resistance Factor Design (LRFD) approach. In order to characterize the uncertainties of the design procedure, the RFD approach employs the overall standard deviation that is the first order combination of the standard deviations due to uncertainties of design parameters and systematic errors in the design model, while the LRFD approach considers the overall safety factor based on the partial safety factors of all design variables and a professional factor, which is a ratio of measured to predicted rut-depth. Both approaches use an iterative algorithm where the computation is continued until the limit-state function converges to zero in order to produce an optimal pavement cross-section.

This work is d

Sung-Ji Kim, v

emotional and t

DEDICATION

This work is dedicated to my parents, Hyun-Suk Kim and Soo-Ja Choi, and my sister, Sung-Ji Kim, without whom this work would have not been possible. Their ceaseless emotional and financial support has been invaluable.

Thank you for everything and God bless you.

I woul

and guidance t

I also

Wolff and Dr

would have not

My app

(MDOT) and th

University for sp

I would like to

deflectometer tes

collection of field

I would a

works on develo

correction factor

this research work

Acknowle

Eu-Jin Oh, Jin-K

ACKNOWLEDGEMENTS

I would first like to express my best gratitude to Dr. Neeraj Buch for his support and guidance throughout my research career at Michigan State University.

I also wish to thank Dr. Gilbert Baladi, Dr. Ronald Harichandran, Dr. Thomas Wolff, and Dr. Vince Melfi who are my Ph.D. guidance committee members. This work would have not been completed without their valuable advice.

My appreciation is extended to the Michigan Department of Transportation (MDOT) and the Pavement Research Center of Excellence (PRCE) at Michigan State University for sponsoring this research work and providing financial support. In addition, I would like to thank MDOT personnel for performing coring and falling weight deflectometer testing as well as providing the necessary traffic control for carrying out the collection of field data.

I would also like to give my sincere gratitude to Mr. Dong-Yeob Park for his works on developing a pavement temperature prediction model and a temperature correction factor for backcalculated moduli. His research results have fully contributed to this research work.

Acknowledgment is given to Jung-Kyu Yu (President), Kyung-Won Cho (CEO), Eu-Jin Oh, Jin-Kyu Song, and Jin-Ho Jung (Executive Directors) of Yoo-Shin

Engineering C

graduate study

Finally

engineering fo

Engineering Corporation, Seoul, Korea, for their willingness to allow me to continue my graduate study without any inconvenience.

Finally, thanks to Korean students in the department of civil and environmental engineering for their valuable supports during my graduate study.

TABLE OF CONTENTS

CHAPTER Page

CHAPTER Page

TABLE

LIST OF TABLES

FIGURE

LIST OF FIGURES

FIGURE Page

General

The
evolutionar
expanded b
The proper
and interrela
by laboratory
efforts regard
rational new d
designing flexi
mechanistic-em
simplified proc
themselves may
more reasonable
control various
performance leve

Problem Statem

The Mich
changing its desi

CHAPTER I

INTRODUCTION

General

The structural design of flexible pavements and bituminous overlays has been an evolutionary process, based primarily on the experience and judgment of engineers, and expanded by empirical relationships developed through research and field observations. The proper design of flexible pavements requires the consideration of several complex and interrelated factors. In previous research efforts, these factors were mainly identified by laboratory and field investigations, and combined with statistical analysis. Recent efforts regarding the interaction of these factors have resulted in the development of rational new design models employing mechanistic theories. Today, design methods for designing flexible pavements and overlays can be divided into two groups, empirical and mechanistic-empirical. Since both methods typically incorporate deterministic inputs and simplified procedure, the uncertainties of design parameters and design procedures themselves may have significant effects on the accuracy of design outputs. Therefore, more reasonable design procedures require comprehensive reliability techniques to control various uncertainties of pavement design and produce a consistent pavement performance level.

Problem Statement

The Michigan Department of Transportation (MDOT) is in the process of changing its design procedures of flexible pavements from one based on the AASHTO

guide to a

MICHBAC

are intend

MICHPAV

responses.

There is a

observations

(PMS), and e

effects of cha

Background

In rece

change their c

methods (AAS

perform this obj

of M-E design ap

depend on severa

1. The accuracy
pavement.

2. The accurate
layers.

3. The selection
functions.

4. The accuracy
deterioration

guide to a mechanistic approach. MICHPAVE, for flexible pavement design, and MICHBACK, for back-calculation of pavement layer moduli from FWD deflection data, are intended to be cornerstones of MDOT's mechanistic design procedure [1]. MICHPAVE has linear and non-linear finite element models to predict primary responses, and field-derived fatigue and rut models to predict the secondary response. There is a need to verify/calibrate the distress models in MICHPAVE using field observations and the distress database in the MDOT Pavement Management System (PMS), and establish a mechanistic flexible pavement design procedure that considers the effects of changing design inputs and bias of the design model.

Background

In recent years, most state highway agencies (SHA's) recognized the need to change their current flexible pavement design practices which are based on empirical methods (AASHTO) to mechanistic based approaches [2]. In order to successfully perform this objective, many SHA's have conducted studies to determine the feasibility of M-E design approaches. In general, the success of the new design practice is known to depend on several factors:

1. The accuracy of the pavement structural model to obtain primary responses of the pavement.
2. The accurate characterization of the material properties in the different pavement layers.
3. The selection of reasonable design criterion based on functional and structural functions.
4. The accuracy of the mechanistic-based pavement performance models to predict the deterioration of these functions.

5. The

T

the State

change th

and desig

MICHBA

(NDT) dat

considerabl

accuracy in

verified with

County, Mich

With r

development c

responses of th

version include

hundred paveme

mechanistic-emp

inventory data fr

a recently compl

affecting paveme

Michigan paveme

period of four ye

5. The application of reliability concept to treat uncertainties of the design procedure

The solutions related to first and second items have been successfully achieved in the State of Michigan; Two computer programs have been developed in an effort to change the state's design practice. One is a nonlinear finite element pavement analysis and design program, called MICHPAVE [3], and the other is a computer program, called MICHBACK, for backcalulation of layer moduli from nondestructive deflection testing (NDT) data [4]. Since the development of the program in 1988, MICHPAVE has had considerable reputation both within and outside the United States of America with the accuracy in computed results. The results from MICHPAVE and MICHBACK have been verified with the field test conducted at two pavement sections along I-96 in Ingham County, Michigan [5].

With reliable results from the computer programs that are commented above, the development of the pavement performance model that is based on mechanistic primary responses of the pavement such as strains and deflections is required. The MICHPAVE version includes rut and fatigue distress models that were derived from about five hundred pavement sections in Michigan and five neighboring states. These models have mechanistic-empirical features in the sense that they are based on a combination of inventory data from the PMS database, field distress data, and mechanistic responses. In a recently completed three-year study aimed at identifying asphalt concrete mix factors affecting pavement rutting and fatigue cracking, field data were collected from sixty four Michigan pavement sections (forty nine flexible and fifteen composite sections) over a period of four years [6]. It is intended that, in addition to other pavement sections and

PMS distress

purpose of ca

Objectives of

The ob

1. Verify cali
spectrum
model if n

2. Develop th
empirical (

3. Develop th
cross-sectio

Organization

This the

- In chapter
rutting, fact
mechanistic
- In chapter 3
raw field dat
- Chapter 4 d
summarizes
- In chapter 5
flexible pave
techniques (e

PMS distress data, most of these pavement sections will be monitored over time for the purpose of calibrating the distress models in MICHPAVE.

Objectives of the Research

The objectives of this research are to:

1. Verify/calibrate the rut prediction model in MICHPAVE using field data from a spectrum of in-service flexible pavement in the state of Michigan or improve the model if necessary. Figure 1 summarizes the calibration process.
2. Develop the reliability analysis model for evaluating uncertainties in the mechanistic-empirical (M-E) flexible pavement design procedure.
3. Develop the reliability-based pavement design algorithms that can output pavement cross-sections satisfying distress thresholds at a desired level of reliability.

Organization

This thesis is divided into seven chapters, including the introduction.

- In chapter 2, a comprehensive literature review on the mechanics of pavement rutting, factors affecting pavement rutting, existing rut prediction models, and the mechanistic-empirical design procedures is presented.
- In chapter 3, the data collection procedure is explained, and preliminary analysis of raw field data is described.
- Chapter 4 describes the revision of the rut prediction model. The chapter also summarizes model validation results.
- In chapter 5, a reliability analysis model for evaluating uncertainties in the M-E flexible pavement design procedure is introduced employing practical probabilistic techniques (e.g. FOSM, PEM, and FORM).

Cross S
Data
Deflect
Moduli
Pavemen
Mechanistic
of the Paveme
Physical P
Bituminou
Environme
Traffic
Measured Dis
(Rut Depth):

Figure

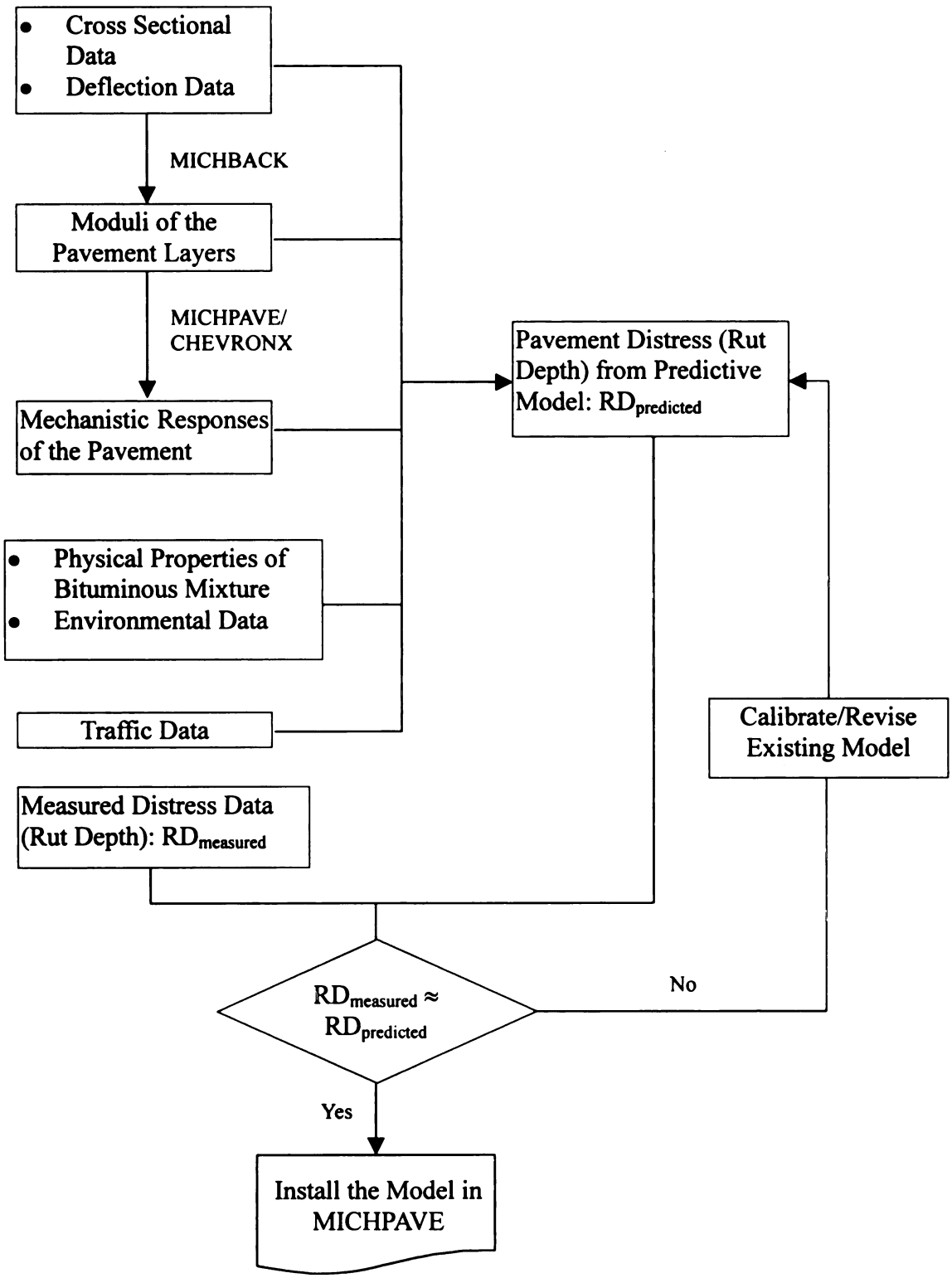

Figure 1 Framework for the Calibration of Existing Rut Prediction Model

- In chapt
  the revi
  introduce
  quantifyi
- In chapt
  provided.

- In chapter 6, two reliability-based M-E flexible pavement design procedures using the revised rut prediction model as a major performance/transfer function are introduced. In the two design procedures, different reliability methodologies for quantifying uncertainties of the M-E design components are exhibited.
- In chapter 7, the results of the research are summarized and conclusions are provided. Finally, recommendations for future research are proposed.

General

The l
distributing ch
of multiple lay
pavement stre
load over the
pavements:

Rut - R
concrete surfac
by environment
pavement mater

Fatigue -
by fatigue failur
traffic loading. It
accelerated by en
minimized by us
construction pract

CHAPTER II

LITERATURE REVIEW

General

The load-carrying capacity of flexible pavements is brought about by the load distributing characteristics of the individual layers. In general, flexible pavements consist of multiple layers with the highest strength material placed at near the surface. Hence, the pavement strength is derived from building up thick layers and thereby distributing the load over the roadbed soil. Two types of load related distress can be found in flexible pavements:

Rut - Rut can be defined as the sum of the permanent deformation in the asphalt concrete surface, base, subbase and roadbed soil. Rut is a load-related distress accelerated by environmental factors. In general, rutting can be minimized by using the appropriate pavement materials, proper design thickness, and construction practices [6].

Fatigue - Fatigue or alligator cracking is a series of interconnecting cracks caused by fatigue failure of the asphalt concrete surface (or stabilized base) under repeated traffic loading. It is a load-associated distress that can be found in both wheel paths and is accelerated by environmental factors. Fatigue cracking potential of any pavement can be minimized by using the appropriate pavement materials, proper design procedure, and construction practices [6].

It sh

rutting due t

theoretical n

layer is main

Rut p

steps during t

and constructi

1. Engineered
plastic yiel
AC layer.

2. Balanced pa
the compres
top of the ro
layers.

3. Good const
various pave

Existing

empirical and

equations deri

Mechanistic-em

criteria:

1. Minimizing t
compressive

2. Maximizing t
at the bottom

It should be noted that the contribution of the AC layer to the total pavement rutting due to densification is negligible, since this layer is typically compacted to near its theoretical maximum density during construction. Permanent deformation in the AC layer is mainly the result of lateral distortion due to repeated shear deformation.

Rut potential of pavements can be minimized by taking balanced engineering steps during the material design (asphalt mix design), the cross-section design process and construction, These steps include:

1. Engineered asphalt mix design that can withstand the expected traffic loading without plastic yielding and resist repeated shear deformation that causes lateral distortion of AC layer.
2. Balanced pavement design process that provides adequate layer thickness to reduce the compressive stresses induced at the top of the base and subbase layers, and at the top of the roadbed soil. These stresses cause permanent deformation (rut) in pavement layers.
3. Good construction practices that deliver adequate and uniform compaction to the various pavement layers.

Existing flexible pavement design methods can be divided into two categories: empirical and mechanistic-empirical. Most empirical methods are based on statistical equations derived from field observations of pavement rutting and roughness. Mechanistic-empirical design methods, on the other hand, are mainly based on two criteria:

1. Minimizing the rut potential of each pavement layer by limiting the magnitude of the compressive stress induced at the top of that layer by a moving wheel load.
2. Maximizing the fatigue life of the AC layer by minimizing the induced tensile stress at the bottom of the layer due to a moving wheel load.

Mechanics o

Perm

wheel paths.

pavement up

noticeable on

permanent de

soil, the subb

magnitude of

1. Constructi
or compac

2. Asphalt n
cement, h

3. Environm
and high
inadequat

4. Tire facto

As s

AC, base, su

the transver

evident tha

contributio

depending

Mechanics of Permanent Deformation (Rut)

Permanent deformation in flexible pavements manifests itself as rutting in the wheel paths, thereby causing permanent distortion in the transverse profile. In addition, pavement uplift may occur along the sides of the rut channel. In many instances, ruts are noticeable only after a rainfall, when the wheel paths are filled with water. Nevertheless, permanent deformation of the pavement surface is the result of rutting of the roadbed soil, the subbase and base layers, and the AC surface. Several other factors affect the magnitude of the rut and its time rate of accumulation. These factors include:

1. Construction factors, including inadequate compaction (either low compaction effort or compaction at lower temperatures than those specified).
2. Asphalt mix factors, which include soft (low viscosity or high penetration) asphalt cement, high air voids, rounded aggregate, and excess sand in the mix.
3. Environmental factors, which include high temperatures, which soften the AC layer, and high moisture content or saturation of the lower layers (base and subbase) due to inadequate drainage.
4. Tire factors, such as studded tires and high tire pressure.

As stated earlier, pavement rutting is the sum of permanent deformations in the AC, base, subbase layers, and in the roadbed soil. Figure 2 shows the results of a study of the transverse profile of loops 4 and 6 at the AASHO Road Test [7]. From the figure, it is evident that rutting has occurred in all pavement layers and roadbed soil. The contribution of each layer to the total pavement rut varies from one pavement to another depending on material properties of layers.

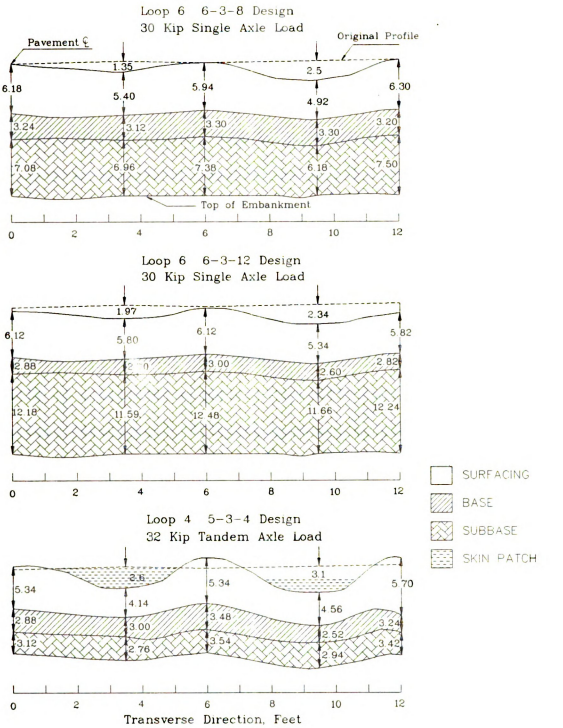

Figure 2 Transverse Profile of Loops 4 and 6 of the AASHO Road Test [7]

Factors Aff

- **Tire In**

In th

rutting and

in the state

has increase

of 130psi (8

average tire

(1069kPa) [8

Typi

magnitude o

and at the to

tire pressure

type and tir

concluded th

1. The effe

pressure.

increase

inflation

percent

mechani

MICHP

stresses

Factors Affecting Rutting of Asphalt Surfaced Pavements

- **Tire Inflation and Tire-Pavement Contact Pressure**

In the U.S.A. asphalt surfaced pavement are in general, experiencing premature rutting and fatigue cracking due to increased traffic load and truck tire pressure. Surveys in the state of Illinois and Texas indicate that, over the last few decades, the tire pressure has increased substantially. An average tire pressure of 96psi (662kPa), with a maximum of 130psi (896kPa) was recorded in the Illinois survey. The Texas survey showed an average tire pressure of 110psi (758kPa), with a maximum tire pressure of 155psi (1069kPa) [8].

Typically, the rut potential of a flexible pavement is evaluated on the basis of the magnitude of the compressive strains induced at the top of the base and subbase layers and at the top of the roadbed soil due to an 18kip (80kN) single axle load and a constant tire pressure (typically 85psi (586kPa)). An experimental study about the influence of tire type and tire pressure on pavement performance conducted by Smith and Bonquist concluded that [9]:

1. The effect of wheel load on pavement response is greater than the effect of tire pressure. The measured pavement responses (stresses and strains) doubled for an increase in load from 9400lb (42kN) to 19000lb (84.5kN), while increasing the tire inflation pressure from 76psi (524kPa) to 140psi (965kPa) resulted in a less than 10 percent increase in the measured response. This conclusion supports the results of mechanistic analysis of flexible pavement structures by Baladi, who used MICHPAVE, linear/nonlinear finite element computer program, to analyze the stresses and strains induced in the pavement layers due to various wheel loads and tire

inflation

induced

wheel lo

2. The effe

thin pav

sections

3. Higher te

wheel loa

fatigue cr

Environmen

Expo

time goes by

strains affilia

function of t

asphalt film

and material

during mixin

that early pav

when it is op

150°F (66°C)

inflation pressures [10]. He reported that the effects of increasing tire pressure on the induced stresses and strains in the pavement are much smaller than those of increasing wheel load.

2. The effects of tire pressure and wheel load on pavement rutting are much higher for thin pavement sections (less than 2-inch (5cm) AC surface) than for typical or thick sections (more than 4-inch (10cm) thick AC surface).

3. Higher temperatures cause higher rut potential. Hence, the magnitude of tire pressure, wheel load, temperatures, and AC thickness are key to the deterioration of rutting and fatigue cracking in asphalt surfaced pavements.

Environmental Factors

Exposure to the environment causes bituminous materials to harden over time. As time goes by, the bituminous binder becomes so brittle that it can no longer sustain the strains affiliated to daily temperature changes and traffic loads. The rate of hardening is a function of the oxidation resistance of the binder, temperature, and thickness of the asphalt film [10]. Therefore, the rate of hardening varies with the binder type, climate, and material design. It should be noted that most of the asphalt hardening takes place during mixing, agitating, transporting, and construction. Hughes and Maupin reported that early pavement rutting is a function of the pavement temperature of the pavement when it is opened to traffic [8]. They suggested that pavement temperatures of less than 150°F (66°C) lead to a stable asphalt mix under traffic.

Permanent

Pav

performanc

life, or the

that must b

prediction

mechanistic

elasticity, p

model can

because of it

to be made

with the mec

researches to

rutting. In an

assumed that

magnitude of

strain and th

field observa

Mechanistic

As m

can be define

The cumulati

Permanent Deformation (Rutting) Prediction Models

Pavement design and pavement performance systems have to include the performance prediction models. Such models should address rate of deterioration, service life, or the remaining service life of the pavement structures. Rut is one type of distress that must be predicted in the pavement design and analysis procedures. Current rut prediction models can be divided into two categories: (1) mechanistic, and (2) mechanistic/empirical. The mechanistic models are based on either the theory of elasticity, plasticity, or visco-elasticity. Even though nonlinear plastic or visco-elastic model can provide more accurate results, the use of this model has been restricted because of its complex nature. In other words, the pavement rutting prediction is difficult to be made directly from plastic stress-strain relationships. The complexities involved with the mechanistic prediction models using nonlinear plastic or visco-elastic theory led researches to develop simplified mechanistic/empirical models for predicting pavement rutting. In an effort to develop practical alternatives for predicting rutting, it is generally assumed that the initial elastic strain and the number of load repetitions can explain the magnitude of cumulative plastic deformation. The relationship between the initial elastic strain and the number of load repetitions can be obtained from both laboratory tests and field observations using linear or nonlinear elastic theory.

Mechanistic Rutting Prediction Model

As mentioned above, rutting on the surface of a pavement due to a specific traffic can be defined as the sum of cumulative permanent deformations in the pavement layers. The cumulative permanent deformation of a layer can be calculated by integrating the

plastic strai

total rut-de

layers. The

calculated.

applications

task to an

correspondi

Beca

estimating t

including mu

elastic soluti

which the de

components:

the total strai

where:

ε

ε_e

ε_p

From equatic

If the total

calculating th

strains at loa

plastic strain in the layer due to the amount of applied traffic load [11]. So, theoretically, total rut-depth of a pavement can be estimated by integrating plastic strains through the layers. Therefore, if the plastic strain of each layer per cyclic load (traffic) can be calculated, one can exactly predict the total rut-depth due to the number of load applications at a given time. However, it is an extremely difficult and time-consuming task to analytically calculate plastic strains with time-series material properties corresponding to the number of load repetitions.

Because of the reasons stated above, it is necessary to find alternatives for estimating the plastic strain with common analysis tools in pavement engineering, including multi-layered elastic theory and finite element analysis with elastic and visco-elastic solution. To this end, many researchers have suggested elastoplastic theory in which the deformation under loading from the load is assumed to be composed of two components: the elastic and plastic, or the recoverable and the unrecoverable [12]. Thus, the total strains can be expressed by the following equation;

$$\varepsilon = \varepsilon_e + \varepsilon_p \tag{1}$$

where:

ε	=	total strain,
ε_e	=	elastic strain, and
ε_p	=	plastic strain

From equation 1, the plastic strain can be expressed:

$$\varepsilon_p = \varepsilon - \varepsilon_e \tag{2}$$

If the total stress is assumed to be constant, the plastic strain can be estimated by calculating the elastic strain. In order to avoid complex procedure for calculating elastic strains at loading stages with different resilient moduli, another assumption needs to be

made, whic

due to repe

model illus

where:

ε_p

ε_r

N

α and μ

Several atter

model based

Review of M

- **VESYS**

The method i

based on the

[11]. The two

in which ε_p(

the n^{th} applica

application nu

proportionality

parameter indi

made, which is the rate of increase of permanent strain in each element of a given layer due to repeated wheel loads is proportional to the resilient strain. The general form of the model illustrating this assumption is followed as [12];

$$\frac{\partial \varepsilon_p}{\partial N} = \mu N^{-\alpha} \varepsilon_r \tag{3}$$

where:

ε_p	=	permanent strain,
ε_r	=	resilient strain,
N	=	number of load repetitions, and
α and μ	=	permanent strain parameters.

Several attempts have been made to develop the mechanistic-based rutting prediction model based on these theories and assumptions.

Review of Mechanistic-Based Rutting Prediction Models

- **VESYS Model**

The method incorporated in the VESYS computer program for predicting the rut depth is based on the assumption that the permanent strain is proportional to the resilient strain [11]. The two are related as follows:

$$\varepsilon_p(N) = \mu \varepsilon N^{-\alpha} \tag{4}$$

in which $\varepsilon_p(N)$ is the permanent or plastic strain due to a single load application, i.e., at the n^{th} application; ε is the elastic or resilient strain at the 200^{th} repetition; N is the load application number; μ is a permanent deformation parameter representing the constant of proportionality between permanent and elastic strains; and α is a permanent deformation parameter indicating the rate of decrease in permanent deformation as the number of load

application

equation 4

From equat

So the slope

The intercep

To determine

for the indivi

strains due t

200th repetiti

in which ε_r(

equation 4 in

Under the sa

can be rewrit

applications increase. The total permanent deformation can be obtained by integrating equation 4

$$\varepsilon_p = \int_0^N \varepsilon_p(N)dN = \varepsilon\mu\frac{N^{1-\alpha}}{1-\alpha} \tag{5}$$

From equation 5

$$\log\varepsilon_p = \log\left(\frac{\varepsilon\mu}{1-\alpha}\right) + (1-\alpha)\log N \tag{6}$$

So the slope of the straight line $S=1-\alpha$, or

$$\alpha = 1\text{-}S \tag{7}$$

The intercept at $N=1$, $I=\varepsilon\mu/(1-\alpha)$, or

$$\mu = \frac{IS}{\varepsilon} \tag{8}$$

To determine the permanent deformation parameters of the layer system, α_{sys} and μ_{sys}, for the individual layers, it is further assumed that the sum of permanent and recoverable strains due to each load application is a constant and equals to the elastic strain at the 200th repetition. This means that after the 200th repetition

$$\varepsilon = \varepsilon_p(N) + \varepsilon_r(N) \tag{9}$$

in which $\varepsilon_r(N)$ is the recoverable strain due to each load application. Substituting equation 4 into equation 9, we obtain

$$\varepsilon_r(N) = \varepsilon(1-\mu N^{-\alpha}) \tag{10}$$

Under the same stresses, strains are inversely proportional to the moduli, so equation 10 can be rewritten as follows:

in which E

loading at t

individual l

These unlo

different val

in which w

equation. 4.

in which μ

When the

accumulated

integrating e

So, the sum

expressed a

$$E_r(N) = \frac{E}{1-\mu N^{-\alpha}} = \frac{EN^{\alpha}}{N^{\alpha}-\mu} \tag{11}$$

in which $E_r(N)$ is the elastic modulus due to unloading and E is the elastic modulus due to loading at the 200th repetitions. Note that $E_r(N)$, which is the unloading modulus for each individual layer, is not a constant but increases with the increasing of load applications. These unloading moduli are used to determine the recoverable deformation $w_r(N)$ at different values of N. The permanent deformation $w_p(N)$ can then be computed by ;

$$w_p(N) = w - w_r(N) \tag{12}$$

in which w is the elastic deformation due to loading at the 200th applications. Similar to equation. 4, $w_p(N)$ can be expressed by

$$w_p(N) = \mu_{sys} w N^{-\alpha_{sys}} \tag{13}$$

in which μ_{sys} and α_{sys} are permanent deformation parameters of a pavement system. When the number of traffic load applications, n, is applied on a pavement, the accumulated permanent deformation of a layer of the pavement can be obtained by integrating equation 13 with respect to n;

$$w_p(n) = w\mu_{sys} \frac{n^{1-\alpha_{sys}}}{1-\alpha_{sys}} \tag{14}$$

So, the sum of rut depths of all layers due to the number of load applications, n, can be expressed as;

$$\text{Rut Depth} = \sum_{i=1}^{l} w_i \mu_{sys_i} \frac{n^{1-\alpha_{sys_i}}}{1-\alpha_{sys_i}} \tag{15}$$

• **Revise**

For a layer

rut-depth, c

where:

ρ

ε

h_i

According to

and 0.006 to

by them hav

parameters,

common ma

equation 15,

pavement.

where :

RUT

A

C_1, C_2, C_3

An importan

compressive

- **Revised VESYS Model with the Consideration of Actual Field Condition.**

For a layer of pavement structure, the vertical compression, which is related to the true rut-depth, can be calculated using equation 14. This equation can be rewritten as [13];

$$\rho_i = \frac{\mu_i}{1-\alpha_i} h_i \left(\varepsilon_{ri}^{\frac{1}{1-\alpha_i}} N \right)^{1-\alpha_i} \tag{16}$$

where:

ρ_i	=	vertical compression in layer i,
ε_{ri}	=	resilient vertical strain in layer i, and
h_i	=	thickness of layer i.

According to Leahy and Witczack, typical values for α and μ range from 0.006 to 0.92 and 0.006 to 8.82, respectively [14]. Furthermore, results from extensive laboratory work by them have shown that α and μ are significantly influenced by mix design and test parameters, which is a background of the assumption that α and μ are constant for common material specification of each layer. Based on this assumption and from equation 15, the following regression can be used to predict rut-depth in a flexible pavement.

$$RUT = C_1 A^{C_2} \left[\sum_{i=1}^{l} h_i \left(N_i \varepsilon_{i,k}^{\frac{1}{1-\alpha_i}} \right)^{1-\alpha_i} \right]^{C_3} \tag{17}$$

where :

RUT	=	rut depth due to vertical compression [in],
A	=	a scaling variable related to the environment and the permanent strain coefficient, μ, and
C_1, C_2, C_3	=	regression coefficients obtained from field data.

An important requirement for using this model is a simple procedure for obtaining the compressive strain in the pavement layers. This requires establishing locations for the

strains to

applied lo

portion of

into three

calculated

1. AC laye
2. Base lay
3. Subgrad

Fina

strain calcu

developed f

$RUT = 0.2$

where:

AGE

α_1

α_2

α_3

The releva

1. Numbe
2. Coeffi
3. Standa

- **Calib**

Ali, et al.

deformati

strains to ensure that they properly reflect the average strain responses from a given applied load, and do not result in over or underestimation of the permanent deformation portion of the layer. Owusu-Antwi, et al. suggests that pavement layers should be divided into three courses of AC, base and subgrade and the critical strains for those layers be calculated at the following locations [13];

1. AC layer -at the middle of the AC surface layer thickness
2. Base layer - at the middle of the base layer thickness
3. Subgrade - at the top of the subgrade.

Finally, using data from Long Term Pavement Performance (LTPP) database and strain calculated at the critical location of each layer, the following equation was developed for predicting the total rut-depth, RUT, in flexible pavements [13];

$$RUT = 0.29 AGE^{0.13} \left[h_{ac} \left(\Sigma n_i \varepsilon_{ac,i}^{\frac{1}{1-\alpha_1}} \right)^{1-\alpha_1} + h_{base} \left(\Sigma n_i \varepsilon_{base,i}^{\frac{1}{1-\alpha_2}} \right)^{1-\alpha_2} + h_{subg} \left(\Sigma n_i \varepsilon_{subg,i}^{\frac{1}{1-\alpha_3}} \right)^{1-\alpha_3} \right]^{0.77} \quad (18)$$

where:

AGE	=	age of pavement, years
α_1	=	0.6,
α_2	=	0.7, and
α_3	=	0.7

The relevant statistics of the model are as follows;

1. Number of data points, N =80
2. Coefficient of determination, $R^2 = 0.35$
3. Standard error estimate, SEE = 0.1

- **Calibrated VESYS Model with LTPP Database**

Ali, et al. suggest a basic equation for predicting rut-depth in which the permanent deformation of each layer by various axle groups can be estimated [15];

where:

ρ_p

ε^e_{ij}

h_j

With a calib

the followin

$\rho_p = 0.000$

$+ 0.022\, h_{sub}$

Advantages

- The mo

  means t

  satisfy v
- The cor

  manner.

  controll

  layer thi
- The mo

  progress

$$\rho_p = \sum_{j=1}^{L} h_j \frac{\mu_j}{1-\alpha_j} \left(\sum_{i=1}^{k} n_i \left(\varepsilon e_{i,j} \right)^{\frac{1}{1-\alpha_j}} \right)^{1-\alpha_j} \tag{19}$$

where:

ρ_p = cumulative permanent deformation in all layers, from all load groups (rut-depth),

$\varepsilon e_{i,j}$ = vertical compressive strain in the middle of layer j, due to a passage of an axle of group i, and

h_j = thickness of layer j. The subgrade may be divided into several layers and the calculations performed until the vertical elastic strain approaches zero, the subgrade thickness is determined accordingly.

With a calibration procedure of α and μ for each layer using the data in LTPP database, the following equation is introduced as a final form of the model;

$$\rho_p = 0.00011\, h_{AC} \left(\sum_{i=1}^{k} n_i \left(\varepsilon e_{i,AC} \right)^{1.111} \right)^{0.9} + 23.26 * h_{base} \left(\sum_{i=1}^{k} n_i \left(\varepsilon e_{i,base} \right)^{20} \right)^{0.05} + 0.022\, h_{subg} \left(\sum_{i=1}^{k} n_i \left(\varepsilon e_{i,subg} \right)^{2.81} \right)^{0.356} \tag{20}$$

Advantages of Mechanistic-Based Rutting Prediction Models

- The models follow mechanistic fundamentals without any physical violation. It means that a mechanistic design procedure adopting this model has a potential to satisfy various regional conditions.
- The contribution of each layer to total rut-depth can be quantified in a reasonable manner. It means that the model can allow one to have various options for controlling rutting in pavement design by changing material properties of layers and layer thickness.
- The models can account for rate-hardening (load applications vs. rut-depth) in the progression of rutting with increased load applications.

- The n
chang
pavem

Disadvanta

- The ea
materia
in labor
in field
- The rec
vertical
load. In
variatio
the criti
- Even th
load spe
can cau
develop
of varic
effects
groups'
paveme
axles is

- The models consider the rut-depth as performance function and hence can easily change failure criteria like rut-depth of 0.4in (1cm) or 0.5in (1.3cm). It means that pavements can be designed at various terminal service levels using this model.

Disadvantages of Mechanistic-Based Rutting Prediction Models

- The early models such as VESYS model require laboratory tests to determine basic material properties of all layers in the pavement. The material properties determined in laboratory tests vary in accordance with test methods and are different from those in field full-scale tests.
- The recent models such as the revised VESYS assume that the locations of critical vertical strains are equivalent to the average strain responses from a given applied load. In multi-layered elastic analysis or finite element analysis, one can see a high variation of vertical strain along the thickness in each layer. So, "determining where the critical strain can be measured" greatly affects the amount of total rut-depth.
- Even though the rut-depth prediction model is developed considering the actual axle load spectrum, there are some limits to estimate the effects of multiple wheels, which can cause the model to under or overestimate actual rut-depth. In the models developed by Ali et. al., the model has been formulated considering the contribution of various axle load groups to total rut-depth [15]. Definitely, axle load groups' effects on the pavement should be separately evaluated since the change in load groups' configuration cannot be linearly related to that of the damage amount to the pavement. For example, the AASHO road test verified that one passage of tandem axles is not equivalent to two passages of single axles, but 1.38 passages [16]. The

mech

layere

actual

variou

pavem

Accord

comput

practica

- The ru

tempera

asphalt-

two co

develop

the mo

be expr

where:

$n_{i,m}$

$\alpha_{j,m} \cdot \mu$

Rutting Pr

In g

categories.

mechanistic pavement analysis algorithms using finite element method, multi-layered elastic analysis method, and so on can compute vertical strains considering actual wheel configurations of vehicles in order to correctly consider effects of various load groups. Unfortunately, most computer programs currently available for pavement analysis calculate vertical strains based on the superposition principle. According to this principle, principal stress and strain under multiple wheels are computed by superimposing those due to each single wheel load [12]. Thus, it is not practical to consider the actual axle load spectrum in rut-depth prediction.

- The rutting prediction model proposed in the section above should include temperature or seasonal variations because the material properties of especially, asphalt-aggregate mixtures are highly sensitive to temperature variation. There are two common ways for the addition of temperature consideration to the model: (1) develop a temperature correction factor for the surface layer modulus and add it to the model, and (2) consider seasonal traffic damage. A conceptual model for this can be expressed as;

$$\rho_p = \sum_{m=1}^{N}\left[\sum_{j=1}^{L} h_j \frac{\mu_{j,m}}{1-\alpha_{j,m}}\left(\sum_{i=1}^{k} n_{i,m}\left(\varepsilon_{i,j,m}\right)^{\frac{1}{1-\alpha_{j,m}}}\right)^{1-\alpha_{j,m}}\right] \qquad (21)$$

where:

$n_{i,m}$ = number of load applications of load group i in seasonal term, m, and

$\alpha_{j,m}$, $\mu_{j,m}$ = permanent strain coefficients of layer j in seasonal term, m.

Rutting Prediction Models Based on Mechanistic-Empirical Approach

In general, mechanistic-empirical modeling approach can be divided into two categories. One approach is to simplify the prediction model with a few components and

emphasiz

vertical st

mechanist

violating p

Mechanist

- **Type I**

where:

ε_t

Table 1 sum

- **Type II**

Allen et. al.

the paveme

control rutti

layers is ex

where:

N

C_3
C_2
C_1
C_0

T

σ_1

emphasize on the key phenomenon of the rutting mechanism such as the magnitude of vertical strain at the top of subgrade (type I), and the other is to statistically organize mechanistic, material, geometric, environmental, and traffic components without violating physical rules (type II).

Mechanistic-Empirical Rutting Prediction Models

- **Type I**

$$N_d = f_1(\varepsilon_v)^{-f_2} \tag{22}$$

where:

ε_v = vertical compressive strain at the top of subgrade.

Table 1 summarizes the values of f_1 and f_2 used by several agencies [12].

- **Type II**

Allen et, al. performed a comprehensive laboratory testing program to determine where in the pavement structure and to what extent rutting occurs and to determine the factors that control rutting [17]. As a result of the tests, the model for predicting plastic strains (ε_p) of layers is expressed as follows:

$$\log \varepsilon_p = C_0 + C_1(\log N) + C_2(\log N)^2 + C_3(\log N)^3 \tag{23}$$

where:

N = number of stress repetitions in the asphalt layer
C_3 = 0.00938,
C_2 = 0.10392,
C_1 = 0.63974
C_0 = $(-0.000663T^2+0.1521T-13.304) + [(1.46-0.00572T)(\log_{\sigma_1})]$
T = temperature (F), and
σ_1 = stress (psi)

Table 1 Su

Asphalt Ir
Shell (revi
50% Reli
85& Reli
95% Reli
U.K. Trans Laboratory
Belgian Ro

Table 1 Summary of Coefficients of Type I Rutting Prediction Models [12]

Agency	f_1	f_2	Rut Depth (in.)
Asphalt Institute	$1.365*10^{-9}$	4.477	0.5
Shell (revised 1985)			
50% Reliability	$6.15*10^{-7}$	4.0	0.5
85& Reliability	$1.94*10^{-7}$	4.0	0.5
95% Reliability	$1.05*10^{-7}$	4.0	0.5
U.K. Transport & Road Research Laboratory (85% Reliability)	$6.18*10^{-8}$	3.95	0.4
Belgian Road Research Center	$3.05*10^{-9}$	4.35	0.4

for a dens

C_3
C_2
C_1
C_0

w

σ_1

σ_3

in the subgr

C_3
C_2
C_1
C_0

w

σ_1

σ_3

Thus,

b. Baladi

collecte

model a

Log(RD
=0.15*
0.7*log

where:

RD
AV
KV

for a dense-graded aggregate base layer

C_3	=	0.0066-0.004log(w),
C_2	=	-0.142+0.092log(w),
C_1	=	0.72
C_0	=	[-4.41+(0.173+0.003w)(σ_1)] -[(0.00075+0.0029w) (σ_3)]
w	=	moisture content (percent)
σ_1	=	deviator stress (psi), and
σ_3	=	confining pressure (psi)

in the subgrade

C_3	=	0.007+0.001(logw),
C_2	=	0.018(logw),
C_1	=	$10^{(-1.1+0.1w)}$
C_0	=	[(-6.5+0.38w)-(1.1log$_{\sigma_3}$)]+(1.86log$_{\sigma_3}$)

w	=	moisture content (percent)
σ_1	=	deviator stress (psi), and
σ_3	=	confining pressure (psi)

Thus,

$$\varepsilon_{p_{total}} = \varepsilon_{p_{AC}} + \varepsilon_{p_{base}} + \varepsilon_{p_{subgrade}} \quad (24)$$

b. Baladi and Harichandran suggest a rut-depth prediction model based on data collected from field sites in Michigan and Indiana. Equation 25 summarizes the model attributes [18]:

$$\text{Log(RD)}=-1.6+0.067*\text{AV}-1.4*\log(\text{TAC})+0.07*\text{AAT}-0.000434*\text{KV} +0.15*\log(\text{ESAL})-0.4*\log(\text{MR}_{\text{RB}})-0.5*\log(\text{MR}_{\text{B}})+0.1*\log(\text{SD})+0.01*\log(\text{CS})- 0.7*\log(\text{TB}_{\text{EQ}})+0.09*\log[50-(\text{TAC}+\text{TB}_{\text{EQ}})] \quad (25)$$

where:

RD	=	rut depth (in.),
AV	=	air void,
KV	=	kinematic viscosity (centistroke),

ESAL

SD
CS
AAT
TAC
TB_{EQ}
MR_{RB}
MR_B

c. Carper

field si

$RUT = -0$

$+0.05238$

$+0.000419$

where:

RUT
40-80

STAB
DIFFS40

AVEHOT

ESAL

200

D
RDEN

Advantages

a. Type I

- One car

rutting a

easily co

loads. Ef

ESAL	=	the number of 18-kip ESALS at which the rut depth is being calculated,
SD	=	pavement surface deflection (in.),
CS	=	compressive strain at the bottom of AC,
AAT	=	average annual temperature (°F),
TAC	=	thickness of AC,
TB_{EQ}	=	equivalent thickness of base material,
MR_{RB}	=	resilient modulus of the roadbed soil, and
MR_{B}	=	resilient modulus of base material

c. Carpenter suggests a rut-depth prediction model based on field data collected from field sites in Illinois [19].

$$RUT = -0.040930187(-40+80)^{1.0849} - 0.0002569715(STAB) + 0.083705(DIFFS40) + 0.0523817(AVEHOT) + 0.313578(ESAL)^{0.045565} - 1.27458(-200)^{-1.24927} + 0.00041937(D) + 0.0106828(RDEN) - 1.38669 \quad (26)$$

where:

RUT	=	rut-depth (in.),
-40+80	=	percent passing the No. 40 seive, retained on the No. 80 sieve of the surface mix (%),
STAB	=	Marshall stability of the surface mixture (lb.),
DIFFS40	=	hump in the FHWA 0.45 power gradation curve on the No. 40 sieve in the surface mixture (%),
AVEHOT	=	average of the maximum monthly temperature during June, July, and August (°C),
ESAL	=	cumulative 18-kip ESALs using the overlay since placement (millions),
-200	=	percent passing the No. 200 sieve in the binder level mix (%),
D	=	theoretical maximum density (pcf), and
RDEN	=	relative density of the surface mixture (%).

Advantages of Mechanistic-Empirical Rutting Prediction Models

a. Type I

- One can have a simple design criterion. By using a unique relationship between rutting and a pavement response such as the strain at the top of subgrade, one can easily control the magnitude of rutting amount in a pavement due to given traffic loads. Effects of various factors on pavement rutting can be integrated and quantified

in th

the e

magni

pavem

b. Type II

- This ty

analysis

asphalt

moisture

performa

- The effec

monthly te

Disadvantages

a. Type I

- The model

Universal a

- In the stati

variable is r

model predi

of rut-depth.

design crite

in the vertical strain at the top of subgrade soil. If a pavement designer understands the effects of various material properties and environmental conditions on the magnitude of vertical strain at the top of roadbed soil, he/she can easily design a pavement structure that successfully meets a mechanistic design criterion of rutting.

b. Type II

- This type of rutting prediction model can be used very effectively in the pavement analysis for evaluating the effects of asphalt mix variables (i.e. air void, viscosity, asphalt content, aggregate angularity and so on) or subgrade soil properties (i.e. moisture content, relative density, and so on) on overall pavement rutting performance.
- The effect of environmental factor such as ambient annual temperature or maximum monthly temperature on asphalt modulus can be incorporated.

Disadvantages of Mechanistic Empirical Rutting Prediction Models

a. Type I

- The models are based on statistical analysis of observed field or laboratory data. Universal applicability of such models is somewhat limited.
- In the statistical analysis of this type of rutting prediction model, the independent variable is not rut-depth but the number of load applications. As seen in Table 1, the model predicts the number of load applications corresponding to the design criterion of rut-depth. It means that whenever a pavement design engineer wants to change the design criteria of rut-depth, he/she must find different model parameters that

corre

Asph

paran

to the

- In pav

most

subgra

vertica

b. Type II

- Applica
- Variabl

highly

model.

contribu

Mechanisti

In o

AASHTO r

deflection in

or moisture.

pavement pe

modeled by

correspond to the design criteria. For instance, when the design criterion in the Asphalt Institute model is changed from 0.5 inch of rut-depth to 0.3 inch, the parameters in the model should be changed, otherwise the model cannot be applied to the changed criterion.

- In pavements with thick asphalt-concrete layer that is subjected to heavy traffic load, most of permanent deformation occurs in the bituminous layer, rather than in the subgrade [6]. In such cases, it is difficult to control the pavement rutting only by vertical compressive strain on the top of roadbed soil.

b. Type II

- Applicability is somewhat limited.
- Variables assigned in a rutting mechanistic-empirical prediction model may be highly correlated with each other, which may lead to high multi-colinearity of the model. These multi-colinearity effects can prevent the model from showing the contributions of highly correlated variables to total rut-depth.

Mechanistic-Empirical Flexible Pavement Design

In order to overcome the shortcomings from empirical design such as the AASHTO method [16], the numerical capability to calculate the stress, strain, or deflection in a pavement, when subjected to external loads or the effects of temperature or moisture, has been developed. However, various investigators have recognized that pavement performance is likely to be influenced by many factors that cannot be precisely modeled by mechanistic methods. Hence, it is necessary to calibrate the models with

observed

develope

E) desig

procedure

available

empirical

related to

Thickness-

procedure.

specificatio

assurance

considered.

NC

procedure a

for a mecha

that transfer

models to

rutting, cra

empirical de

model throu

requirement

NCHRP 1-2

models and

observed performance data, i.e. empirical correlation. So, the procedure that is being developed as a new design method of the pavement is called mechanistic-empirical (M-E) design procedure. The current effort of developing mechanistic-empirical design procedures does not require new technology but assessing, evaluating, and applying available mechanistic-empirical technology. It should be noted that a mechanistic-empirical design procedure cannot adequately address all pertinent factors and issues related to load responses, distresses development, and ultimate system performance. Thickness-related factors are most readily addressed by mechanistic-empirical design procedure. Some other important factors such as material selection process and material specification, construction policy and specifications, quality control and quality assurance procedures, and maintenance and rehabilitation practices should also be considered.

NCHRP 1-26 reports that the major inputs to the mechanistic-empirical design procedure are structural models, transfer functions, and reliability [20]. The framework for a mechanistic empirical model is illustrated in Figure 3. The report also concludes that transfer functions which relate the pavement responses determined from mechanistic models to pavement performance as measured by the type and severity of distress (rutting, cracking, roughness, and so on) are the weakest part in the mechanistic-empirical design procedure [20]. Hence, the achievement of rigorous distress prediction model through extensive field calibration and verification is the most important requirement in the complete implementation of M-E design procedure. In Phase I of NCHRP 1-26 project, it was concluded that the available flexible pavement structural models and computer codes (such as MICHPAVE, ILLIPAVE, CHEVRONX, ELSYM5,

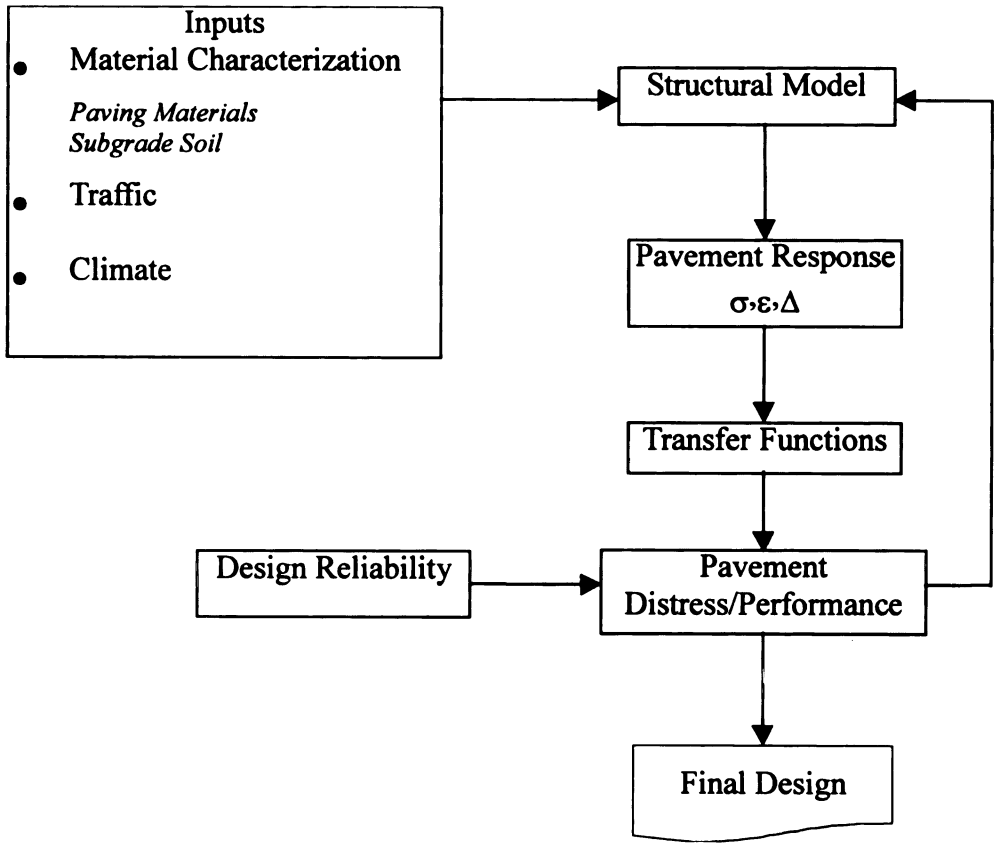

Figure 3 Framework of a M-E Flexible Pavement Design Model [20]

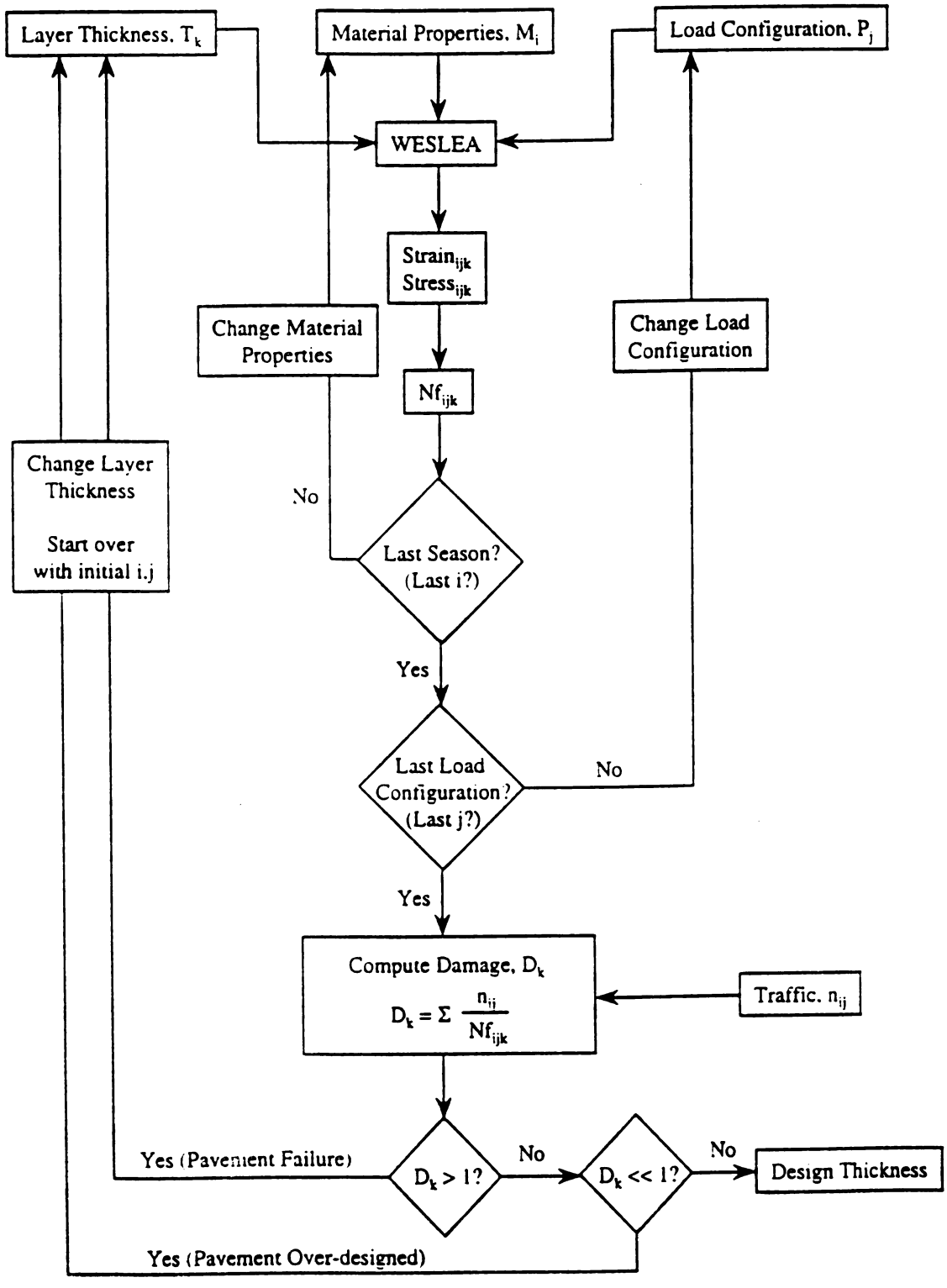

Figure 4 M-E Flexible Pavement Design Flowchart in Minnesota Practice [21]

BISAR.

develop

C

design pr

which th

flowchart

Research

Based on t

- Altho

  structu

  rutting

  the m

  mecha

  flexibl

  temper

  mechar

  many i

  both pr

  many

  procedu

  load-rel

  mechani

BISAR, WESLEA and so on) for mechanistic analysis are adequate for supporting the development and initiating the implementation of M-E thickness design procedures [20].

Currently, some of SHA's are in the process of piloting M-E flexible pavement design procedures. Recently, Minnesota DOT has proposed a M-E design procedure in which the major design components have been calibrated to regional conditions. A flowchart regarding this design procedure is shown in Figure 4 [21].

Research Work Needed

Based on the literature review presented above the following conclusions are drawn:

- Although great amount of research efforts have been conducted to develop pavement structural performance models in terms of mechanistic-oriented distress such as rutting, or fatigue cracking, less effort has been devoted towards the applicability of the models to various regional and environmental conditions by combining mechanistic and non-mechanistic factors. It is obvious that fatigue and rutting of the flexible pavements are highly affected by non-mechanistic factors such as temperature, specific regional condition, and material properties as well as primary mechanistic factors (i.e. deflection, loading pressure, etc.). The models suggested by many investigators have not had enough success to accommodate systematically both primary mechanistic factors and non-mechanistic factors, which prevented many SHA's from adopting mechanistic-empirical flexible pavement design procedure. Therefore, in brief, there is an urgent need to develop comprehensive load-related pavement distress prediction models that include both primary mechanistic factors and non-mechanistic factors in a reasonable manner, as

pave

appr

M-E

deter

theor

analy

desig

affect

be n

compr

design

pavement design procedure is moving from empirical to mechanistic-empirical approaches.

- M-E design procedures presently suggested by many researchers incorporate deterministic design parameters and simplification of exact formula based on theoretical assumptions such as perfect elasticity, homogeneity, or two-dimensional analysis. The present M-E design procedure cannot prevent the uncertainties from design input variables and pragmatic simplification of the design from significantly affecting the accuracy of design outputs. In conclusion, it is necessary that in order to be more reasonable and practical, M-E design procedures must contain comprehensive reliability techniques to control various uncertainties of pavement design and produce a consistent pavement performance level.

Data Coll

On

pavement

included

- Traff
- Asph
- Cross
- Road
- Paver
- Distr

Table 2 pr

pavement s

Site Select

Bas

The length

presented in

Types of Fa

For

cracking), c

CHAPTER III

FIELD STUDY - DATA COLLECTION

Data Collection Criteria

One of the first tasks of this study was to select test sites from in-service highway pavements in Michigan. A set of criterion for choosing the sites was developed and it included the following variables:

- Traffic volume and load
- Asphalt course thickness
- Cross-sections
- Roadbed type
- Pavement surface age
- Distress(rutting) severity

Table 2 provides a list of the combination of variables used to prioritize the various pavement sections.

Site Selection

Based on the above criteria and variables, thirty-nine test sections were selected. The length of each section ranged from 300 to 500-ft. The locations of these sites are presented in Figure 5. The detailed information of selected sections is shown in Table 3.

Types of Field Data Collected

For each selected pavement section, the distress data (e.g. rut-depth, fatigue cracking), cross-sectional properties, traffic, and deflection data were collected and stored

Table 2. I

Table 2. Pavement Selection Criterion

Selection Criteria	Level
Traffic Volume	Light Medium Heavy
HMAC Thickness	Thin < 3inch Medium ≈ 3 inch ~6 inch Thick > 6inch
Cross-Section	3 layers 4 layers
Roadbed Soil	Stiff Soft
Pavement Age	Less than 3 years since last rehabilitation New construction Old pavement
Pavement Distress (Rutting) Severity	High Medium Low

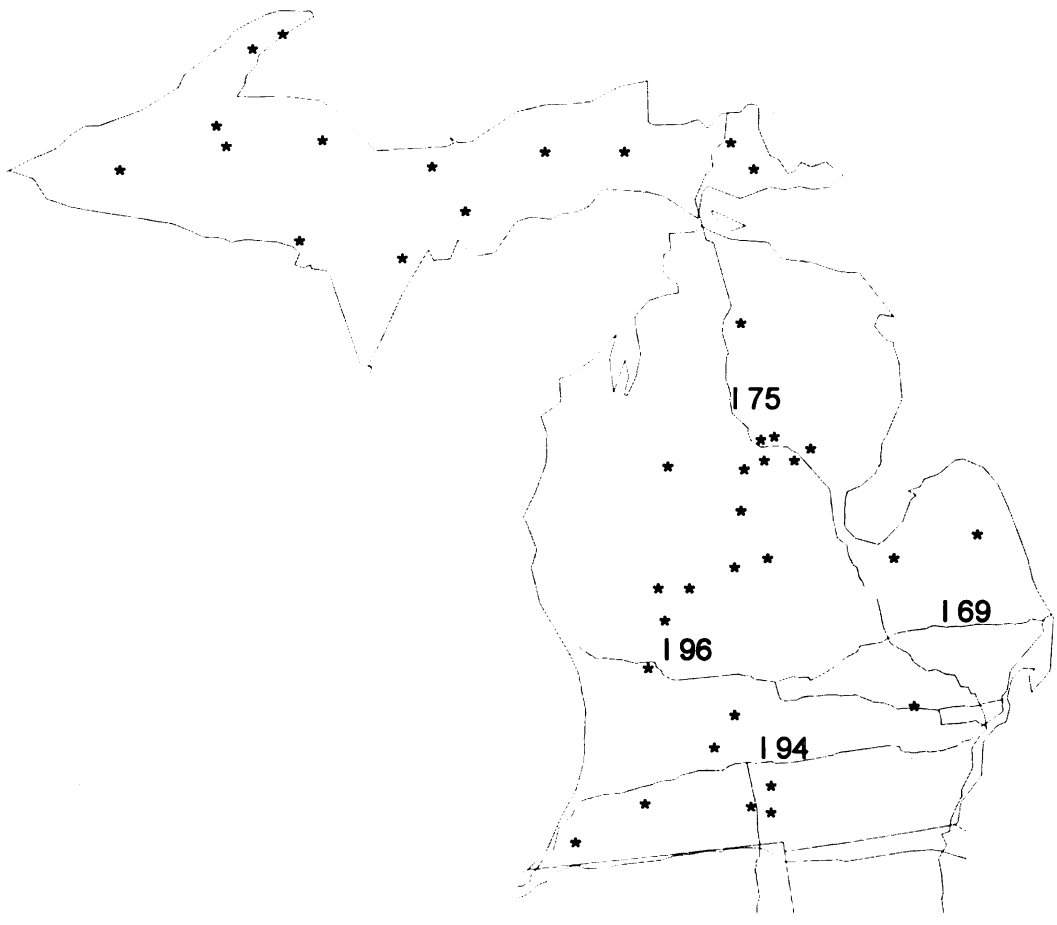

Figure 5 Distribution of Test Sites across the State of Michigan

Table 3

District No.
Superior
Grand
Grand
Grand
North
North
North
North
Bay
Grand
Superior
University
North
Bay
University
North
Grand
Superior
North
North
North
North
Superior
North
North
Southwest
North
North
North
North
Superior
Superior
Superior

Table 3 Summary of Selected Sites

District No.	Code	Control Section	Route	Dir.	Mile Post		Asphalt Grade	1991 Test	1997 Test	1998 Test
					From	To				
Superior	MSU05F	66022	M-28	NB	13.7	13.8	AC2.5			
Grand	MSU06F	34021	M-50	WB	7.4	7.3	AC10			
		34021	M-50	WB	5.3	5.2				
Grand	MSU11F	41051	M-44	EO	4.7	4.8	AC10			
Grand	MSU12F	61152	I-96	EB	1.8	1.9	AC10			
		61152	I-96	EB	2.1	2.2				
North	MSU15F	20016	US-27	SO	2.3	2.4	AC5			
North	MSU16F	83031	US131	NB	2.3	2.4	AC5			
North	MSU18F	20016	US-27	NO	2.3	2.4	AC5			
North	MSU19F	69013	I-75	NB	4.2	4.3	AC5			
		69013	I-75	NB	5.3	5.4				
Bay	MSU21F	74032	M-19	NB	0	0.1	AC10			
		74032	M-19	NB	1.9	2				
Grand	MSU22F	59041	M-82	WB	0.2	2	AC10			
Superior	MSU23F	66023	M-28	EB	7.6	7.7	AC2.5			
University	MSU24F	33011	M-99	NB	4.3	4.6	AC10			
North	MSU25F	83031	US131	SB	2.4	2.3	AC5			
Bay	MSU26F	25102	M-57	EB	2.8	2.9	AC10			
University	MSU29F	23092	M-99	NB	2.5	2.6	AC10			
		23092	M-99	NB	5.8	5.9				
North	MSU30F	69013	I-75	NB	6.7	6.8	AC5			
Grand	MSU32F	59012	US-131	NO	11.2	11.3	AC10			
Superior	MSU34F	17072	M-129	NB	17.3	17.4	AC2.5			
North	MSU35F	16091	I-75	NB	0.9	1	AC5			
		16091	I-75	NB	1.1	1.2				
North	MSU36F	72061	I-75	SO	11.9	12	AC5			
North	MSU37F	72061	I-75	NO	19.3	19.4	AC5			
North	MSU38F	57013	M-66	NB	10.1	10.2	AC5			
Superior	MSU39F	21024	US-2	EB	10.9	11	AC2.5			
North	MSU40F	20015	I-75	NB	8.3	8.4	AC5			
North	MSU41F	20015	I-75	NB	13.8	13.9	AC5			
Southwest	MSU42F	11015	I-94	EB	13.1	13.2	AC10			
North	MSU45F	20014	I-75	NO	4.7	4.8	AC5			
North	MSU46F	40031	M-66	NB	0	0.1	AC5			
North	MSU47F	18041	M-61	EB	8.8	8.9	AC5			
North	MSU49F	72061	I-75	SO	17.2	17.3	AC5			
Superior	MSU50F	28106	M-28	WB	3.3	3.4	AC2.5			
Superior	MSU51F	31095	OLD M-69	SB	9	9.1	AC2.5			
Superior	MSU52F	261004	M-26	NB	0.1	0.2	AC2.5			

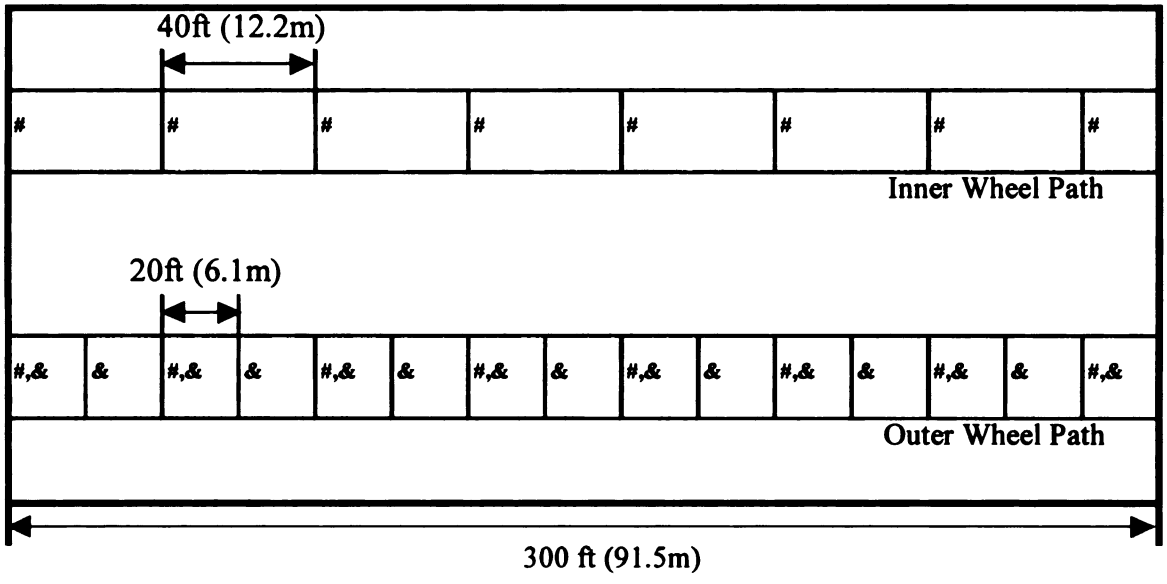

: measurement of rut-depth
&: measurement of deflection using FWD

Figure 6 Description of Typical Test Site

in a co

yearly

- Dis
Measur
0.05inc
for both
study, r
sections

- Cro
Pavemer
this data

- Tra
By revie
obtained.
data for t

- Defl
Nondestr
conducte
in Figure
deflection
inches (cn
the load o
conceptua
locations

- Temp
The air an
FWD. In o
database
temperatur
Table 4.

in a comprehensive database. During the research period, the database was updated on a yearly basis.

- Distress (rutting) data

Measuring the rut-depth, a six-foot long straight-edge leveling rod with an accuracy of 0.05inch (1.27mm) was used. The rut-depth was measured at an interval of 40ft (12.2m) for both inner and outer wheel paths and recorded in inches as shown in Figure 6. In this study, rut-depths of 930 locations were measured on 39 in-service Michigan pavement sections from 1991 to 1998.

- Cross sectional properties.

Pavement cross-sectional data was obtained from the MDOT PMS database. In the event this data was not available, pavement cores were extracted and measured.

- Traffic

By reviewing MDOT data sufficiency books, a set of traffic data for the test sites was obtained. This traffic data includes average daily traffic (ADT) and percent commercial data for the construction or last rehabilitation year of each test site.

- Deflection Data

Nondestructive deflection tests (NDT) using a fall weight deflectometer (FWD) were conducted at uniform interval of 20-ft (6.1m) at the beginning of each section as shown in Figure 6. All tests were conducted on the surface along outer wheel path. The 7 deflection sensors (0 (0), 8 (20.3), 12 (30.5), 18 (45.7), 24 (61), 36 (91.5), 60 (152.4) inches (cm) from the center of loading plate) along outer wheel path were installed, and the load of 9000lb (40kN) was applied on the plate with the radius of 5.91in (15cm). A conceptual drawing is shown in Figure 7. In this study, FWD test was conducted on 930 locations at 39 in-service Michigan pavement sections from 1991 to 1998.

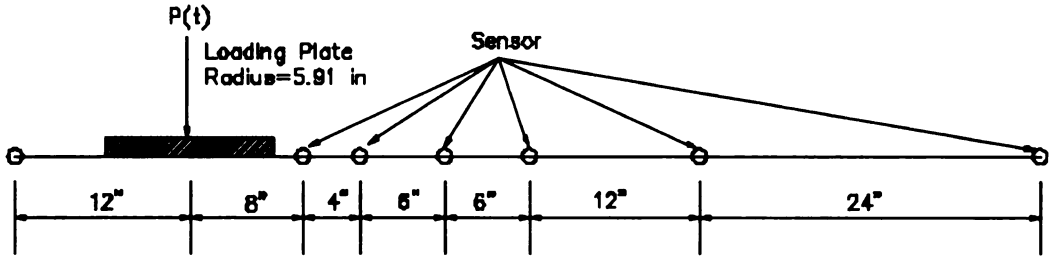

Figure 7 Conceptual Configuration of FWD Test

- Temperature

The air and surface temperature at the test were recorded using a sensor attached to the FWD. In order to obtain comprehensive ambient temperature history of each test site, the database of the department of agriculture was used. From the database, 30 years temperature history data of 27 major cities in Michigan was collected and tabulated in Table 4.

Overvie

T

pavemer

monitor

across th

sections

complen

(GPS) u

second s

are desig

Data is c

Performa

equipme

Manager

which it

DATAP

easy-to-u

Data Acc

T

cross-sec

LTPP_IM

available

Overview of Long Term Pavement Performance (LTPP) Database

The Long Term Pavement Performance (LTPP) is a 20-year study of in-service pavements. It is the largest and most comprehensive pavement study in the world, monitoring more than 2,400 asphalt and portland cement concrete pavement test sections across the United States and Canada. The LTPP program will collect data on pavement sections in the study during the 20-year period. The LTPP program has two complementary experiments to meet the objectives. The General Pavement Studies (GPS) use in-service pavements as originally constructed or after the first overlay. The second set of LTPP experiments is the Specific Pavement Studies (SPS.) These studies are designed to meet LTPP objectives that the GPS experiments cannot completely meet. Data is collected on forms found in the Data Collection Guide for Long Term Pavement Performance and other documents, or in machine-readable form from monitoring equipment. Data collected is available from a database known as the LTPP Information Management System (LTPP-IMS or IMS). Most recently, LTPP is providing the data which it has collected over the past 10 years to the highway community via DATAPAVE, a new software package introduced in 1998 that presents LTPP data on an easy-to-use CD-ROM [22].

Data Acquisition from LTPP Database

Twenty-four GPS sections were selected (Table 5). The data regarding rut-depth, cross-sectional properties, material properties, FWD data, and traffic were extracted from LTPP_IMS using DATAPAVE. The temperature information that is not currently available in DATAPAVE CD-ROM was obtained from a climatic database provided by

Table 4

C
Easte
E
North
North
Soutl
Sout
Soutl
Weste

Table 4 Temperature History of Major Cities in Michigan

Region	City	Ambient Temperature (°F)	Ambient Temperature (°C)
Central Lower	Alma	46.91	8.28
	Gladwin	43.67	6.48
Eastern Central Lower	Badaxe	46.05	7.81
	Sandusky	46.36	7.98
Eastern Upper	Chatham	41.60	5.33
	Grandmar	41.47	5.26
	Newberry	40.55	4.75
North Eastern Lower	Alpena	42.68	5.93
	Easttawa	43.01	6.12
	Garyling	42.52	5.85
North Western Lower	Cheboygan	43.28	6.27
	Eastjordan	44.38	6.88
	Traverse City	44.64	7.02
South Central Lower	Lansing	46.86	8.26
	Battle Creek	48.02	8.90
South Eastern Lower	Detroit	48.57	9.21
	Pontiac	48.37	9.10
	Toledo	48.37	9.10
South Western Lower	Grandrapid	47.75	8.58
	Southbend	49.40	9.67
Western Central Lower	Hart	46.63	8.13
	Muskegon	47.16	8.42
Eastern Upper	Herman	28.66	-1.86
	Houghton	40.01	4.45
	Ironmountain	41.72	5.40
	Ironwood	39.85	4.36
	Stephenson	39.48	4.15

Table 5 Summary of Selected LTPP-GPS Sections
(a)Site Information

Section I.D.	State	Climatic Region	Length of Section (ft)	Interval of Location of FWD Test (ft)	Traffic Open Date	T_{annual} (F)	Kinematic Viscosity (centistoke)
33-1001	NH	Wet Freeze	500	25	81-1-1	46.1	388.5
42-1599	PA	Wet Freeze	500	25	87-7-31	47.8	452
25-1002	MA	Wet Freeze	500	25	82-4-30	47.7	425.5
27-1016	MN	Wet Freeze	500	25	76-1-1	40.4	304.5
27-1019	MN	Wet Freeze	500	25	80-1-1	42.4	461
89-1021	PQ	Wet Freeze	500	25	81-6-1	39.2	159
34-1031	NJ	Wet Freeze	500	25	73-3-31	52.5	438.5
87-1622	ON	Wet Freeze	500	25	76-5-31	41.0	350
84-1684	NB	Wet Freeze	500	25	78-8-31	44.3	210
26-1013	MI	Wet Freeze	500	25	79-12-31	45.6	305
42-1605	PA	Wet Freeze	500	25	71-8-31	50.4	440
8-1053	CO	Dry Freeze	500	25	84-2-1	49.1	240
26-1001	MI	Wet Freeze	500	25	71-8-31	43.9	315
51-1464	VA	Wet Freeze	500	25	79-4-30	58.0	424
87-1620	ON	Wet Freeze	500	25	81-5-31	41.0	350
34-1011	NJ	Wet Freeze	500	25	70-2-28	52.7	356
25-1004	MA	Wet Freeze	500	25	74-6-30	51.4	390
30-8129	MT	Dry Freeze	500	25	88-6-1	41.4	356
29-1005	MO	Wet Freeze	500	25	74-5-1	51.0	389
30-7066	MT	Dry Freeze	500	25	81-6-1	46.4	325
32-1021	NV	Dry Freeze	500	25	81-3-1	54.9	460
29-1002	MO	Wet Freeze	500	25	86-4-1	54.8	381.5
23-1001	ME	Wet Freeze	500	25	72-11-1	44.0	367.1
2-1002	AK	Wet Freeze	500	25	84-10-1	40.8	140

(b) Summary of Preliminary Analysis of Data from Selected LTPP-GPS Sections

Section I.D	Cumulative Traffic	AC	Base	Subbase	Corrected Modulus of	Average Modulus of	Average Modulus of	Average Modulus of Subgrade	Surface Deflection	Strain at the top of Base	Strain at the top of	Average Rut-Depth

(b) Summary of Preliminary Analysis of Data from Selected LTPP-GPS Sections

Section I.D.	Cumulative Traffic (ESAL)	AC Thickness	Base Thickness	Subbase Thickness	Corrected Modulus of AC	Average Modulus of Base	Average Modulus of Subbase	Average Modulus of Subgrade (C=0.33)	Surface Deflection	Strain at the top of Base	Strain at the top of Subgrade	Average Rut-Depth Measured
33-1001	1566000	8.4	33		1078220	25562		14233	8.997E-03	2.498E-04	7.413E-05	0.24
42-1599	1010002	12.3	12		897766	11188		17982	7.387E-03	2.058E-04	6.921E-05	0.23
25-1002	1779457	7.8	4	8.4	566518	199528	7752	11133	1.339E-02	1.392E-04	1.763E-04	0.2
27-1016	433000	3	6.5		516584	45754		11281	2.627E-02	9.249E-04	1.060E-03	0.29
27-1019	645177	5	6.4		185922	69946		7398	2.859E-02	6.009E-04	9.240E-04	0.23
89-1021	3915296	6	15		844822	31260		8285	1.710E-02	4.344E-04	3.029E-04	0.46
34-1031	4418550	7.3	11		336859	13332		10747	2.060E-02	8.164E-04	3.780E-04	0.35
87-1622	3749000	6	6.6	26.3	420336	41541	22609	10392	1.587E-02	5.488E-04	1.395E-04	0.24
84-1684	4325000	5	3.3	21.4	392794	44709	18979	6881	2.406E-02	6.439E-04	3.036E-04	0.52
26-1013	1961000	6.7	23.4		471915	25745		10994	1.543E-02	5.786E-04	1.888E-04	0.22
42-1605	4142000	8.1	16.2		895022	14378		18582	1.038E-02	3.710E-04	1.153E-04	0.59
8-1053	524000	4.6	28		536711	38572		6996	1.813E-02	7.050E-04	2.004E-04	0.35
26-1001	346000	3	10		808061	43223		9828	2.383E-02	8.395E-04	7.199E-04	0.17
51-1464	6988000	8.4	10.5		474508	97116		16270	9.439E-03	2.158E-04	1.940E-04	0.27
87-1620	1924000	5	29.6		1438520	21922		6164	1.841E-02	4.826E-04	1.986E-04	0.36
34-1011	2613000	9	31.1		547759	23268		14813	1.075E-02	3.587E-04	8.780E-05	0.22
25-1004	3096000	9.6	25.6		662770	19437		12974	1.084E-02	3.038E-04	1.022E-04	0.31
30-8129	249000	3.2	22.8		989148	21014		12332	2.202E-02	1.103E-03	2.790E-04	0.27
29-1005	1752000	8.9	39		373782	47657		13393	9.443E-03	3.352E-04	6.390E-05	0.21
30-7066	1989000	5.4	18.9		274101	20532		9488	2.405E-02	1.129E-03	3.669E-04	0.33
32-1021	136000	7.8	6		1288722	3124		8257	1.633E-02	6.318E-04	1.603E-04	0.34
29-1002	50000	7	4		1178206	11517		8329	1.707E-02	3.840E-04	3.201E-04	0.09
23-1001	5986000	8.9	12		617317	14887		11876	1.340E-02	3.905E-04	1.974E-04	0.35
2-1002	299000	3.3	6	7.5	341564	53889	51700	16990	1.702E-02	8.714E-04	4.026E-04	0.19

the Nati

from 30

Prelimir

- **Bac**

The bac

elastic m

WESDE

lowest e

reasonab

machine.

individua

individua

individua

be noted

Accordin

usually g

Design (

comparab

adjusted t

the backc

number is

project [1

the National Oceanic and Atmospheric Administration (NOAA). The averaged values from 30 years temperature histories at same coordinates of the test sites were used.

Preliminary Data Analysis

- **Backcalculation**

The backcalculation program MICHBACK was used to back-calculate pavement layer elastic moduli [23]. According to a report of LTPP-GPS data analysis, MODCOMP3.6, WESDEF, and MICHBACK produced most reasonable solutions of layer moduli with lowest errors [24]. Thus, the moduli back-calculated by MICHBACK can be considered reasonable. The deflections in the Michigan database measured by KUAB, a FWD machine, were normalized to a 9000lb (40kN) load level and then backcalculated on an individual drop basis, while that of LTPP-GPS database were backclaculated on an individual drop basis without the normalization. The backcalculated moduli on an individual drop basis were, then, filtered and averaged on a per test site basis. It is should be noted that more than 15 individual drops of FWD were conducted at each test section. According to Elliott and Darter et al., the backcalualted or in-situ moduli of subgrade are usually greater than the laboratory moduli that are used as standard values in AASHTO Design Guide [25]. In order for the M-E design procedure to be consistent and comparable with the AASHTO Design Guide, all the backcalulated moduli should be adjusted to values that are consistent with laboratory determined moduli. In this study, the backclaulated moduli by MICHBACK was multiplied by a factor of 0.33. This number is recommended in AASHTO Design Guide and the final report of NCHRP 1-32 project [16,26].

Temper

In an eff

adjust th

mid-dep

parts: 1

backcalc

In

by Michi

estimatin

based on

at MSU

Thus, in

with the

T_{pav}

where:

T_{pav}

T_{surf}

h

Time

The foll

modulus

Temperature Correction Procedure

In an effort to obtain effective annual layer moduli of a flexible pavement, the process to adjust the moduli to a reference temperature was applied. This procedure is based on the mid-depth temperature of an asphaltic layer as an effective temperature and has two parts: 1) prediction of the AC mid-depth temperature and 2) adjustment of the backcalculated AC modulus to a reference temperature.

In order to calculate the AC mid-depth temperature, a new procedure developed by Michigan State University was used [27]. The procedure suggests two approaches for estimating the AC mid-depth temperature: (1) use a finite difference method (FDM) based on heat transfer theory and (2) use a statistical model. A research study conducted at MSU shows that the two methods produce similar results with the MDOT database. Thus, in this study, the statistical equation was used to avoid the complexity associated with the FDM procedure. The equation is as follows [27]:

$$T_{pav} = T_{surf} + \sin(-6.3252Time + 5.0967) * (-0.8767h - 0.2788h^2 + 0.0321h^3) \quad (27)$$

where:

T_{pav}	=	AC pavement temperature at a depth, °C,
T_{surf}	=	AC pavement temperature at surface, °C,
h	=	pavement depth, in., and
Time	=	Time at the temperature measurement (e.g. 1:30PM → 13.5/24 = 0.5625)

The following equation, developed recently by Park, et al., was used to adjust the AC modulus to a reference temperature of 20 °C [27]:

$$E_{20} = 10^{0.0224(T-20)} * E_T \quad (28)$$

where :

E_{20}

E_T

T

Table 6

• **Prin**

With the

structura

was con

available

and nonli

pavement

primary

[28]. The

• **Estim**

In general

classifica

18,000lb (

estimating

relatively

more com

where :

E_{20}	=	adjusted AC modulus to the reference temperature of 20 °C,
E_T	=	backcalculated AC modulus from FWD testing at temperature T (°C), and
T	=	the mid-depth temperature (°C) of the AC layer at the time of FWD testing.

Table 6 shows backcalculated and adjusted moduli of pavement layers in the test sites.

- **Primary Pavement Responses**

With the backcalculated and temperature-adjusted elastic moduli of pavement layers, a structural analysis of the pavement using the mechanistic-based load-deformation model was conducted to calculate the critical pavement responses. There are many models available based on linear layered-elastic, nonlinear layered-elastic, linear finite element, and nonlinear finite element theory. In this study, CHEVRONX, a computer program for pavement analysis based on a linear layered-elastic theory was used to calculate the primary pavement responses because of its relative simplicity and excellent accuracy [28]. The pavement responses are summarized in Table 7.

- **Estimation of Cumulative Traffic Volume**

In general, traffic volume is usually represented in terms of particular vehicle classifications and equivalent single axle loads (ESALs). In Michigan, standard EASL is 18,000lb (80kN) as developed at the AASHO Road Test. The current MDOT method for estimating the number of 18-kips ESALs over the design period for the highway is relatively simplistic and easy to use, while the 1993 AASHTO Design Guide adopts a more complex procedure that utilize axle load distributions and vehicle classifications.

Table 6

TESTS I

Code
MSU05F
MSU06F
MSU12F
MSU15F
MSU16F
MSU18F
MSU19F
MSU21F
MSU22F-1
MSU22F-2
MSU23F
MSU24F
MSU25F
MSU26F
MSU29F
MSU30F
MSU32F
MSU34F
MSU35F
MSU36F
MSU37F
MSU38F
MSU39F
MSU40F
MSU41F
MSU42F
MSU45F
MSU46F
MSU47F

Table 6 Summary of Backcalculated Moduli of Test Sites

TESTS IN 1991

Code	Cross Section (inch)			Moduli (psi)					Temperature (F)		Correction Factor
	AC	Base	Subbase	AC	AC (corrected)	Base	Subbase	Subgrage	Surface	Mid-Depth	
MSU05F	4	7	12	659062	545313	66294	15669	5559	64	61	0.827
MSU06F	4	12	22	469419	1294039	35324	12300	11060	106	103	2.757
	5	12	22	337538	682417	29943	8123	7053	96	93	2.022
MSU12F	5.5	8	32	580761	822575	26448	60708	19853	84	80	1.416
	5.5	8	32	563315	975080	28067	52935	14271	91	87	1.731
MSU15F	6.4	8	28	652992	830492	53329	46313	9801	81	76	1.272
MSU16F	5	8	28	544164	981022	35649	32441	8455	92	89	1.803
MSU18F	6.4	8	28	748854	478804	90748	22626	7989	57	52	0.639
MSU19F	4.8	12	12	506129	999114	72798	81942	17807	95	92	1.974
	4.5	12	12	452136	1067515	70331	83556	14915	101	98	2.361
MSU21F	3	7.5	10	352397	1113975	69039	5435	9257	110	108	3.161
	2.7	8	10	381159	1284082	53845	6830	7668	112	110	3.369
MSU22F-1	3.5	10		729997	2218024	134133		8786	109	107	3.038
MSU22F-2	3.5	10		820202	2715810	54417		7782	112	110	3.311
MSU23F	4.5	10	21	572524	807046	38035	28698	7264	83	80	1.410
MSU24F	12.5	14		555825	916862	9617		18331	94	85	1.650
MSU25F	5	8	28	899805	1767789	136776	28920	10325	95	92	1.965
MSU26F	3.5	11	20	485418	1107431	42816	13257	10041	99	97	2.281
MSU29F	14.5	11.5		564251	734914	16547		8059	86	77	1.302
	12	10		354768	903834	7687		19885	109	101	2.548
MSU30F	7.5	11		297639	401942	47872		16855	84	78	1.350
MSU32F	7	6.2	18	355962	862669	173118	25177	10933	104	99	2.423
MSU34F	5.5	9.5		665394	749379	18650		4731	76	72	1.126
MSU35F	6.3	6	18	556688	1122519	32061	83579	13022	97	92	2.016
	7.5	6	24	396153	1064152	21311	66269	9416	108	102	2.686
MSU36F	8.2	22		689328	1088132	32635		11532	90	84	1.579
MSU37F	6	8	28	1064052	1366377	134013	24903	11102	81	77	1.284
MSU38F	8	10		959568	1706258	31822		14506	94	88	1.778
MSU39F	6.5	20		759473	543263	43178		10194	61	56	0.715
MSU40F	7.9	11		536314	658549	66606		17353	81	75	1.228
MSU41F	8	11		482834	702515	31256		18867	87	81	1.455
MSU42F	10	12	25	311297	531344	94529	30279	11777	94	87	1.707
MSU45F	7.9	11		466854	430433	28789		13880	71	65	0.922
MSU46F	8.5	10		539247	1126262	49657		11741	100	94	2.089
MSU47F	4	10	15	582286	784173	53878	24205	11782	81	78	1.347

Table 6

TESTS

Code
MSU11F
MSU15F
MSU18F
MSU22F-
MSU22F-
MSU23F
MSU32F
MSU34F
MSU36F
MSU37F
MSU39F
MSU45F
MSU47F
MSU50F
MSU51F
MSU52F

TESTS

Code
MSU15F
MSU18F
MSU22F-
MSU22F-
MSU23F
MSU32F
MSU34F
MSU36F
MSU39F
MSU50F
MSU51F
MSU52F

Table 6 (cont'd)

TESTS IN 1997

Code	Cross Section (inch)			Moduli (psi)					Temperature (F)		Correction Factor
	AC	Base	Subbase	AC	AC (corrected)	Base	Subbase	Subgrage	Surface	Mid-Depth	
MSU11F	9.5	27		342272	741636	32412		10991	102	95	2.167
MSU15F	6.4	8	28	657559	610202	37895	86289	9045	70	65	0.928
MSU18F	6.4	8	28	490866	606661	63153	43751	7300	80	75	1.236
MSU22F-1	3.5	10		619881	1778544	154876		9650	107	105	2.869
MSU22F-2	3.5	10		402914	1001720	96239		7839	102	100	2.486
MSU23F	4.5	10	21	341017	1202550	52293	32897	6664	115	112	3.526
MSU32F	7	6.2	18	741688	1311514	107047	36438	10679	93	88	1.768
MSU34F	5.5	9.5		373937	364921	36138		4488	71	67	0.976
MSU36F	8.2	22		453639	1069519	49193		10850	104	98	2.358
MSU37F	6	8	28	565343	1181613	42985	47241	8519	98	94	2.090
MSU39F	6.5	20		245517	619633	61989		9906	105	100	2.524
MSU45F	7.9	11		269367	639346	57715		13954	104	98	2.374
MSU49F	8.2	20		398914	648007	68548		15809	91	85	1.624
MSU50F	5.8	5.5	20	438141	504126	47779	40177	7552	77	73	1.151
MSU51F	4.5	9	18	442553	442320	44472	19072	30933	71	68	0.999
MSU52F	5.5	20		821372	1098573	26611		15822	82	78	1.337

TESTS IN 1998

Code	Cross Section (inch)			Moduli (psi)					Temperature (F)		Correction Factor
	AC	Base	Subbase	AC	AC (corrected)	Base	Subbase	Subgrage	Surface	Mid-Depth	
MSU15F	6.4	8	28	326197	652424	65547	54800	9361	96.8	92	2.000
MSU18F	6.4	8	28	280745	655484	94619	37111	7440	102	98	2.335
MSU22F-1	3.5	10		882305	1989948	88425		8372	99	96	2.255
MSU22F-2	3.5	10		1023133	2191568	160818		9316	97	95	2.142
MSU23F	4.5	10	21	249072	829398	62177	28369	6556	113	110	3.330
MSU32F	7	6.2	18	590779	1164838	109446	55602	10991	97	92	1.972
MSU34F	5.5	9.5		399242	339549	39136		4537	66	62	0.850
MSU36F	8.2	22		500926	823098	43719		11202	91	85	1.643
MSU39F	6.5	20		229717	692471	60656		9493	111.2	107	3.014
MSU50F	5.8	5.5	20	373686	408349	61543	36079	7669	75.2	71	1.093
MSU51F	4.5	9	18	214071	579957	49911	21145	31273	105.8	103	2.709
MSU52F	5.5	20		795964	1393671	26878		16214	91.4	88	1.751

Table 7

Tests ir

Coc
MSU
MSU
MSU1
MSU1
MSU1
MSU1
MSU1
MSU2
MSU22
MSU22
MSU2
MSU2
MSU2
MSU2
MSU2
MSU3
MSU32
MSU34
MSU35
MSU36
MSU37
MSU38
MSU39
MSU40
MSU41
MSU42
MSU45
MSU46
MSU47

Table 7 Summary of Pavement Responses in Test Sites

Tests in 1991

Code	Pavement Responses		
	Surface Deflection (in)	Vertical Compressive Strain at the top of Base	Vertical Compressive Strain at the top of Subgrade
MSU05F	2.713E-02	5.930E-04	4.534E-04
MSU06F	2.106E-02	9.002E-04	1.591E-04
	2.617E-02	9.003E-04	2.081E-04
MSU12F	9.966E-03	6.297E-04	6.070E-05
	1.054E-02	5.481E-04	7.194E-05
MSU15F	1.085E-02	3.575E-04	9.027E-05
MSU16F	1.463E-02	5.262E-04	1.253E-04
MSU18F	1.462E-02	3.356E-04	1.215E-04
MSU19F	9.928E-03	3.790E-04	8.419E-05
	1.122E-02	3.970E-04	9.169E-05
MSU21F	2.473E-02	5.410E-04	3.355E-04
	2.774E-02	6.564E-04	4.324E-04
MSU22F-1	1.488E-02	2.454E-04	3.366E-04
MSU22F-2	1.943E-02	3.525E-04	4.582E-04
MSU23F	1.789E-02	6.388E-04	1.821E-04
MSU24F	8.342E-03	2.575E-04	6.958E-05
MSU25F	1.014E-02	1.917E-04	8.920E-05
MSU26F	1.919E-02	6.508E-04	1.802E-04
MSU29F	1.178E-02	1.758E-04	1.365E-04
	8.424E-03	3.220E-04	7.418E-05
MSU30F	1.252E-02	4.410E-04	2.734E-04
MSU32F	1.083E-02	1.585E-04	1.262E-04
MSU34F	3.265E-02	6.971E-04	7.206E-04
MSU35F	9.683E-03	4.141E-04	1.144E-04
	1.046E-02	4.105E-04	9.750E-05
MSU36F	1.059E-02	2.680E-04	1.297E-04
MSU37F	9.898E-03	1.821E-04	8.376E-05
MSU38F	9.308E-03	1.998E-04	1.594E-04
MSU39F	1.443E-02	4.907E-04	2.116E-04
MSU40F	9.788E-03	2.726E-04	2.050E-04
MSU41F	1.052E-02	3.667E-04	1.994E-04
MSU42F	8.876E-03	1.842E-04	6.515E-05
MSU45F	1.467E-02	5.139E-04	2.974E-04
MSU46F	1.080E-02	2.009E-04	1.993E-04
MSU47F	1.577E-02	5.972E-04	1.986E-04

Table 7 (cont'd)
Tests in 1997

Code	Pavement Responses		
	Surface Deflection (in)	Vertical Compressive Strain at the top of Base	Vertical Compressive Strain at the top of Subgrade
MSU11F	1.079E-02	2.770E-04	1.092E-04
MSU15F	1.125E-02	5.202E-04	7.976E-05
MSU18F	1.301E-02	3.796E-04	1.056E-04
MSU22F-1	1.400E-02	2.435E-04	3.253E-04
MSU22F-2	1.954E-02	4.070E-04	4.927E-04
MSU23F	1.567E-02	4.258E-04	1.621E-04
MSU32F	1.011E-02	1.712E-04	1.217E-04
MSU34F	3.488E-02	7.573E-04	8.480E-04
MSU36F	1.001E-02	2.296E-04	1.253E-04
MSU37F	1.138E-02	3.510E-04	9.640E-05
MSU39F	1.265E-02	3.692E-04	1.817E-04
MSU45F	1.157E-02	1.203E-03	2.397E-04
MSU49F	8.877E-03	2.623E-04	1.207E-04
MSU50F	1.637E-02	5.137E-04	1.941E-04
MSU51F	1.308E-02	7.498E-04	1.028E-04
MSU52F	1.421E-02	5.017E-04	1.809E-04

Tests in 1998

Code	Pavement Responses		
	Surface Deflection (in)	Vertical Compressive Strain at the top of Base	Vertical Compressive Strain at the top of Subgrade
MSU15F	1.073E-02	3.579E-04	8.645E-05
MSU18F	1.225E-02	2.837E-04	1.026E-04
MSU22F-1	1.750E-02	3.316E-04	4.239E-04
MSU22F-2	1.374E-02	2.237E-04	3.068E-04
MSU23F	1.654E-02	4.615E-04	1.707E-04
MSU32F	9.179E-03	1.821E-04	1.100E-04
MSU34F	3.408E-02	7.487E-04	8.238E-04
MSU36F	1.068E-02	2.832E-04	1.348E-04
MSU39F	1.251E-02	3.524E-04	1.793E-04
MSU50F	1.695E-02	4.996E-04	2.009E-04
MSU51F	1.223E-02	6.161E-04	9.583E-05
MSU52F	1.187E-02	4.329E-04	1.625E-04

The c

terms

1) Ini
2) Ini
3) Dir
4) Tru

In this

lanes i

5) Gro

where:

r
n

In this s

Michiga

6) Truc

In Mich

In this st

Given th

of 18-kip

The cum

Table 9 s

in this ch

model in

The current MDOT technique for estimating traffic volume during a design period in terms of ESALs requires the following inputs [12];

1) Initial Average Daily Traffic (ADT_o)
2) Initial Proportion of Trucks in ADT_o (Percent Commercial: PCOM)
3) Directional Distribution Factor (DDF)
4) Truck lane Distribution Factor (LDF)

In this study, the factor is assumed to be 1.0 for one lane in one direction and 0.9 for two lanes in one direction, as it is in MODT practice.

5) Growth Factor of Trucks (GF): this can be calculated as follows [16];

$$GF = \frac{\left[(1+r)^n - 1\right]}{r} \tag{29}$$

where:

r	=	annual growth rate (a proportion), and
n	=	design period, years

In this study, annual growth rates for all test sections are assumed to be 1.5% (for local Michigan road) or 2% (for interstate).

6) Truck Equivalency Factor (TEF):

In Michigan, the truck equivalency factor of 0.57 (SN=6) or 0.59 (SN=5) has been used. In this study, the mean truck equivalency factor of 0.58 was used for all test sections.

Given these inputs, the following equation was used to estimate the cumulative number of 18-kip ESAL for given performance period as follows

$$\text{Cum. ESAL} = (ADT_o)\,(PCOM)(LDF)(DDF)(GF)(TEF) \tag{30}$$

The cumulative ESAL estimated by equation 24 for all test sections is shown in Table 8. Table 9 shows the summary of statistics of the variables that were preliminarily analyzed in this chapter. These variables were incorporated in the calibration of the existing rutting model in MICHPAVE, which will be presented in next chapter.

Table

Co
MSU(
MSU(
MSU:
MSU1
MSU1
MSU1
MSU1
MSU1
MSU2
MSU2:
MSU23
MSU24
MSU25
MSU26
MSU29
MSU30
MSU32
MSU34
MSU35
MSU36
MSU37
MSU38
MSU39
MSU40
MSU41
MSU42
MSU45
MSU46
MSU47
MSU49
MSU50
MSU51
MSU52

Table 8 Summary of Traffic in Test Sites

Code	Construction or Last Rehabilitation Date	Initial ADT	% Commercial	1991 Cum. Traffic	1997 Cum. Traffic	1998 Cum. Traffic
MSU05F	1965	550	10	366933		
MSU06F	1976	700	9	222491		
MSU11F	1979	7000	5		1518160	
MSU12F	1961	1900	9	1358927		
MSU15F	1977	2300	18	1354130	2026646	2144690
MSU16F	1966	800	5	254574		
MSU18F	1977	2300	18	1354130	2026646	2144690
MSU19F	1980	1600	7	281283		
MSU21F	1984	700	10	108519		
MSU22F	1963	2000	7	1021962	1302089	1351258
MSU23F	1984	600	13	120922	235087	255126
MSU24F	1978	800	12	289338		
MSU25F	1966	800	5	254574		
MSU26F	1975	2275	10	863654		
MSU29F	1980	1500	10	376718		
MSU30F	1980	1600	7	281283		
MSU32F	1980	1750	6	263703	426817	455448
MSU34F	1977	1000	6	196251	293717	310825
MSU35F	1977	1450	8	379418		
MSU36F	1985	3051	12	482838	1010793	1103463
MSU37F	1985	3051	12	482838	1010793	
MSU38F	1980	450	10	113015		
MSU39F	1984	1550	11	264322	513876	557679
MSU40F	1980	2150	9	485966		
MSU41F	1979	1600	12	530078		
MSU42F	1979	5250	19	2753922		
MSU45F	1979	3000	11	911072	1431408	
MSU46F	1980	400	10	100458		
MSU47F	1971	400	12	234973		
MSU49F	1979	1550	13		874027	
MSU50F	1993	2800	7		169745	213784
MSU51F	1993	800	8		55427	69807
MSU52F	1985	11125	3		921425	1005901

Table 9 Summary of Statistics of Analyzed Variables

(a) Data from '91 and 97' Field Observation in Michigan

Table 9 Summary of Statistics of Analyzed Variables

(a) Data from '91 and 97' Field Observation in Michigan

	AC Thickness (in)	Base Thickness (in)	Subbase Thickness (in)	AC Modulus (psi)	Base Modulus (psi)	Subbase Modulus (psi)	Subgrade Modulus (psi)	Annual Ambient Temperature (F)	Average Rut-Depth (in)	Traffic (ESAL)
Mean	6.34	11.04	21.64	823,442	57,070	37,858	11,605	43.90	0.203	660,510
Stdev	2.44	4.71	6.69	466,998	36,992	24,533	4,792	2.53	0.098	586,431
Max	14.50	27.00	32.00	2,699,344	173,118	86,289	30,933	49.40	0.538	2,753,922
Min	2.70	5.50	10.00	301,277	7,687	5,435	4,488	40.00	0.045	55,427

(b) Data from '98 Field Observation in Michigan

	AC Thickness (in)	Base Thickness (in)	Subbase Thickness (in)	AC Modulus (psi)	Base Modulus (psi)	Subbase Modulus (psi)	Subgrade Modulus (psi)	Annual Ambient Temperature (F)	Average Rut-Depth (in)	Traffic (ESAL)
Mean	5.81	12.17	22.17	847,056	69,995	38,851	11,120	42.69	0.215	883,900
Stdev	1.54	5.96	4.67	558,773	35,849	13,922	6,723	2.58	0.135	675,780
Max	8.20	22.00	28.00	2,069,484	160,818	55,602	31,273	46.90	0.507	2,144,690
Min	3.50	5.50	18.00	277,594	26,878	21,145	4,537	39.99	0.071	69,807

Table 9 (cont'd)

Table 9 (cont'd)

(c) Data from LTPP-GPS Database

	AC Thickness (in)	Base Thickness (in)	Subbase Thickness (in)	AC Modulus (psi)	Base Modulus (psi)	Subbase Modulus (psi)	Subgrade Modulus (psi)	Annual Ambient Temperature (F)	Average Rut-Depth (in)	Traffic (ESAL)
Mean	6.65	15.87	15.90	672,414	39,129	25,260	11,484	46,94	0.315	2,245,687
Stdev	2.40	10.67	9.40	338,557	40,200	18,727	3,594	5.353	0.093	1,947,070
Max	12.30	39.00	26.30	1,438,520	199,528	51,700	18,582	58.03	0.544	6,988,000
Min	2.40	3.30	7.50	185,922	3,124	7,752	6,164	39.16	0.140	50,000

Vali

mech

prope

total r

layers

where

PD_1

PD_2

PD_3

The abb

existing

the traff

rut pred

MDOT d

Table 10

CHAPTER IV

MODEL DEVLOPEMENT AND SENSITIVITY ANALYSIS

Validation of Existing Rut Prediction Model

The existing rut model in MICHPAVE predicts rut-depth as a function of various mechanistic and empirical parameters including primary pavement responses, material properties, cross-sectional properties, environmental conditions, and traffic volume. The total rut-depth is calculated by integrating permanent deformations of different pavement layers. The general format of the model is expressed as follows:

$$\text{Total Rut-Depth} = PD_1 + PD_2 + PD_3 \tag{31}$$

where :

PD_1 = permanent deformation of AC surface layer,
= f_{PD_1} (AV,AAT,KV,ESAL,SD,CS,T_{AC}),
PD_2 = permanent deformation of base and subbase layer,
= f_{PD_2} (MR_B,MR_{SB},SD,ESAL,T_B,T_{SB}), and
PD_3 = permanent deformation of subgrade.
= f_{PD_3} (ESAL,M_{RB}, T_B,T_{SB}, T_{AC})

The abbreviations PD_1, PD_2, and PD_3 have been described previously in equation 25. The existing rut prediction model was evaluated using the field data, as obtained in 1997 and the traffic volume projected up to the testing date. Among the input variables for existing rut prediction model, air void and kinematic viscosity which are not available in the MDOT database were assumed based on engineering judgement and are summarized in Table 10.

Table 10 Assumptions for Kinematic Viscosity and Air Void

MDOT Region	Superior	North	Others
Asphalt Grade	AC2.5	AC5	AC10
Kinematic Viscosity (Centistoke)	159	212	270
Air Void (%)	4	4	4

The comparison between predicted rut-depths and observed rut-depth is presented in Figure 8. 32 data points out of 69 test points plotted outside the ±0.1 inch (0.25cm) of the deviation. This difference was statistically significant and warrants calibration.

Proposed Rut Prediction Model

There is an implicit assumption in statistical model development that the variables that predict the dependent variable are mutually independent. When linear combinations of independent variables are highly correlated, multicollinearity exists. Hence, in engineering practice, when building performance models based on statistical regression, mutually less correlated variables should be selected in the process of modeling. The existing rut prediction model includes 12 independent variables to predict a dependent variable of the rut-depth. Some of these variables which have the same mechanistic origins are highly correlated and suspected to result in multicollinearity. For example the relationship between surface deflection and AC thickness, kinematic viscosity and AC modulus or kinematic viscosity and annual ambient temperature. Thus, they must be rearranged to clearly identify their effects and reasonable contributions to the model without introducing multicollinearity.

Framework for Calibration and Modification of Rut Prediction Model

The first step was to select variables used in the format of the new model and the second step was to develop a conceptual form. Based on these two steps, coefficients of the regression were determined through the calibration procedure described in Figure 1.

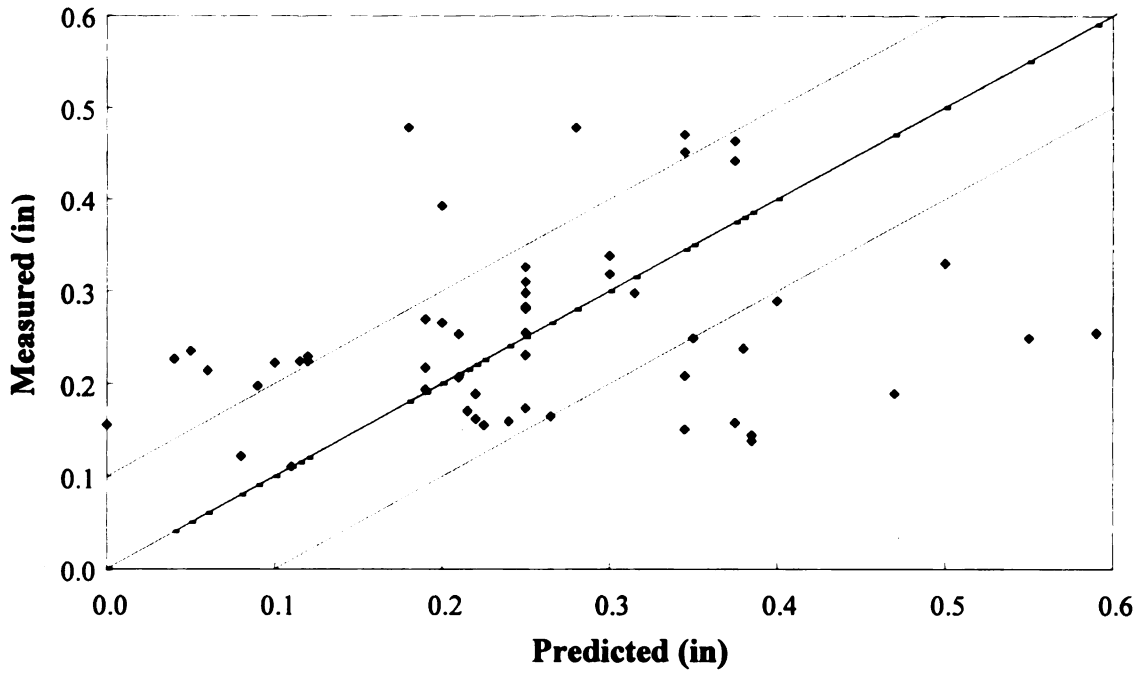

Figure 8 Measured vs. Predicted Rut-Depth Using Existing Model

Variable Selection

With respect to mechanistic responses, two factors must be present in the rutting prediction model in order to characterize the mechanism; vertical permanent strains of the pavement layers and the number of load applications. Typically, these two factors have been key components of all the models that have been developed in the past. In addition, environmental conditions should be considered to explain regional differences of rutting rate with traffic. A correlation matrix was developed using SPSS [29] to investigate the impact of pavement response, environmental condition and traffic on rut-depth based on field data (refer to table 11).

Considering mechanistic and statistical relationships between rut-depth and all variables affecting pavement performance, the following variables were selected for building a rutting prediction model;

SD	:	Pavement surface deflection (in.),
KV	:	Kinematic viscosity (centistroke),
T_{annual}	:	Annual ambient temperature (^{o}F),
H_{AC}	:	Thickness of asphalt concrete (in.),
N	:	Cumulative traffic volume (ESAL),
$\varepsilon_{v,base}$	:	Vertical compressive strain at the top of base layer (10^{-3}),
$\varepsilon_{v,SG}$	:	Vertical compressive strain at the top of subgrade (10^{-3}),
E_{AC}	:	Resilient modulus of asphalt concrete (psi), and
E_{SG}	:	Resilient modulus of subgrade (psi).

Basic Concept of the Model

As outlined previously, the existing multiple regression analysis assumes that the variables have only linear relationships with each other. Theoretical considerations or model formulation may suggest otherwise. A reasonable conceptual model that consists of two categories: non-mechanistic (or empirical) function and mechanistic function was developed:

Table 11 Correlation Matrix of Pavement Variables

	Kinematic Viscosity	T_{AC}	T_{Base}	E_{AC}	E_{Base}	E_{SG}	Compressive strain - Subgrade	Compressive strain - Base	Surface Deflection	T_{annual}	Traffic	Rutmax	Rutave
Kinematic Viscosity	1.000												
T_{AC}	0.131	1.000											
T_{Base}	-0.088	0.303	1.000										
E_{AC}	0.326	-0.386	-0.143	1.000									
E_{Base}	0.201	-0.314	-0.216	0.384	1.000								
E_{SG}	0.041	0.267	0.133	-0.177	-0.167	1.000							
Compressive strain - Subgrade	-0.174	-0.358	-0.111	0.124	0.001	-0.441	1.000						
Compressive strain - Base	-0.195	-0.402	-0.132	-0.319	-0.388	-0.025	0.335	1.000					
Surface Deflection	-0.152	-0.522	-0.185	-0.022	-0.112	-0.527	0.838	0.570	1.000				
T_{annual}	0.921	0.222	-0.049	0.254	0.170	0.129	-0.208	-0.228	-0.224	1.000			
Traffic	0.255	0.157	0.123	-0.092	0.103	-0.054	-0.222	-0.093	-0.293	0.270	1.000		
Rutmax	0.432	-0.429	-0.115	0.374	0.094	-0.146	0.231	0.227	0.255	0.407	0.219	1.000	
Rutave	0.357	-0.375	-0.112	0.327	0.112	-0.096	0.205	0.171	0.158	0.379	0.256	0.934	1.000

$$\text{Rut Depth} = g(\underline{x}) * f(\underline{x}') \quad (32)$$

where:

$g(\underline{x})$ = non-mechanistic function considering the adjustment of theoretical pavement rutting mechanism to field conditions based on statistically significant variables for pavement rutting, and

$f(\underline{x}')$ = mechanistic function reflecting basic mechanism for pavement rutting.

The $g(\underline{x})$ may be modified with varying regions and is assumed as a deterministic number based on engineering judgement.

Nonlinear Regression Approach

Using the conceptual model determined above, a nonlinear regression analysis was conducted with data collected from 39 test sections in 1991 and 1997. More than 760 data points from the 39 test sections were analyzed and then were grouped into 51 statistical samples representing every test site. Based on the process of numerical optimization using SYSTAT [30], a statistical computer program, the model is as follows:

$$RD = g(\underline{x}) * f(\underline{x}')$$

$$g(\underline{x}) = a1 * H_{AC} + a2 * \ln(SD) + a3 * T_{annual} + a4 * \ln(KV)$$

$$f(\underline{x}') = a5 + a6 * (\varepsilon_{v,base})^{a7} + a8 * (\varepsilon_{v,SG})^{a9} + a10 * \ln(N) - a11 * \ln(E_{AC}/E_{SG})$$

where :

RD = average rut depth along a specified wheel path segment (inch). The results from this nonlinear regression analysis are summarized in Table 12. Finally, the revised rut prediction model is as follows:

$$RD = \left(-0.016H_{AC} + 0.033\ln(SD) + 0.011T_{annual} - 0.01\ln(KV)\right)\cdot$$
$$\left(-2.703 + 0.657\left(\varepsilon_{v,base}\right)^{0.097} + 0.271\left(\varepsilon_{v,SG}\right)^{0.883} + 0.258\ln(N) - 0.034\ln\left(\frac{E_{AC}}{E_{SG}}\right)\right) \quad (33)$$

The R^2 of 90.5% indicates that the rut prediction of this nonlinear regression equation can be considered relatively useful. From the p-value of 2.044E-18 for the regression relation between predicted rut-depth and independent variables, one can conclude that the regression relation is very significant and useful for making predictions of rut-depths. The comparison between measured versus predicted rut-depth is shown in Figure 9.

There is a certain amount of bias associated with the measurement of rut, estimation of traffic and determination of material and cross-sectional properties. Hence, rut-depth prediction should include a confidence interval. For the purpose of this study, a tolerance level of ±0.1 inch was set up. If the difference between the observed and predicted rut-depth is within this tolerance level, it can be considered that the rutting prediction by the model is accurate. As shown in Figure 9, 43 of 51 samples are within this tolerance level indicating that a reasonable fit between the model and the data exists.

Sensitivity Analysis

There are two objectives associated with the sensitivity analysis

- Examine the possibility that the rutting prediction model violates physical rules of pavement performance.
- Determine the effects of major design parameters such as material and cross-sectional properties on the magnitude of pavement rutting.

Table 12 Statistical Results of Nonlinear Regression Analysis

DEPENDENT VARIABLE IS RD

SOURCE	SUM-OF-SQUARES	DF	MEAN-SQUARE	F	P-value
REGRESSION	2.336	9	0.260	43.333	2.044E-18
RESIDUAL	0.188	42	0.004		
TOTAL	2.583	51			
CORRECTED	0.477	50			

RAW R-SQUARED (1-RESIDUAL/TOTAL) = 0.905

PARAMETER	ESTIMATE	A.S.E.	CONFIDENCE INTERVAL (95%)	
			LOWER BOUND	UPPER BOUND
a1	-0.016	0.036	-0.089	0.058
a2	0.033	0.094	-0.157	0.223
a3	0.011	0.023	-0.037	0.058
a4*	-0.010			
a5	-2.703	0.181	-3.708	-1.698
a6	0.657	3.300	-6.002	7.317
a7	0.097	0.670	-1.255	1.448
a8	0.271	0.912	-1.569	2.111
a9	0.883	1.601	-2.348	4.114
a10	0.258	0.587	-0.926	1.443
a11	0.034	0.114	-0.196	0.264

*A4 is assumed to be a constant value before running statistical analysis due to the difficulty of convergence in the regression model

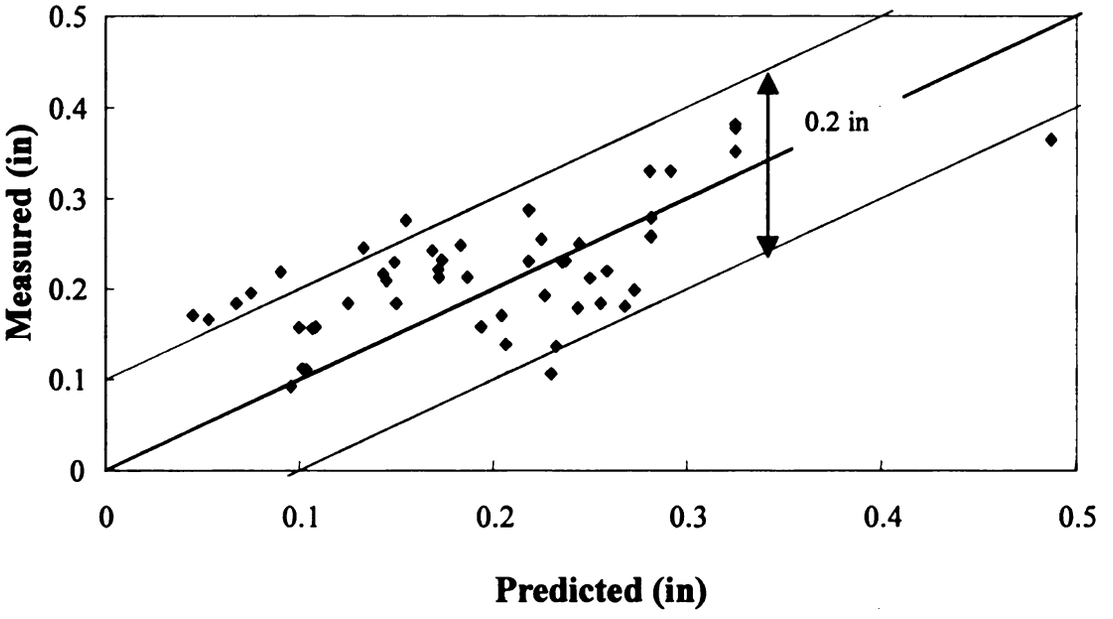

Figure 9 Measured vs. Predicted Rut-Depth Using Revised Model

For this analysis, an experimental matrix was set up that include low, medium, and high values for AC, base, subgrade modulus and AC thickness. The representative low, medium, and high values for each input were determined based on comments of pavement design engineers of MDOT and the catalog of current state pavement design features of NCHRP 1-32 project [26]. During this sensitivity analysis, other design parameters were held constant. Table 13 shows the experimental matrix and the resulting rut-depths. Figure 10 illustrates the results of the sensitivity analysis. In Figure 10-(a), when the resilient modulus of subgrade soil was changed from low (3,000psi (20,682kPa)) to strong (10,000psi (68,940kPa)) value, the rut-depth decreases by a factor of 10%. In Figure 10-(b), when AC thickness was changed from thin (3in.) to thick (9in.), the rut-depth decreases by a factor of around 48%. These results of the sensitivity analysis indicate that the revised rutting prediction model is more sensitive to AC thickness than other design parameters selected in this analysis. Figure 11 presents the relationship between traffic and rut-depth development based on observed data from the sections of AASHO Road Test and a prediction made by the developed model. In the figure, the rate of pavement rutting development increases rapidly at the beginning of pavement performance and then stabilizes as the pavement age increases. This trend of pavement rutting behavior corresponds well with the results from several field investigations regarding rutting development of in-service pavements [19,50,51,52]. Since the field data from pavements that had reached the end of their service lives was not collected in this study, the pavement rutting development at the final stage of pavement service life, which is known to increase with highly rapid rate [19,50], is out of the predictive range by the revised model.

Table 13 Experimental Design Matrix for Sensitivity Analysis

Matrix

AC Modulus			100			300			500		
Base Modulus			20	50	80	20	50	80	20	50	80
Roadbed Modulus											
AC Thickness											
3		3	1	2	3	4	5	6	7	8	9
		7	10	11	12	13	14	15	16	17	18
		10	19	20	21	22	23	24	25	26	27
6		3	28	29	30	31	32	33	34	35	36
		7	37	38	39	40	41	42	43	44	45
		10	46	47	48	49	50	51	52	53	54
9		3	55	56	57	58	59	60	61	62	63
		7	64	65	66	67	68	69	70	71	72
		10	73	74	75	76	77	78	79	80	81

Rut-Depth

AC Modulus			100			300			500		
Base Modulus			20	50	80	20	50	80	20	50	80
Roadbed Modulus											
AC Thickness											
3		3	0.632	0.561	0.531	0.599	0.536	0.509	0.583	0.524	0.498
		7	0.598	0.535	0.507	0.567	0.512	0.486	0.551	0.500	0.476
		10	0.586	0.526	0.498	0.556	0.503	0.477	0.539	0.491	0.467
6		3	0.490	0.445	0.425	0.452	0.415	0.397	0.435	0.402	0.385
		7	0.462	0.422	0.403	0.424	0.391	0.375	0.406	0.378	0.362
		10	0.452	0.413	0.395	0.413	0.382	0.366	0.395	0.368	0.353
9		3	0.368	0.337	0.323	0.332	0.308	0.295	0.316	0.295	0.284
		7	0.342	0.315	0.302	0.305	0.284	0.272	0.289	0.271	0.260
		10	0.333	0.308	0.294	0.295	0.275	0.263	0.279	0.261	0.251

(a)

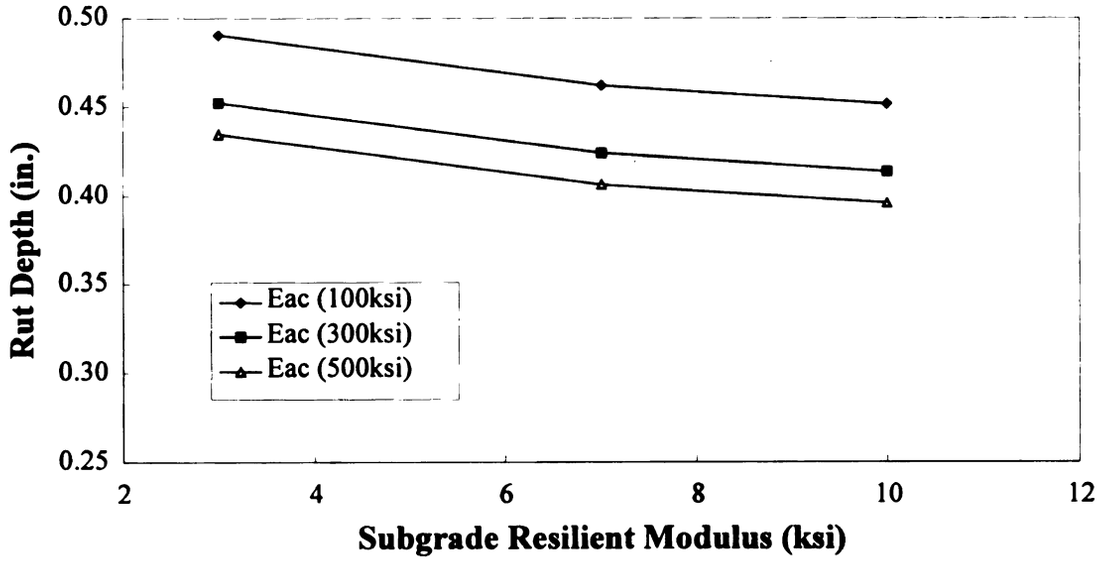

(b)

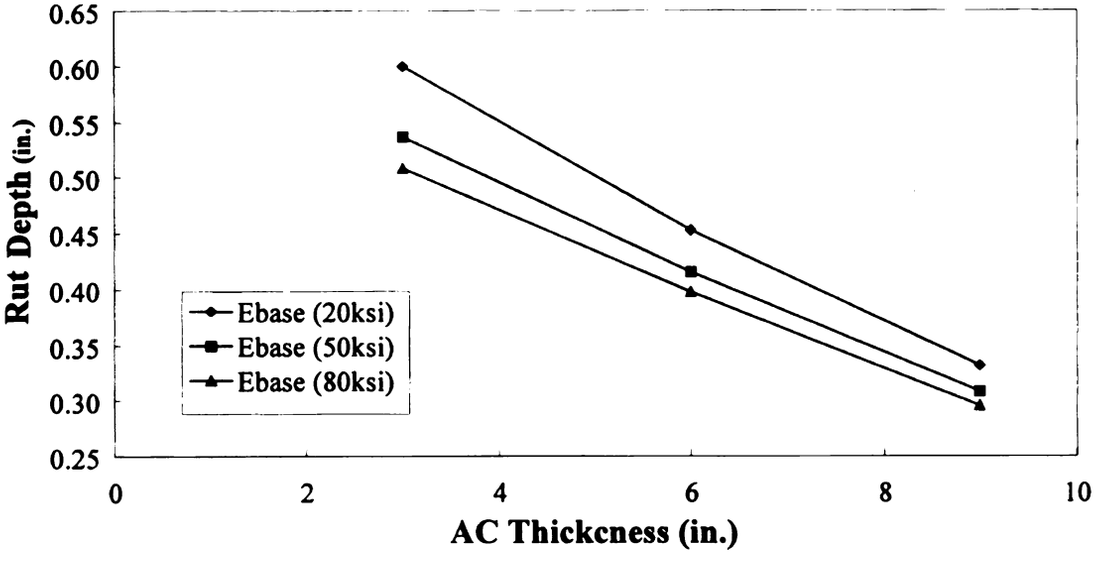

Figure 10 Sensitivity of Pavement Rutting to pavement design variables :

(a) Rut-Depth vs. Resilient Modulus of Subgrade, (b) Rut-Depth vs. AC Thickness, and

(c) Rut-depth vs. Resilient Modulus of Base Layer

(c)

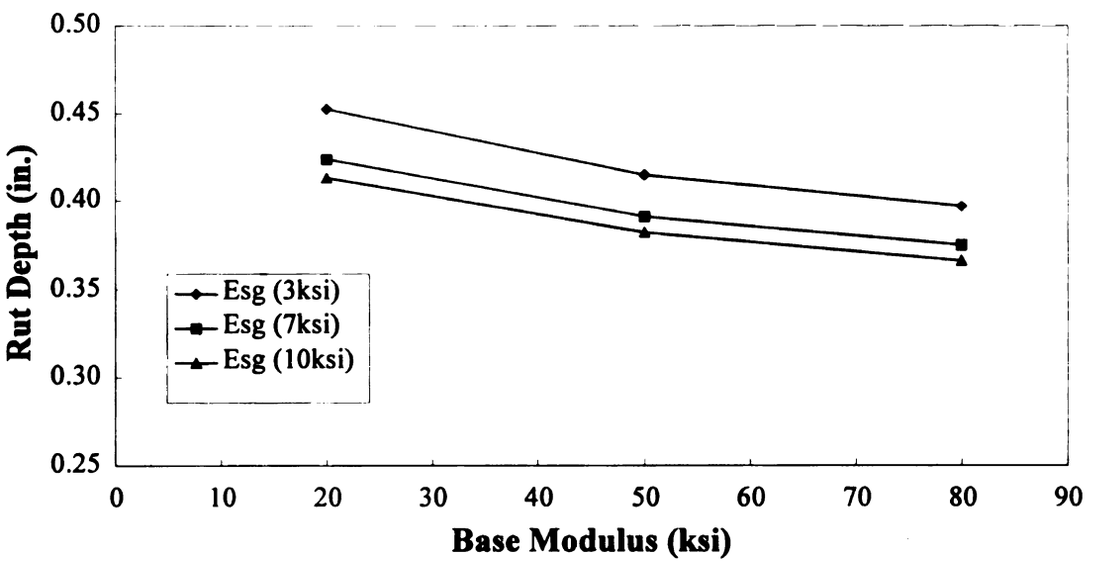

Figure 10 (cont'd) (c) Rut-depth vs. Resilient Modulus of Base Layer

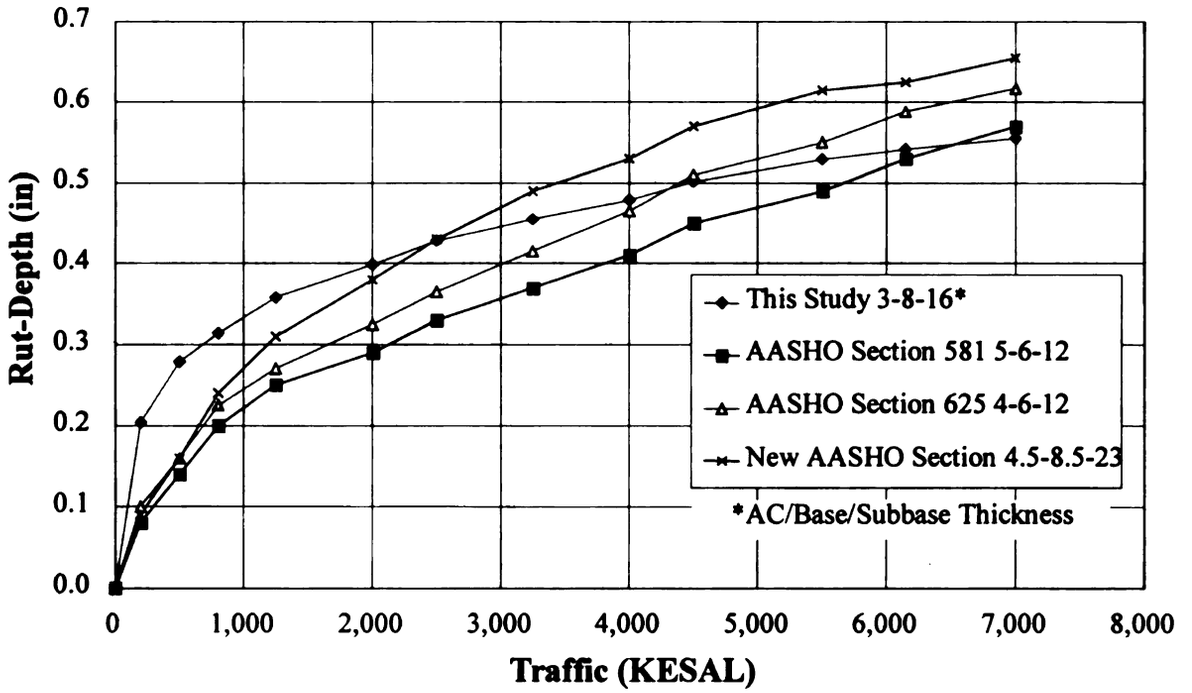

Figure 11 Rut-Depth Development with Increase of Traffic

In this sensitivity analysis, no violation of mechanistic rules of pavement performance was found implying that the model can successfully explain the relationship between the pavement rutting behavior and material/cross-sectional properties.

Validation with Field Data Collected in Michigan 1998

The data collected in 1998 was used to evaluate the accuracy of new rut prediction model and confirm the model's validity. Figure 12 is a graphical presentation of this evaluation. The observation points are distributed around the 45degree line – an indication of a reasonable fit between the model and the data. The sections on which data collection was conducted sequentially in 1991,1997 and 1998 were selected to compare their rutting development as a function of traffic volume, as predicted using the model, to the actual measured rut-depths. The results are shown in Table 14. Figure 13 is a typical presentation of the comparison in a graphical form. Because of little accumulated traffic volume and small changes of material properties between 1997 and 1998, there are no significant changes of rut-depths in the test sections.

Validation with LTPP Database

Data from twenty-four LTPP-GPS sections were used in order to further validate new rutting prediction model. Figure 14 shows a plot of predicted versus observed rut-depths in LTPP sections. In 19 (79%) of the 24 sites, the differences between measured and predicted rut-depth were less than 0.1in, implying that a new rutting prediction model developed in this study has potential for nation-wide application.

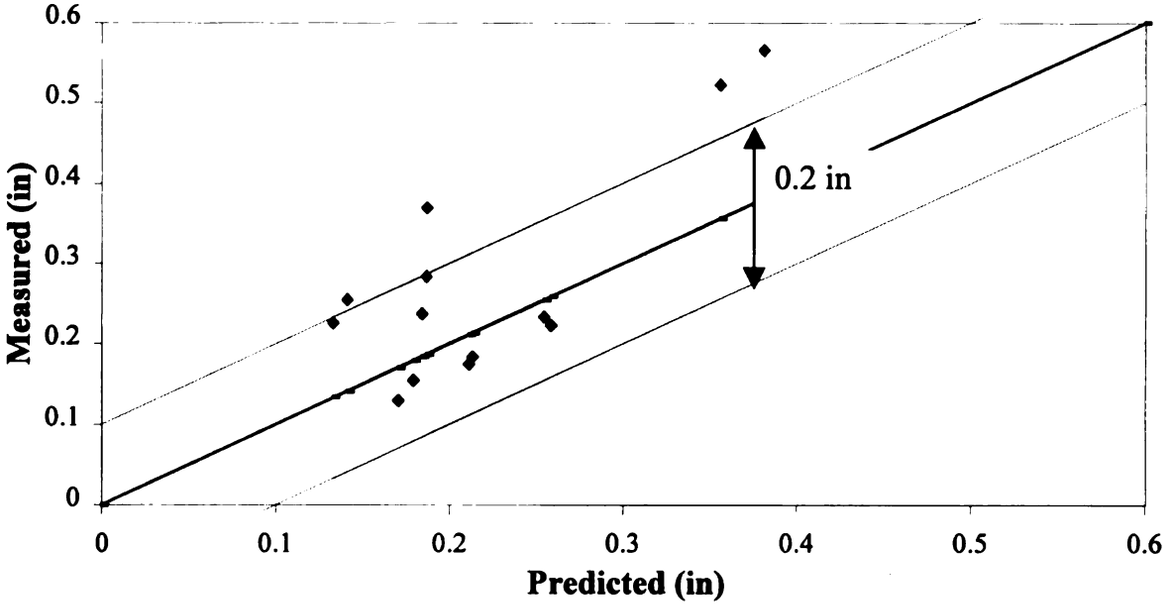

Figure 12 Measured vs. Predicted Rut-Depth Based on '98 Michigan Data Set

Table 14 Rutting Development at Test Sites with Increase of Traffic

	1991			1997			1998		
	ESAL	predicted rut-depth	measured rut-depth	ESAL	predicted rut-depth	measured rut-depth	ESAL	predicted rut-depth	measured rut-depth
MSU23F	117089	0.16	0.11	226268	0.18	0.24	255126	0.18	0.24
MSU34F	196251	0.22	0.17	293717	0.26	0.23	310825	0.26	0.23
MSU39F	264322	0.16	0.11	513876	0.18	0.15	557679	0.19	0.15
MSU18F	1354130	0.24	0.17	2026646	0.26	0.28	2144690	0.25	0.23
MSU45F	911072	0.21	0.15	1431408	0.23	0.24			
MSU36F	482838	0.16	0.19	1010793	0.18	0.26	1103463	0.19	0.28
MSU32F	263703	0.20	0.08	426817	0.21	0.17	455448	0.22	0.18
MSU15F	1354130	0.23	0.17	2026646	0.25	0.24	2144690	0.25	0.25

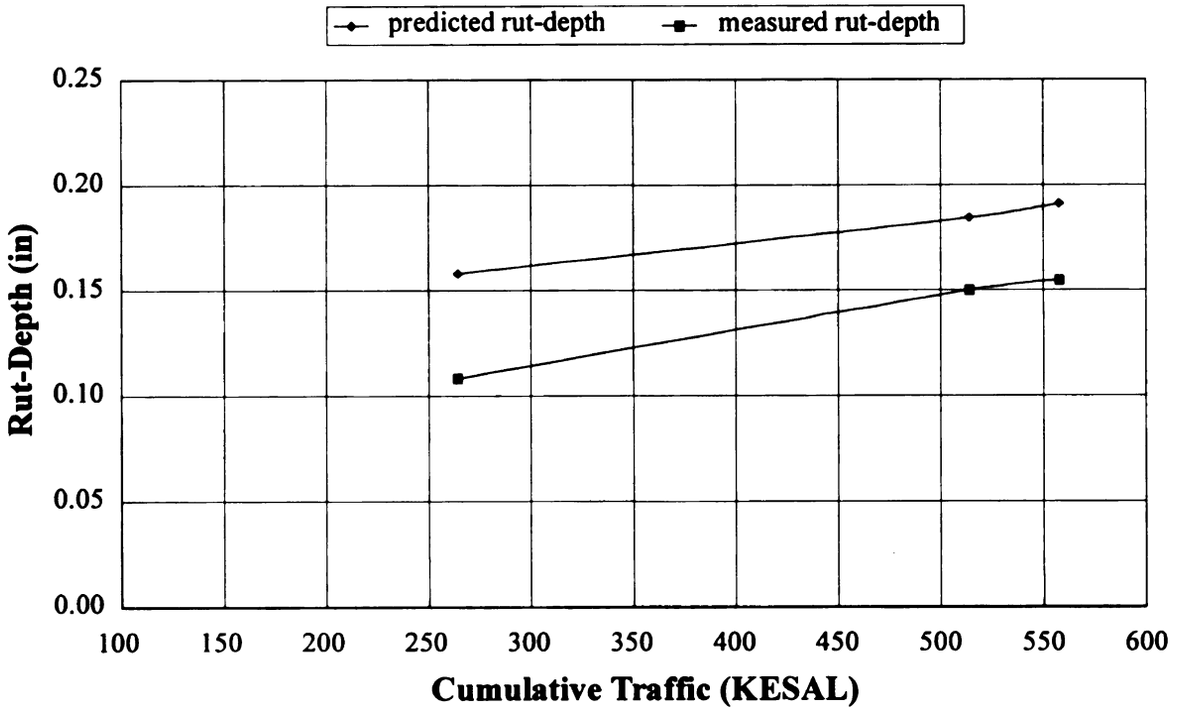

Figure 13 Typical Rutting Development with Increase of Traffic (MSU39F)

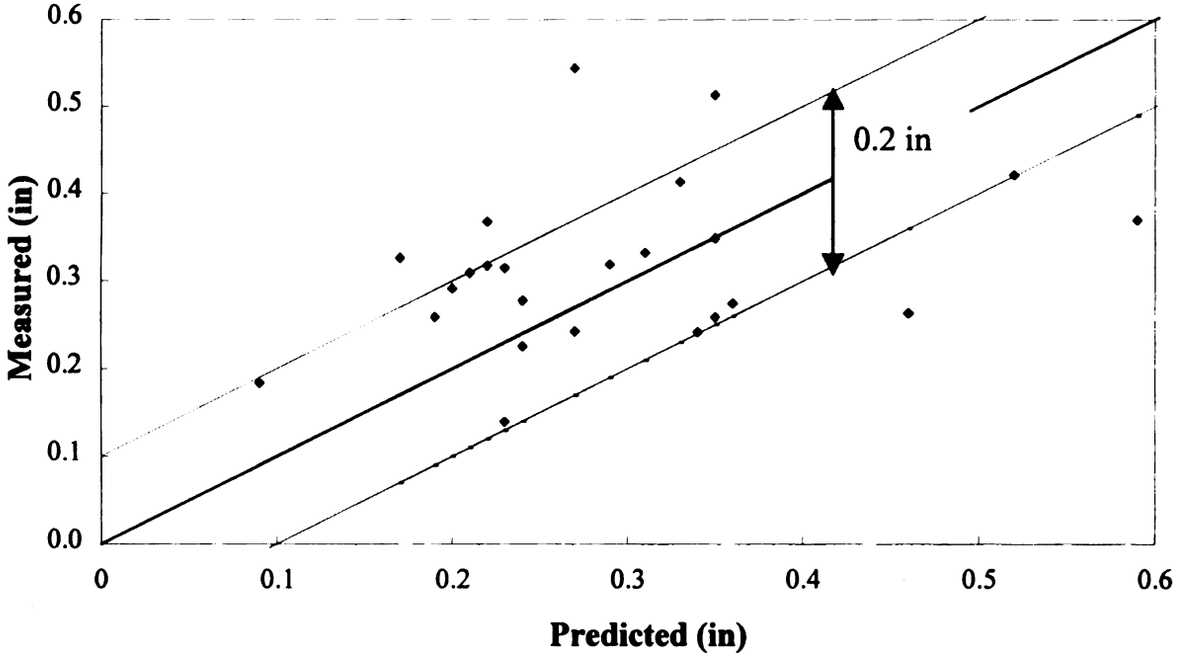

Figure 14 Measured vs. Predicted Rut-Depth Based on Selected LTPP-GPS Data Set

CHAPTER V

RELIABILITY-BASED APPROACH TO M-E FLEXIBLE PAVEMENT ANALYSIS

General

As described in Chapter II, there are still some issues that need to be resolved before implementing M-E flexible pavement design procedure. According to Thompson et al., following issues exist [2]:

- Deterministic nature of design parameters, and
- Lack of fit of transfer functions.

In the current M-E design procedures that are analytical in nature, the pavement performance is predicted by deterministic nominal design parameters based on engineering judgement and then compared with established failure criteria. Outputs such as pavement thickness and material properties are derived based on an intended limit state. Limit state is defined as a state of the structure including parameters at which the structure is just on the point of not satisfying its function [31]. In other words, the current M-E design procedures predict average pavement performance using average values of design parameters without considering variability of design parameters and model bias. The reliability theory provides a rational framework for addressing these uncertainties. The objective of reliability analysis is to provide a specific degree of confidence that the pavement will perform satisfactorily while being subjected to traffic and environmental loads during its service life. The following advantages can be derived by the reliability theory if applied to the M-E flexible pavement design procedure [32].

- Be able to consider in design construction variability, differences between design and as-built parameters, material variability, and variability associated with traffic prediction during pavement design life.

- Simplify the design process by encouraging the use of same design philosophy and procedure to be adopted for all materials of construction.

- Overcome the lack of fit of the transfer function that is statistical in nature, and the uncertainties of simplified structural analysis algorithms by quantifying model bias factors.

- Provide designed pavement structures with a uniform performance level without which the comparison of life-cycle costs of alternative pavement types would be misleading and could result in the selection of a less cost-effective pavement type.

- Provide a tool for updating standards in a rational manner, as more data becomes available.

Reliability Concepts

The pavement design reliability is defined as the probability that the pavement's traffic load capacity exceeds the cumulative traffic loading on the pavement or the cumulative amount of pavement distress does not exceed a specified level regarded as a failure criterion during a specified design life. Since there are uncertainties in the major parameter values of pavements such as moduli of layers, thickness of layers, traffic volume, etc., it is reasonable to define each parameter as a random variable with its mean and standard deviation or its complete probability distribution. Once the statistical information for each random variable is obtained, one can calculate mean and standard deviation of the pavement performance function, which in this study, is taken as :

$$SM_{rut} = RD_{\max} - RD_{predict} \tag{34}$$

where :

SM_{rut}	=	safety margin between maximum allowable and predicted rut-depth,
RD_{max}	=	maximum allowable rut depth in the design period, and
$RD_{predict}$	=	predicted rut depth in the design.

If a probability distribution function (pdf) of the pavement performance function is assumed and its limit state is taken as SM = 0, the area of pdf below the limit state is the probability of failure, Pr(f). The U.S. Army Corps of Engineers uses the term probability of unsatisfactory performance, Pr(U) rather than the probability of failure to recognize that the considered cases for rehabilitation projects are not disastrous [33]. Theoretically, the probability of unsatisfactory performance can be determined by constructing a pdf on the performance function (e.g. SM) and calculating the area under the curve that is less than the value of the limit state. However, Pr(U) is not practical because of the incomplete probability information of the design parameters in pavements. Even though the probability information of all parameters can be obtained, the shape of the probability distribution of the performance function that is likely to be non-linear may be difficult to obtain. Practically, approximate statistical moments of the performance function (E[SM] or SD[SM]) are obtained from the estimated statistical moments of parameters from pavements using several reliability analysis techniques which will be described in later sections. Using these approximate moments of the performance function, the reliability can be characterized by a conventional reliability index β_c, which is the number of standard deviations by which the expected value of the performance function exceeds the limit state [34]. Figure 15 illustrates the concepts of the probability of unsatisfactory performance and the conventional reliability index, β_c.

In this study, using the moments of the safety margin ($E[SM_{rut}]$, $SD[SM_{rut}]$) and the limit state condition (SM = 0), β_c is:

$$\beta_c = \frac{E[SM_{rut}]}{SD[SM_{rut}]} \tag{35}$$

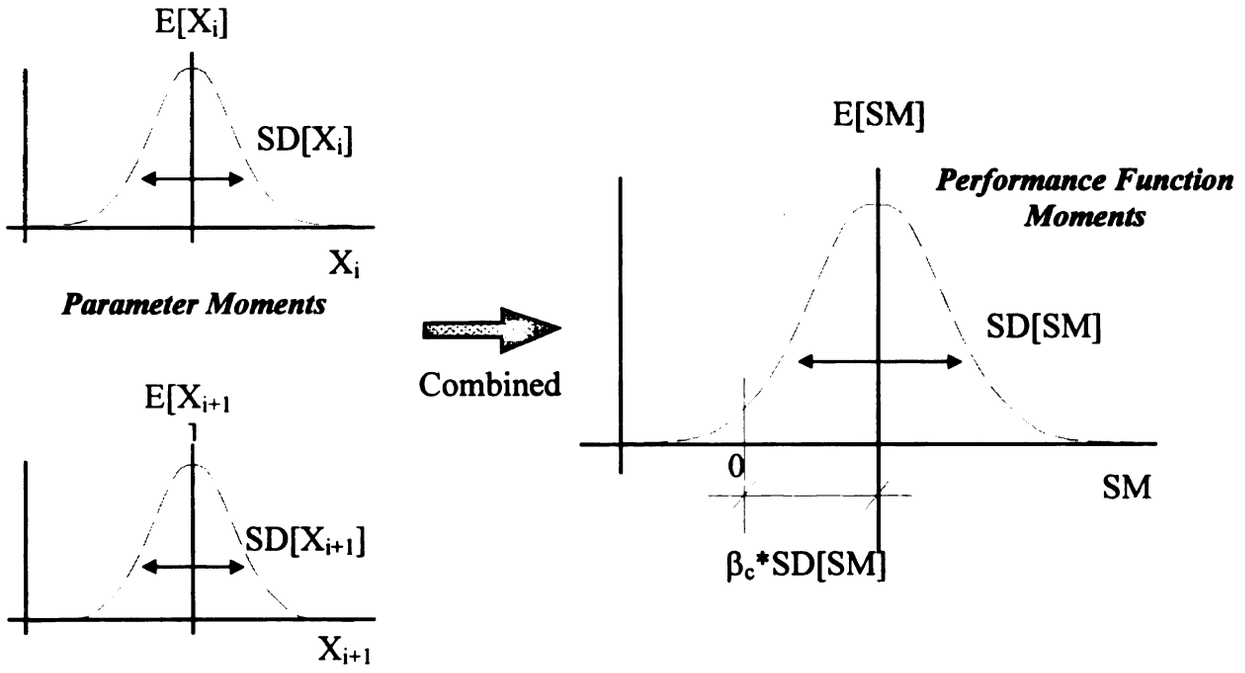

Figure 15 Probability of Unsatisfactory Performance with Specified Variables

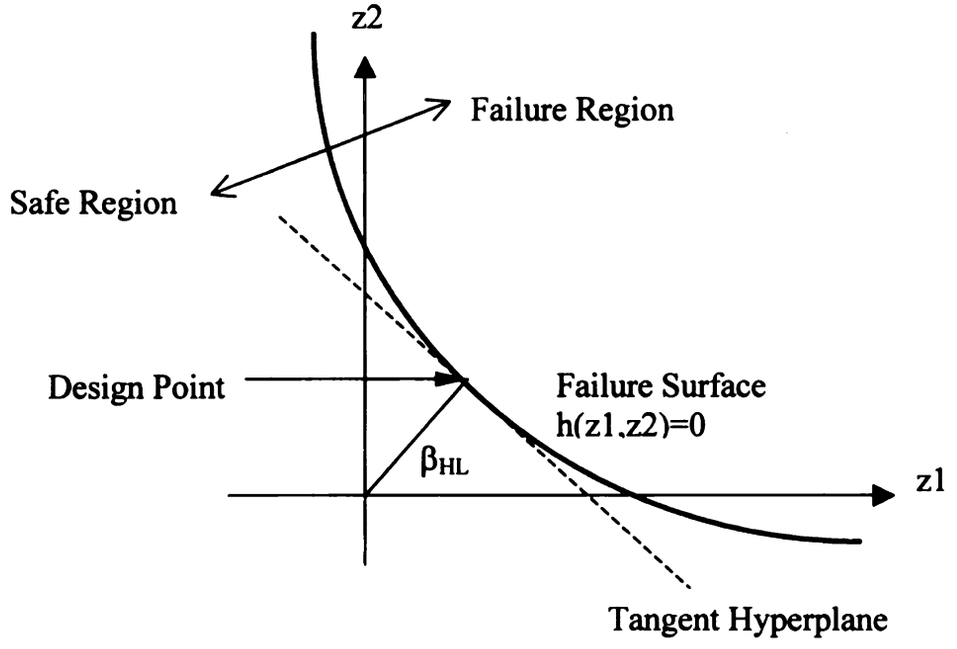

Figure 16 Geometrical Illustration of Haosfer and Lind's Reliability Index [35]

For normal random variables, the probability of unsatisfactory performance, Pr(U), is estimated using following approximate relationship [36]:

$$\Pr(U) = \Phi(-\beta) = \int_{-\infty}^{\beta} g(z)dz \qquad (36)$$

where :

$\Phi(-\beta)$	=	area under the pdf of standard normal variate from -∞ to -β, and
g(z)	=	pdf of pavement performance.

The reliability of pavement performance can now be expressed as: 1-Pr(U). It should be noted that even if no particular distribution was assumed, various designs or trial failure modes could be compared since the lowest value of β_c represents the least safe condition. In other words, engineering system and components with higher β_c values are considered more reliable than those with lower values. The reliability index β_c is a convenient and valid comparative measure of an engineering system that reflects both the mechanics of the problem and uncertainty in the input variables at the same time [37]. However, although the conventional reliability index, β_c is a consistent index of risk measure, it is not invariant to different but mechanically expression of the performance function for non-linear performance functions. To circumvent this problem, Hasofer and Lind proposed an invariant reliability index [35]. In their method, all random variables $\underline{X}$ are transformed into a standardized parameter space $\underline{z}$ by means of an orthogonal transformation such that

$$E\{Z_i\} = 0 \; ; \; \sigma_{Zi} = 1$$

Hasofer and Lind defined the reliability index as the minimum distance between the origin and the surface representing the limit state condition in the standardized parameter space z which was taken as SM = 0 in the section above.

$$\beta_{HL} = \min_{g(\underline{x})\equiv 0} \sqrt{\{(\underline{x} - m_{\underline{x}})^T \underline{C}^{-1} (x - m_{\underline{x}})} \text{ or } \min_{h(\underline{z})\equiv 0} \sqrt{(\underline{z}^T \underline{z})} \quad (37)$$

where :

β_{HL}	=	reliability index defined in Hasofer and Lind's sense,
$\underline{z}$	=	a vector representing the set of random variables in the z space,
$\underline{x}$	=	a vector representing the set of random variables in x space,
$\underline{C}$	=	the covariance matrix of the random variables, and
$h(\underline{z})$ and $g(\underline{x})$	=	the failure criterion in z and x space.

Haosfer and Lind's invariant reliability index is illustrated in Figure 16. If the performance function is linear, the conventional reliability index (β_c) and the Haosfer and Lind reliability index (β_{HL}) will be identical.

Sources of Uncertainties in the M-E Flexible Pavement Design

Uncertainties affecting pavement performance can be grouped into the following four categories as shown in Table 15:

1. Spatial variability that includes a real difference in the basic properties of materials from one point to another in what are assumed to be homogeneous layers and a fluctuation in the material and cross-sectional properties due to construction quality.

2. The variability due to the imprecision in quantifying the parameters affecting pavement performance (i.e. random measurement error in determining the strength of subgrade soil, and estimation of traffic volume in terms of ADT and mean truck equivalency factor).

3. The model bias due to the assumption and idealization of a complex pavement analysis model with a simple mathematical expression.

4. The statistical error due to the lack of fit of the regression equation.

Table 15 Variability Components in M-E Flexible Pavement Design

Uncertainties in the Design			
Uncertainties of Design Parameters		Systematic Errors	
Spatial Variation	Imprecision in Quantifying Parameters	Model Bias	Statistical Error

One can combine the first and second sources of uncertainty into uncertainties of design parameters, which represent the variability from site to site and inconsistent estimation of the parameters, and the third and forth sources of uncertainty into systematic errors, which consistently deviate from predicted actual pavement performance. The uncertainties of design parameters cause the variation within the probability distribution of the performance function, whereas systematic errors cause the variation in possible location of the probability distribution of the performance function [38]. Therefore, design parameters describe the scatter of the pavement properties and the variation of traffic estimation and systematic errors are associated with the uncertainty in the location of the trend of predicted pavement performances. This concept is graphically presented in Figure 17 [39]. The methods and procedure to quantify and combine these variations will be described in the subsequent sections.

Practical Engineering Reliability Techniques

The following numerical reliability techniques are generally used in engineering practices.

- **First Order Second Moment (FOSM) Method**

FOSM method involves approximation based on Taylor series expansion [40]. The mean value and standard deviation of a performance function can be obtained by linearizing the function at the mean centroid. This method is also referred to as the mean value first order second moment (MVFOSM) method, due to linearizing at mean values. For example, if there is a performance function $g(\underline{x})$ with random vector $\underline{x}$'s, its approximate mean value and standard deviation can be mathematically expressed as:

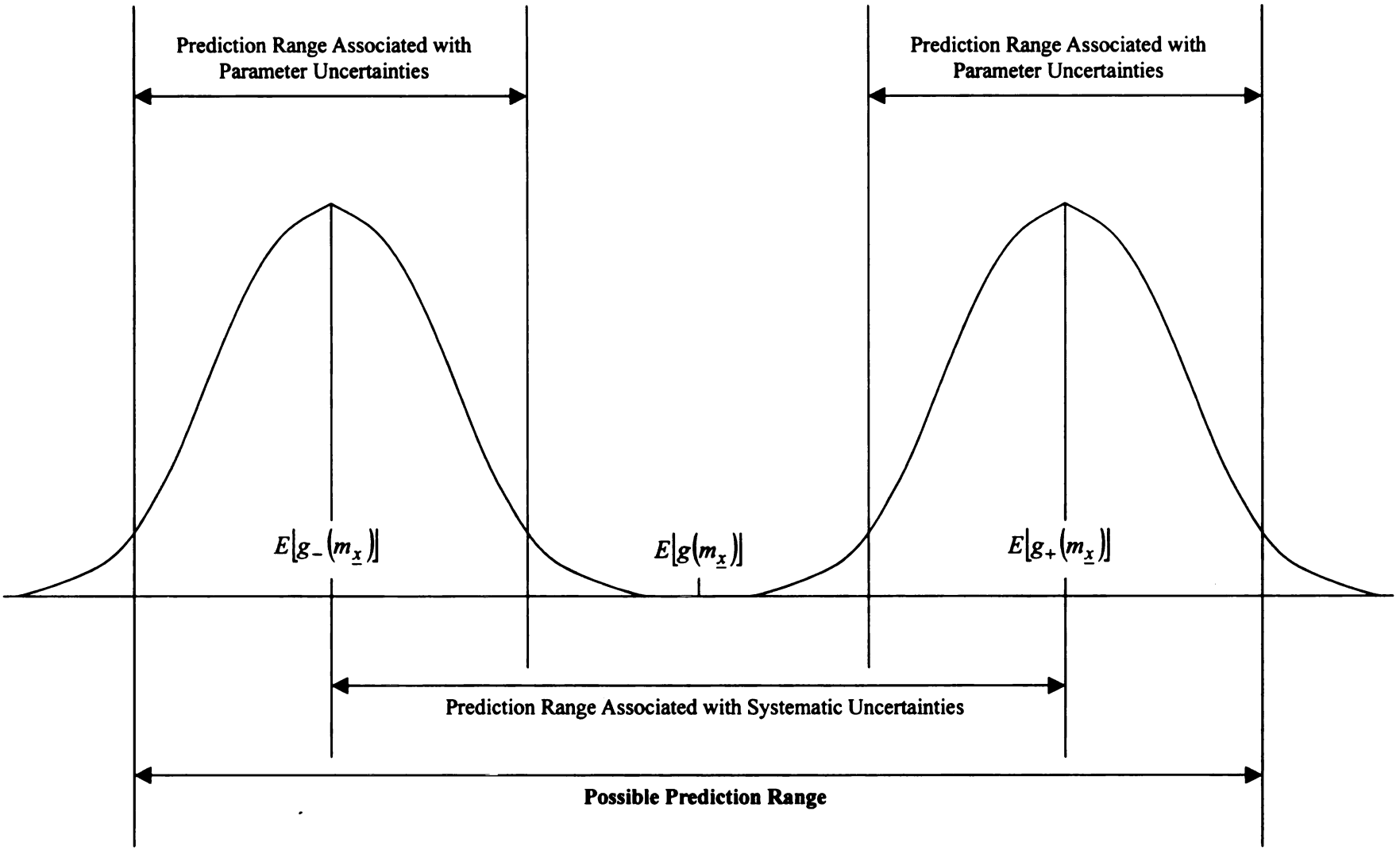

Figure 17 Integrated Presentation of Types of Uncertainties Associated with M-E Flexible Pavement Analysis

$$E[g(\underline{x})] \approx g(m_{\underline{x}}) \tag{38}$$

$$\sigma^2_{g(\underline{x})} = \nabla G^T COV(\underline{x}) \nabla G \tag{39}$$

where :

$m_{\underline{x}}$	=	vector of the mean values of random variables $\underline{x}$,
∇G	=	vector of partial derivatives of the performance function at the mean values of random variables $\underline{x}$,
$COV(\underline{x})$	=	covariance matrix of the random vector $\underline{x}$.

The partial derivatives may be estimated numerically using the finite difference approach as follows:

$$\frac{\partial g(\underline{x})}{\partial x_i} = \frac{g(x_{i+}) - g(x_{i-})}{x_{i+} - x_{i-}} \tag{40}$$

where x_{i+} and x_{i-} represent the random variable x_i taken at some increment above and below its expected values. Theoretically, an extremely small increment gives the most accurate value of the derivative at the expected value, but in practice, one standard deviation increment for each random variable is adequate [41]. The FOSM method allows the designer to see the contribution of each random variable to the total uncertainty and usually requires fewer computations than the point estimate method.

- **Point Estimate Method (PEM)**

PEM is the procedure where probability distributions for continuous random variables are considered by discrete equivalent distributions having two or more values [42]. In order to obtain the expected value for the performance function, PEM requires all possible combinations of one low and one high value for each random variable for determining various possible $g(\underline{x})$'s. The results are weighted by the product of their

associated probability concentrations P_{i+} or P_{i-}, and then summed. The procedure is summarized as:

$$E[g(\underline{x})] = \sum \left(P_{x_1\pm} P_{x_2\pm} \ldots P_{x_n\pm}\right)\left[Y(x_{1\pm}, x_{2\pm}, \ldots x_{n\pm})\right] \tag{41}$$

$$E[g(\underline{x})^2] = \sum \left(P_{x_1\pm} P_{x_2\pm} \ldots P_{x_n\pm}\right)\left[Y^2(x_{1\pm}, x_{2\pm}, \ldots x_{n\pm})\right] \tag{42}$$

$$\sigma^2_{g(\underline{x})} = E[g(\underline{x})^2] - \left(E[g(\underline{x})]\right)^2 \tag{43}$$

When performance functions are significantly nonlinear, the PEM may produce better solutions because of its higher order accuracy in the mean value estimate [37].

- **First Order Reliability Method (FORM)**

As described in the previous sections, an advanced reliability method was developed by Hasofer and Lind, who introduced an invariant second moment method where the failure surface is approximated to a tangent hyperplane at the failure point [35,43]. The shortest distance between the design point on the failure surface and the origin in a standardized normal space is considered as β_{HL}. Rackwitz and Fiessler suggested an alternative iteration method to practically obtain β_{HL} [44]. The method is described as follows:

1. Evaluate the limit state function $h(\underline{z})$ in standardized space, z

$$h(\underline{z}) = g(\sigma_{\underline{z}} \underline{z} + m_{\underline{z}}) \tag{44}$$

2. Select a trial point $\underline{z}^{(n)}$ (usually take $z^{(0)} = \underline{0}$)

3. Evaluate the gradient vector

$$\underline{\nabla} h = \left\{\frac{\partial h}{\partial \underline{z}}\right\} \text{ at } \underline{z}^{(n)} \tag{45}$$

i.e. $\underline{\nabla} h(\underline{z}^{(n)})$, and its magnitude $\left|\underline{\nabla} h(\underline{z}^{(n)})\right|$

4. Compute the unit vector

$$\underline{\alpha}^{(n)} = -\frac{\underline{\nabla} h(\underline{z}^{(n)})}{\left|\underline{\nabla} h(\underline{z}^{(n)})\right|} \tag{46}$$

5. Compare $\underline{z}^{(n)^T}\underline{\alpha}^{(n)}$ and $h(\underline{z}^{(n)})$ and obtain the revised point

$$\underline{z}^{(n+1)} = \left[\underline{z}^{(n)^T}\underline{\alpha}^{(n)} + \frac{h(\underline{z}^{(n)})}{\left|\underline{\nabla} h(\underline{z}^{(n)})\right|}\right]\underline{\alpha}^{(n)} \tag{47}$$

6. Current estimate of β_{HL} is distance from origin to $\underline{z}^{(n+1)}$,

i.e. $$\beta_{HL}^{(n+1)} = \left|\underline{z}^{(n+1)}\right| \tag{48}$$

7. Repeat steps 3 to 6 until the $h(z^{(n)}) \cong 0$, and β_{HL} converge.

For a linear failure criterion, β_{HL} is identical to β_c. For a nonlinear failure criterion, β_{HL} is identical to β_c if the linearization point for FOSM is chosen to be the design point in x-space, which corresponds to the point on the failure surface in z-space that is closest to the origin [45].

Framework for Developing Reliability Model for Pavement Structural Analysis

The reliability model in this study consists of two subsystems: an analytically derived mechanistic subsystem for predicting pavement performance and a reliability subsystem for analyzing the limit state function. When FORM is applied to the reliability model, an iterative loop between these subsystems is established and presented in Figure 18. The rut prediction model developed in this study was employed as a pavement performance function that would predict the development of pavement rut-depth during its service life.

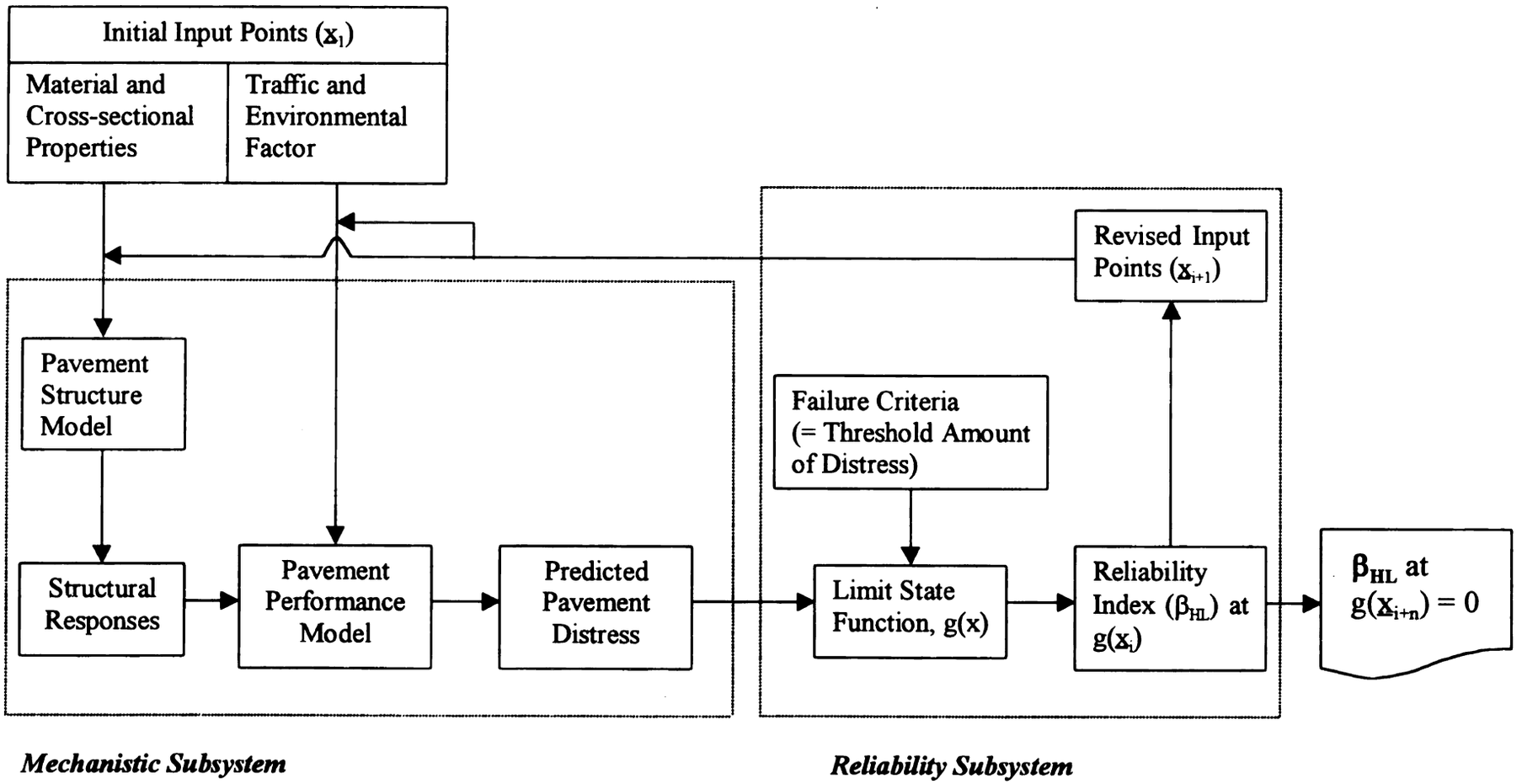

Figure 18 Flow Diagram for Pavement Reliability Analysis

First, a structural analysis of the pavement section was conducted to obtain the relevant pavement structural responses due to traffic loads. Followed by the determination of rut- depth in accordance with equation 32. The reliability subsystem then determines the reliability of the pavement section in terms of the reliability index using the results derived from the mechanistic submodel. At any time, the safety of the pavement section may be characterized by a limit state function, which is expressed as safety margin, SM, in this study.

Illustrative Example

In order to better explain the merits and demerits of pavement reliability models employing MVFOSM, PEM, and FORM, the reliabilities of two typical pavement structures were estimated using the three methods. The variables used in the illustrative example design are summarized in Table 16. They are not based on any specific pavement section but on statistics from the database collected during this study and the MDOT database. A post validation work of the coefficient of variation (COV) of AC thickness using the database acquired from an evaluation study for Michigan pavement construction practice indicates that the selected number (10%) for COV of AC thickness is appropriate as shown in Table 17. In this illustration, six design parameters including AC thickness, moduli of AC, base, subbase, and subgrade, and traffic volume, were considered as statistical variables with normal or log-normal distributions, while annual ambient temperature and kinematic viscosity were considered as deterministic values.

Table 16 Summary of Variables Used in Example Pavement Sections

		Section 1		Section 2	
Description of Variables	Type of Distribution	Mean	Coefficient of Variation	Mean	Coefficient of Variation
Traffic Volume	Log-normal	5.0E+6 ESAL	0.42	1.5E+7 ESAL	0.42
Modulus of Asphalt Concrete	Normal	450,000 psi	0.25	450,000 psi	0.25
Modulus of Base	Normal	30,000 psi	0.2	30,000 psi	0.2
Modulus of Subbase	Normal	15,000 psi	0.2	15,000 psi	0.2
Modulus of Subgrade	Normal	4,000 psi	0.2	8,000 psi	0.2
Thickness of Asphalt Concrete	Normal	7.0 in.	0.1	10.0 in.	0.1
Professional Factor	Normal	0.894	0.2	0.894	0.2
Annual Ambient Temperature	Deterministic	45°F	-	45°F	-
Asphalt Kinematic Viscosity	Deterministic	210 centistokes	-	210 centistokes	-

Table 17 Summary of the Statistics of AC Thickness Cored in Michigan Sections

Route	C.S.	J.N.	Core #	AC Thickness (in)	Mean of AC Thickness	Stdev of AC Thickness	Coefficient of Variation
US-27 (St. Johns)	19032	45595	27111-13	6	5.81	0.293	0.050
			27111-21	6			
			27111-03	5.375			
			27112-08	6			
			27112-18	5.5			
			27112-22	6			
M-66 (Athens)	13031	34497	66111-05	6	6.88	0.629	0.092
			66111-21	7.5			
			66112-15	7			
			66112-22	7			
M-50 (Charlotte)	33081	45984-A	50141-21	5.5	5.50	0.816	0.148
			50141-05	4.5			
			50142-15	5.5			
			50142-22	6.5			
M-99 (Lansing)	MR33011	44738-A	99131-03	10.5	10.33	0.303	0.029
			99131-13	10.5			
			99131-21	10.5			
			99132-08	10.5			
			99132-18	9.75			
			99132-22	10.25			
EB I-96 (weigh Station)	IM47066	37990A	96121-05	5.125	4.78	0.329	0.069
			96121-21	4.5			
			96122-15	5			
			96122-22	4.5			
WB M-89 (Springfield)	39102	32377	89141-05	8.75	9.50	0.736	0.077
			89141-21	9.25			
			89142-15	10.5			
			89142-22	9.5			
EB M-21 (Ionia)	34062	33804	21121-05	4	3.88	0.629	0.162
			21121-21	4.5			
			21122-15	3			
			21122-22	4			
WB M-21 (Ionia)	34062	33804	21141-05	4	4.81	0.688	0.143
			21141-21	4.5			
			21142-15	5.5			
			21142-22	5.25			
WB I-96 (Grand Rapids)	41026	IM9841	96141-03	10.25	10.25	0.354	0.034
			96141-21	9.5			
			96141-13	10			
			96142-08	10			
			96142-22	10			
			96142-18	10.5			
WB I-196 (Grand Rapids)	35988A	32485	196141-03	8.5	9.00	1.173	0.130
			196141-21	8			
			196141-13	8			
			196142-08	10			
			196142-22	10.5			
			196142-18	8			
				Mean of Coefficient of Variations			0.098

Partly reflecting Michigan flexible pavement design practice, the thickness of the base and subbase was fixed at 8 (20.3) and 16 (40.6) inches (cm), while AC thickness was varied with cumulative traffic volume. As mentioned in previous sections, uncertainties affecting the variation of the pavement performance are not only ascribed to the variations of design parameters but also to the uncertainties of the pavement performance model itself. In this illustration, a professional factor that is defined as a representative ratio of measured rut-depth to predicted was employed to reflect the model uncertainties [46]. The statistical information of the professional factor is also given in Table 16. The professional factor and the limit-state function of the pavement reliability model are related as follows:

$$SM_{rut} = RD_{\max} - P \cdot RD_{predict} \tag{49}$$

where P is a professional factor. Further detailed explanation of the professional factor will be presented in the following sections. A rut-depth of 0.5 inch was considered as failure criterion for this illustration. Detailed calculation procedures of the reliability indices for the two given pavement sections are presented in Tables 18 and 19.

At each iteration,

1. The first of all, the limit state function $h(\underline{z})$ on standardized space, z, are calculated.
2. In order to evaluate the gradient vector, $h(z_{i+})$ and $h(z_{i-})$, which are the limit state function with ± one standard deviation increment of a variable, are calculated for all variables. Since 7 variables are involved in this limit state function, 14 runs are needed. Totally, 15 runs for calculating predictive rut-depths are required at each iteration stage as can be seen in Table 18.

3. With calculated $h(z_{i+})$ and $h(z_{i-})$ for all variables, the partial derivatives of the gradient vector are obtained using equation 40, and the gradient vector (*grad(h(z))*) is established as seen in equation 45.

4. The unit vectors (*alpha*) for all variables are calculated as follows:

$$alpha = \frac{\partial h / \partial z_i}{\sqrt{\sum_{i=1}^{n} (\partial h / \partial z_i)^2}} = \frac{grad((h(z_i))}{magnitude} \tag{50}$$

5. The revised points (*New z's and New X's*) and current estimate of β_{HL} are calculated by equation 47 and 48.

The iteration using the steps 1 through 5 are continued until the design point and β_{HL} converge. It should be noted that in Table 18, the estimate of β_{HL} at the 1st iteration is identical to β_c using MVFOSM because the first trial points of variables in z space are zero. Table 20 summarizes the results of reliability analysis for the two given pavement sections. The results from three methods indicate that the reliability indices vary with the methods, reflecting the degree of nonlinearity of the pavement performance model that includes a structural analysis model and a performance prediction equation. For both pavement sections, FORM results in the lowest reliability indices. Especially, for the pavement section 2, the reliability index from FORM is different from reliability indices from the two other methods. If the reliability analysis is conducted on the performance of a structure whose actual reliability index is close to such threshold value, the reliability method using linear approximation at the mean values of design parameters using MVFOSM or PEM may produce higher β and lead the engineer to a fatal misinterpretation about the existing reliability of the pavement structure. Therefore, FORM should be used to evaluate the reliabilities of civil engineering structures that

have higher degrees of non-linearity or are considered to be on critical states, although it requires more computational time. For the pavement structure, the author recommends that MVFOSM or PEM should be used to characterize the effects of parameter uncertainties on the pavement performance for the purpose of analyzing the existing pavement reliability and FORM used to quantify the uncertainties of design parameters and model bias for the purpose of establishing reliability-based M-E pavement design procedure.

Table 18 Spreadsheet for Reliability Analysis of Pavement Performance (on Example Pavement Section 2)
(a) FOSM or the 1st Iteration in FORM

Description of Variables	z	Run	Eac(ksi)	Tac (inch)	Ebase (inch)	Esubbase (ksi)	Esg (ksi)	ln(Traffic Volume)	Professional Factor
		1	**450.0**	**10.0**	**30.0**	**15.0**	**8.00**	16.442	**0.894**
		2	**562.5**	10.0	30.0	15.0	8.0	16.442	0.894
Eac	0.0	3	**337.5**	10.0	30.0	15.0	8.0	16.442	0.894
		4	450.0	**11.0**	30.0	15.0	8.0	16.442	0.894
Tac	0.0	5	450.0	**9.0**	30.0	15.0	8.0	16.442	0.894
		6	450.0	10.0	**36.0**	15.0	8.0	16.442	0.894
Ebase	0.0	7	450.0	10.0	**24.0**	15.0	8.0	16.442	0.894
		8	450.0	10.0	30.0	**18.0**	8.0	16.442	0.894
Esubbase	0.0	9	450.0	10.0	30.0	**12.0**	8.0	16.442	0.894
		10	450.0	10.0	30.0	15.0	**9.6**	16.442	0.894
Esg	0.0	11	450.0	10.0	30.0	15.0	**6.4**	16.442	0.894
		12	450.0	10.0	30.0	15.0	8.0	**16.845**	0.894
ln(Traffic Volume)	0.0	13	450.0	10.0	30.0	15.0	8.0	**16.039**	0.894
		14	450.0	10.0	30.0	15.0	8.0	16.442	**1.072**
Professional Factor	0.0	15	450.0	10.0	30.0	15.0	8.0	16.442	**0.715**

Run	Maximum Deflection	Maximum Vertical Strain at Base	Maximum Vertical Strain at Subgrade	Predicted Rut-Depth	Threshold Rut-Depth	h(z)	grad(h(z))	alpha	New z	New X
1	**1.480E-02**	**2.950E-04**	**1.571E-04**	***0.291***	***0.500***	***0.240***				
2	1.388E-02	2.555E-04	1.455E-04	***0.284***	0.500	0.247				
3	1.609E-02	3.522E-04	1.722E-04	***0.300***	0.500	0.232	0.007	-0.111534	-0.414130	403.4
4	1.388E-02	2.520E-04	1.412E-04	***0.252***	0.500	0.275				
5	1.588E-02	3.489E-04	1.757E-04	***0.330***	0.500	0.205	0.035	-0.541358	-2.010086	8.0
6	1.454E-02	2.729E-04	1.545E-04	***0.289***	0.500	0.242				
7	1.512E-02	3.244E-04	1.595E-04	***0.293***	0.500	0.238	0.002	-0.029274	-0.108696	29.3
8	1.442E-02	2.980E-04	1.556E-04	***0.289***	0.500	0.242				
9	1.527E-02	2.917E-04	1.571E-04	***0.293***	0.500	0.239	0.002	-0.025849	-0.095977	14.7
10	1.360E-02	2.954E-04	1.414E-04	***0.285***	0.500	0.245				
11	1.649E-02	2.947E-04	1.771E-04	***0.298***	0.500	0.234	0.006	-0.086268	-0.320316	7.49
12	1.480E-02	2.950E-04	1.571E-04	***0.305***	0.500	0.227				
13	1.480E-02	2.950E-04	1.571E-04	***0.276***	0.500	0.254	-0.013	0.204581	0.760	16.7485
14	1.480E-02	2.950E-04	1.571E-04	***0.291***	**0.500**	0.188				
15	1.480E-02	2.950E-04	1.571E-04	***0.291***	**0.500**	0.292	-0.052	0.802291	2.979	1.43

magnitude 0.0647 **Beta 3.71**
z*alpha 0.0000

Table 18 (cont'd)
(b) End of the Iteration in FORM

Description of Variables	z	Run	Eac(ksi)	Tac (inch)	Ebase (inch)	Esubbase (ksi)	Esg (ksi)	ln(Traffic Volume)	Professional Factor
		1	**403.5**	**8.2**	**29.2**	**14.7**	**7.53**	**16.761**	**1.298**
		2	**516.0**	8.2	29.2	14.7	7.5	16.761	1.298
Eac	-0.41324	3	**291.0**	8.2	29.2	14.7	7.5	16.761	1.298
		4	403.5	**9.2**	29.2	14.7	7.5	16.761	1.298
Tac	-1.84388	5	403.5	**7.2**	29.2	14.7	7.5	16.761	1.298
		6	403.5	8.2	**35.2**	14.7	7.5	16.761	1.298
Ebase	-0.12904	7	403.5	8.2	**23.2**	14.7	7.5	16.761	1.298
		8	403.5	8.2	29.2	**17.7**	7.5	16.761	1.298
Esubbase	-0.10374	9	403.5	8.2	29.2	**11.7**	7.5	16.761	1.298
		10	403.5	8.2	29.2	14.7	**9.13**	16.761	1.298
Esg	-0.29578	11	403.5	8.2	29.2	14.7	**5.93**	16.761	1.298
		12	403.5	8.2	29.2	14.7	7.5	**17.164**	1.298
ln(Traffic Volume)	0.79004	13	403.5	8.2	29.2	14.7	7.5	**16.358**	1.298
		14	403.5	8.2	29.2	14.7	7.5	16.761	**1.477**
Professional Factor	2.26177	15	403.5	8.2	29.2	14.7	7.5	16.761	**1.119**

Run	Maximum Deflection	Maximum Vertical Strain at Base	Maximum Vertical Strain at Subgrade	Predicted Rut-Depth	Threshold Rut-Depth	h(z)	grad(h(z))	alpha	New z	New X
1	**1.797E-02**	**4.339E-04**	**2.066E-04**	***0.38527***	***0.50000***	***0.000***				
2	1.685E-02	3.737E-04	1.924E-04	***0.377***	0.500	0.011				
3	1.958E-02	5.231E-04	2.252E-04	***0.396***	0.500	-0.014	0.013	-0.134686	-0.413431	403.5
4	1.668E-02	3.641E-04	1.842E-04	***0.343***	0.500	0.055				
5	1.951E-02	5.234E-04	2.329E-04	***0.429***	0.500	-0.057	0.056	-0.601049	-1.844968	8.2
6	1.756E-02	3.983E-04	2.020E-04	***0.382***	0.500	0.004				
7	1.847E-02	4.813E-04	2.112E-04	***0.389***	0.500	-0.004	0.004	-0.042059	-0.129102	29.2
8	1.743E-02	4.375E-04	2.034E-04	***0.383***	0.500	0.003				
9	1.865E-02	4.297E-04	2.081E-04	***0.388***	0.500	-0.003	0.003	-0.033817	-0.103804	14.7
10	1.650E-02	4.343E-04	1.851E-04	***0.379***	0.500	0.008				
11	2.008E-02	4.336E-04	2.344E-04	***0.393***	0.500	-0.010	0.009	-0.096420	-0.295968	7.53
12	1.797E-02	4.339E-04	2.066E-04	***0.404***	0.500	-0.024				
13	1.797E-02	4.339E-04	2.066E-04	***0.367***	0.500	0.024	-0.024	0.257461	0.790	16.76087
14	1.797E-02	4.339E-04	2.066E-04	***0.385***	**0.500**	-0.069				
15	1.797E-02	4.339E-04	2.066E-04	***0.385***	**0.500**	0.069	-0.069	0.736277	2.260	1.30

magnitude 0.0935 **beta 3.07**
z*alpha 3.0701

Table 19 Spreadsheet for Reliability Analysis of Pavement Performance Using PEM

	Input Design Variables							Output Results						
Run	Professional Factor	ln(Traffic Volume)	Eac (ksi)	Tac (in)	Ebase (ksi)	Esubbase (ksi)	Esg (ksi)	Maximum Surface Deflection	Maximum Vertical Strain at Base	Maximum Vertical Strain at Subgrade	Predicted Rut-Depth (RD)	p	p(RD)	p(RD^2)
1	1.072	16.845	563	11.0	36	18	9.6	1.142E-02	2.044E-04	1.159E-04	0.2333	0.0078	1.823E-03	4.252E-04
2	1.072	16.845	563	11.0	36	18	6.4	1.401E-02	2.040E-04	1.431E-04	0.2188	0.0078	1.709E-03	3.739E-04
3	1.072	16.845	563	11.0	36	12	9.6	1.203E-02	2.001E-04	1.145E-04	0.2296	0.0078	1.794E-03	4.119E-04
4	1.072	16.845	563	11.0	36	12	6.4	1.473E-02	1.999E-04	1.452E-04	0.2151	0.0078	1.681E-03	3.615E-04
5	1.072	16.845	563	11.0	24	18	9.6	1.181E-02	2.422E-04	1.182E-04	0.2295	0.0078	1.793E-03	4.115E-04
6	1.072	16.845	563	11.0	24	18	6.4	1.446E-02	2.407E-04	1.464E-04	0.2151	0.0078	1.680E-03	3.613E-04
7	1.072	16.845	563	11.0	24	12	9.6	1.243E-02	2.350E-04	1.172E-04	0.2259	0.0078	1.765E-03	3.987E-04
8	1.072	16.845	563	11.0	24	12	6.4	1.518E-02	2.338E-04	1.490E-04	0.2115	0.0078	1.653E-03	3.496E-04
9	1.072	16.845	563	9.0	36	18	9.6	1.308E-02	2.833E-04	1.445E-04	0.1463	0.0078	1.143E-03	1.673E-04
10	1.072	16.845	563	9.0	36	18	6.4	1.594E-02	2.830E-04	1.786E-04	0.1320	0.0078	1.032E-03	1.362E-04
11	1.072	16.845	563	9.0	36	12	9.6	1.390E-02	2.780E-04	1.439E-04	0.1420	0.0078	1.109E-03	1.574E-04
12	1.072	16.845	563	9.0	36	12	6.4	1.691E-02	2.780E-04	1.829E-04	0.1275	0.0078	9.964E-04	1.271E-04
13	1.072	16.845	563	9.0	24	18	9.6	1.365E-02	3.376E-04	1.487E-04	0.1412	0.0078	1.104E-03	1.559E-04
14	1.072	16.845	563	9.0	24	18	6.4	1.657E-02	3.361E-04	1.845E-04	0.1271	0.0078	9.931E-04	1.262E-04
15	1.072	16.845	563	9.0	24	12	9.6	1.448E-02	3.285E-04	1.487E-04	0.1370	0.0078	1.071E-03	1.467E-04
16	1.072	16.845	563	9.0	24	12	6.4	1.756E-02	3.274E-04	1.895E-04	0.1227	0.0078	9.588E-04	1.177E-04
17	1.072	16.845	338	11.0	36	18	9.6	1.334E-02	2.802E-04	1.375E-04	0.2162	0.0078	1.689E-03	3.653E-04
18	1.072	16.845	338	11.0	36	18	6.4	1.611E-02	2.799E-04	1.697E-04	0.2024	0.0078	1.582E-03	3.202E-04
19	1.072	16.845	338	11.0	36	12	9.6	1.412E-02	2.757E-04	1.369E-04	0.2120	0.0078	1.657E-03	3.513E-04
20	1.072	16.845	338	11.0	36	12	6.4	1.702E-02	2.757E-04	1.737E-04	0.1982	0.0078	1.549E-03	3.070E-04
21	1.072	16.845	338	11.0	24	18	9.6	1.391E-02	3.372E-04	1.417E-04	0.2115	0.0078	1.652E-03	3.494E-04
22	1.072	16.845	338	11.0	24	18	6.4	1.674E-02	3.357E-04	1.756E-04	0.1978	0.0078	1.546E-03	3.058E-04
23	1.072	16.845	338	11.0	24	12	9.6	1.470E-02	3.291E-04	1.417E-04	0.2074	0.0078	1.621E-03	3.361E-04
24	1.072	16.845	338	11.0	24	12	6.4	1.768E-02	3.280E-04	1.804E-04	0.1937	0.0078	1.513E-03	2.930E-04
25	1.072	16.845	338	9.0	36	18	9.6	1.507E-02	3.832E-04	1.675E-04	0.1286	0.0078	1.005E-03	1.292E-04
26	1.072	16.845	338	9.0	36	18	6.4	1.809E-02	3.827E-04	2.068E-04	0.1149	0.0078	8.978E-04	1.032E-04
27	1.072	16.845	338	9.0	36	12	9.6	1.608E-02	3.778E-04	1.681E-04	0.1237	0.0078	9.663E-04	1.195E-04
28	1.072	16.845	338	9.0	36	12	6.4	1.928E-02	3.778E-04	2.135E-04	0.1098	0.0078	8.579E-04	9.421E-05
29	1.072	16.845	338	9.0	24	18	9.6	1.586E-02	4.642E-04	1.742E-04	0.1224	0.0078	9.560E-04	1.170E-04
30	1.072	16.845	338	9.0	24	18	6.4	1.897E-02	4.627E-04	2.159E-04	0.1088	0.0078	8.501E-04	9.250E-05
31	1.072	16.845	338	9.0	24	12	9.6	1.691E-02	4.544E-04	1.757E-04	0.1175	0.0078	9.183E-04	1.079E-04
32	1.072	16.845	338	9.0	24	12	6.4	2.020E-02	4.534E-04	2.239E-04	0.1038	0.0078	8.106E-04	8.410E-05

Table 19 (cont'd)

	Input Design Variables							Output Results						
Run	Professional Factor	ln(Traffic Volume)	Eac (ksi)	Tac (in)	Ebase (ksi)	Esubbase (ksi)	Esg (ksi)	Maximum Surface Deflection	Maximum Vertical Strain at Base	Maximum Vertical Strain at Subgrade	Predicted Rut-Depth (RD)	p	p(RD)	p(RD^2)
33	1.072	16.039	563	11.0	36	18	9.6	1.142E-02	2.044E-04	1.159E-04	0.2596	0.0078	2.028E-03	5.265E-04
34	1.072	16.039	563	11.0	36	18	6.4	1.401E-02	2.040E-04	1.431E-04	0.2466	0.0078	1.926E-03	4.750E-04
35	1.072	16.039	563	11.0	36	12	9.6	1.203E-02	2.001E-04	1.145E-04	0.2563	0.0078	2.002E-03	5.132E-04
36	1.072	16.039	563	11.0	36	12	6.4	1.473E-02	1.999E-04	1.452E-04	0.2433	0.0078	1.901E-03	4.624E-04
37	1.072	16.039	563	11.0	24	18	9.6	1.181E-02	2.422E-04	1.182E-04	0.2560	0.0078	2.000E-03	5.122E-04
38	1.072	16.039	563	11.0	24	18	6.4	1.446E-02	2.407E-04	1.464E-04	0.2431	0.0078	1.899E-03	4.617E-04
39	1.072	16.039	563	11.0	24	12	9.6	1.243E-02	2.350E-04	1.172E-04	0.2528	0.0078	1.975E-03	4.994E-04
40	1.072	16.039	563	11.0	24	12	6.4	1.518E-02	2.338E-04	1.490E-04	0.2399	0.0078	1.875E-03	4.498E-04
41	1.072	16.039	563	9.0	36	18	9.6	1.308E-02	2.833E-04	1.445E-04	0.1808	0.0078	1.412E-03	2.554E-04
42	1.072	16.039	563	9.0	36	18	6.4	1.594E-02	2.830E-04	1.786E-04	0.1679	0.0078	1.312E-03	2.203E-04
43	1.072	16.039	563	9.0	36	12	9.6	1.390E-02	2.780E-04	1.439E-04	0.1769	0.0078	1.382E-03	2.443E-04
44	1.072	16.039	563	9.0	36	12	6.4	1.691E-02	2.780E-04	1.829E-04	0.1639	0.0078	1.280E-03	2.098E-04
45	1.072	16.039	563	9.0	24	18	9.6	1.365E-02	3.376E-04	1.487E-04	0.1760	0.0078	1.375E-03	2.420E-04
46	1.072	16.039	563	9.0	24	18	6.4	1.657E-02	3.361E-04	1.845E-04	0.1633	0.0078	1.276E-03	2.083E-04
47	1.072	16.039	563	9.0	24	12	9.6	1.448E-02	3.285E-04	1.487E-04	0.1722	0.0078	1.345E-03	2.317E-04
48	1.072	16.039	563	9.0	24	12	6.4	1.756E-02	3.274E-04	1.895E-04	0.1593	0.0078	1.245E-03	1.983E-04
49	1.072	16.039	338	11.0	36	18	9.6	1.334E-02	2.802E-04	1.375E-04	0.2437	0.0078	1.904E-03	4.639E-04
50	1.072	16.039	338	11.0	36	18	6.4	1.611E-02	2.799E-04	1.697E-04	0.2313	0.0078	1.807E-03	4.179E-04
51	1.072	16.039	338	11.0	36	12	9.6	1.412E-02	2.757E-04	1.369E-04	0.2399	0.0078	1.874E-03	4.497E-04
52	1.072	16.039	338	11.0	36	12	6.4	1.702E-02	2.757E-04	1.737E-04	0.2275	0.0078	1.777E-03	4.042E-04
53	1.072	16.039	338	11.0	24	18	9.6	1.391E-02	3.372E-04	1.417E-04	0.2392	0.0078	1.869E-03	4.471E-04
54	1.072	16.039	338	11.0	24	18	6.4	1.674E-02	3.357E-04	1.756E-04	0.2270	0.0078	1.773E-03	4.025E-04
55	1.072	16.039	338	11.0	24	12	9.6	1.470E-02	3.291E-04	1.417E-04	0.2356	0.0078	1.841E-03	4.336E-04
56	1.072	16.039	338	11.0	24	12	6.4	1.768E-02	3.280E-04	1.804E-04	0.2232	0.0078	1.744E-03	3.892E-04
57	1.072	16.039	338	9.0	36	18	9.6	1.507E-02	3.832E-04	1.675E-04	0.1641	0.0078	1.282E-03	2.103E-04
58	1.072	16.039	338	9.0	36	18	6.4	1.809E-02	3.827E-04	2.068E-04	0.1518	0.0078	1.186E-03	1.799E-04
59	1.072	16.039	338	9.0	36	12	9.6	1.608E-02	3.778E-04	1.681E-04	0.1597	0.0078	1.247E-03	1.991E-04
60	1.072	16.039	338	9.0	36	12	6.4	1.928E-02	3.778E-04	2.135E-04	0.1471	0.0078	1.149E-03	1.691E-04
61	1.072	16.039	338	9.0	24	18	9.6	1.586E-02	4.642E-04	1.742E-04	0.1582	0.0078	1.236E-03	1.956E-04
62	1.072	16.039	338	9.0	24	18	6.4	1.897E-02	4.627E-04	2.159E-04	0.1460	0.0078	1.141E-03	1.665E-04
63	1.072	16.039	338	9.0	24	12	9.6	1.691E-02	4.544E-04	1.757E-04	0.1539	0.0078	1.202E-03	1.850E-04
64	1.072	16.039	338	9.0	24	12	6.4	2.020E-02	4.534E-04	2.239E-04	0.1414	0.0078	1.105E-03	1.562E-04

Table 19 (cont'd)

	Input Design Variables							Output Results						
Run	Professional Factor	ln(Traffic Volume)	Eac (ksi)	Tac (in)	Ebase (ksi)	Esubbase (ksi)	Esg (ksi)	Maximum Surface Deflection	Maximum Vertical Strain at Base	Maximum Vertical Strain at Subgrade	Predicted Rut-Depth (RD)	p	p(RD)	p(RD^2)
65	0.715	16.845	563	11.0	36	18	9.6	1.142E-02	2.044E-04	1.159E-04	0.3222	0.0078	2.517E-03	8.110E-04
66	0.715	16.845	563	11.0	36	18	6.4	1.401E-02	2.040E-04	1.431E-04	0.3125	0.0078	2.442E-03	7.630E-04
67	0.715	16.845	563	11.0	36	12	9.6	1.203E-02	2.001E-04	1.145E-04	0.3197	0.0078	2.498E-03	7.987E-04
68	0.715	16.845	563	11.0	36	12	6.4	1.473E-02	1.999E-04	1.452E-04	0.3101	0.0078	2.422E-03	7.511E-04
69	0.715	16.845	563	11.0	24	18	9.6	1.181E-02	2.422E-04	1.182E-04	0.3197	0.0078	2.497E-03	7.983E-04
70	0.715	16.845	563	11.0	24	18	6.4	1.446E-02	2.407E-04	1.464E-04	0.3100	0.0078	2.422E-03	7.510E-04
71	0.715	16.845	563	11.0	24	12	9.6	1.243E-02	2.350E-04	1.172E-04	0.3173	0.0078	2.479E-03	7.864E-04
72	0.715	16.845	563	11.0	24	12	6.4	1.518E-02	2.338E-04	1.490E-04	0.3077	0.0078	2.404E-03	7.396E-04
73	0.715	16.845	563	9.0	36	18	9.6	1.308E-02	2.833E-04	1.445E-04	0.2642	0.0078	2.064E-03	5.455E-04
74	0.715	16.845	563	9.0	36	18	6.4	1.594E-02	2.830E-04	1.786E-04	0.2547	0.0078	1.990E-03	5.068E-04
75	0.715	16.845	563	9.0	36	12	9.6	1.390E-02	2.780E-04	1.439E-04	0.2613	0.0078	2.041E-03	5.335E-04
76	0.715	16.845	563	9.0	36	12	6.4	1.691E-02	2.780E-04	1.829E-04	0.2517	0.0078	1.966E-03	4.949E-04
77	0.715	16.845	563	9.0	24	18	9.6	1.365E-02	3.376E-04	1.487E-04	0.2608	0.0078	2.038E-03	5.315E-04
78	0.715	16.845	563	9.0	24	18	6.4	1.657E-02	3.361E-04	1.845E-04	0.2514	0.0078	1.964E-03	4.938E-04
79	0.715	16.845	563	9.0	24	12	9.6	1.448E-02	3.285E-04	1.487E-04	0.2580	0.0078	2.016E-03	5.201E-04
80	0.715	16.845	563	9.0	24	12	6.4	1.756E-02	3.274E-04	1.895E-04	0.2485	0.0078	1.941E-03	4.824E-04
81	0.715	16.845	338	11.0	36	18	9.6	1.334E-02	2.802E-04	1.375E-04	0.3108	0.0078	2.428E-03	7.547E-04
82	0.715	16.845	338	11.0	36	18	6.4	1.611E-02	2.799E-04	1.697E-04	0.3016	0.0078	2.357E-03	7.108E-04
83	0.715	16.845	338	11.0	36	12	9.6	1.412E-02	2.757E-04	1.369E-04	0.3080	0.0078	2.406E-03	7.413E-04
84	0.715	16.845	338	11.0	36	12	6.4	1.702E-02	2.757E-04	1.737E-04	0.2988	0.0078	2.335E-03	6.976E-04
85	0.715	16.845	338	11.0	24	18	9.6	1.391E-02	3.372E-04	1.417E-04	0.3076	0.0078	2.403E-03	7.394E-04
86	0.715	16.845	338	11.0	24	18	6.4	1.674E-02	3.357E-04	1.756E-04	0.2986	0.0078	2.333E-03	6.964E-04
87	0.715	16.845	338	11.0	24	12	9.6	1.470E-02	3.291E-04	1.417E-04	0.3050	0.0078	2.382E-03	7.265E-04
88	0.715	16.845	338	11.0	24	12	6.4	1.768E-02	3.280E-04	1.804E-04	0.2958	0.0078	2.311E-03	6.835E-04
89	0.715	16.845	338	9.0	36	18	9.6	1.507E-02	3.832E-04	1.675E-04	0.2524	0.0078	1.972E-03	4.976E-04
90	0.715	16.845	338	9.0	36	18	6.4	1.809E-02	3.827E-04	2.068E-04	0.2433	0.0078	1.901E-03	4.624E-04
91	0.715	16.845	338	9.0	36	12	9.6	1.608E-02	3.778E-04	1.681E-04	0.2491	0.0078	1.946E-03	4.849E-04
92	0.715	16.845	338	9.0	36	12	6.4	1.928E-02	3.778E-04	2.135E-04	0.2399	0.0078	1.874E-03	4.495E-04
93	0.715	16.845	338	9.0	24	18	9.6	1.586E-02	4.642E-04	1.742E-04	0.2482	0.0078	1.939E-03	4.814E-04
94	0.715	16.845	338	9.0	24	18	6.4	1.897E-02	4.627E-04	2.159E-04	0.2392	0.0078	1.869E-03	4.470E-04
95	0.715	16.845	338	9.0	24	12	9.6	1.691E-02	4.544E-04	1.757E-04	0.2450	0.0078	1.914E-03	4.690E-04
96	0.715	16.845	338	9.0	24	12	6.4	2.020E-02	4.534E-04	2.239E-04	0.2358	0.0078	1.842E-03	4.345E-04

Table 19 (cont'd)

	Input Design Variables							Output Results						
Run	Professional Factor	ln(Traffic Volume)	Eac (ksi)	Tac (in)	Ebase (ksi)	Esubbase (ksi)	Esg (ksi)	Maximum Surface Deflection	Maximum Vertical Strain at Base	Maximum Vertical Strain at Subgrade	Predicted Rut-Depth (RD)	p	p(RD)	p(RD^2)
97	0.715	16.039	563	11.0	36	18	9.6	1.142E-02	2.044E-04	1.159E-04	0.3397	0.0078	2.654E-03	9.017E-04
98	0.715	16.039	563	11.0	36	18	6.4	1.401E-02	2.040E-04	1.431E-04	0.3311	0.0078	2.586E-03	8.562E-04
99	0.715	16.039	563	11.0	36	12	9.6	1.203E-02	2.001E-04	1.145E-04	0.3375	0.0078	2.637E-03	8.900E-04
100	0.715	16.039	563	11.0	36	12	6.4	1.473E-02	1.999E-04	1.452E-04	0.3289	0.0078	2.569E-03	8.449E-04
101	0.715	16.039	563	11.0	24	18	9.6	1.181E-02	2.422E-04	1.182E-04	0.3374	0.0078	2.636E-03	8.892E-04
102	0.715	16.039	563	11.0	24	18	6.4	1.446E-02	2.407E-04	1.464E-04	0.3287	0.0078	2.568E-03	8.443E-04
103	0.715	16.039	563	11.0	24	12	9.6	1.243E-02	2.350E-04	1.172E-04	0.3352	0.0078	2.619E-03	8.780E-04
104	0.715	16.039	563	11.0	24	12	6.4	1.518E-02	2.338E-04	1.490E-04	0.3266	0.0078	2.552E-03	8.335E-04
105	0.715	16.039	563	9.0	36	18	9.6	1.308E-02	2.833E-04	1.445E-04	0.2872	0.0078	2.244E-03	6.444E-04
106	0.715	16.039	563	9.0	36	18	6.4	1.594E-02	2.830E-04	1.786E-04	0.2786	0.0078	2.177E-03	6.065E-04
107	0.715	16.039	563	9.0	36	12	9.6	1.390E-02	2.780E-04	1.439E-04	0.2846	0.0078	2.223E-03	6.326E-04
108	0.715	16.039	563	9.0	36	12	6.4	1.691E-02	2.780E-04	1.829E-04	0.2759	0.0078	2.156E-03	5.948E-04
109	0.715	16.039	563	9.0	24	18	9.6	1.365E-02	3.376E-04	1.487E-04	0.2840	0.0078	2.219E-03	6.301E-04
110	0.715	16.039	563	9.0	24	18	6.4	1.657E-02	3.361E-04	1.845E-04	0.2755	0.0078	2.153E-03	5.931E-04
111	0.715	16.039	563	9.0	24	12	9.6	1.448E-02	3.285E-04	1.487E-04	0.2815	0.0078	2.199E-03	6.190E-04
112	0.715	16.039	563	9.0	24	12	6.4	1.756E-02	3.274E-04	1.895E-04	0.2729	0.0078	2.132E-03	5.818E-04
113	0.715	16.039	338	11.0	36	18	9.6	1.334E-02	2.802E-04	1.375E-04	0.3291	0.0078	2.571E-03	8.462E-04
114	0.715	16.039	338	11.0	36	18	6.4	1.611E-02	2.799E-04	1.697E-04	0.3209	0.0078	2.507E-03	8.043E-04
115	0.715	16.039	338	11.0	36	12	9.6	1.412E-02	2.757E-04	1.369E-04	0.3266	0.0078	2.552E-03	8.334E-04
116	0.715	16.039	338	11.0	36	12	6.4	1.702E-02	2.757E-04	1.737E-04	0.3183	0.0078	2.487E-03	7.916E-04
117	0.715	16.039	338	11.0	24	18	9.6	1.391E-02	3.372E-04	1.417E-04	0.3261	0.0078	2.548E-03	8.310E-04
118	0.715	16.039	338	11.0	24	18	6.4	1.674E-02	3.357E-04	1.756E-04	0.3180	0.0078	2.484E-03	7.899E-04
119	0.715	16.039	338	11.0	24	12	9.6	1.470E-02	3.291E-04	1.417E-04	0.3237	0.0078	2.529E-03	8.187E-04
120	0.715	16.039	338	11.0	24	12	6.4	1.768E-02	3.280E-04	1.804E-04	0.3155	0.0078	2.465E-03	7.774E-04
121	0.715	16.039	338	9.0	36	18	9.6	1.507E-02	3.832E-04	1.675E-04	0.2760	0.0078	2.157E-03	5.953E-04
122	0.715	16.039	338	9.0	36	18	6.4	1.809E-02	3.827E-04	2.068E-04	0.2678	0.0078	2.092E-03	5.604E-04
123	0.715	16.039	338	9.0	36	12	9.6	1.608E-02	3.778E-04	1.681E-04	0.2731	0.0078	2.134E-03	5.827E-04
124	0.715	16.039	338	9.0	36	12	6.4	1.928E-02	3.778E-04	2.135E-04	0.2647	0.0078	2.068E-03	5.475E-04
125	0.715	16.039	338	9.0	24	18	9.6	1.586E-02	4.642E-04	1.742E-04	0.2721	0.0078	2.126E-03	5.786E-04
126	0.715	16.039	338	9.0	24	18	6.4	1.897E-02	4.627E-04	2.159E-04	0.2640	0.0078	2.062E-03	5.445E-04
127	0.715	16.039	338	9.0	24	12	9.6	1.691E-02	4.544E-04	1.757E-04	0.2692	0.0078	2.103E-03	5.664E-04
128	0.715	16.039	338	9.0	24	12	6.4	2.020E-02	4.534E-04	2.239E-04	0.2609	0.0078	2.038E-03	5.319E-04
											Sum:	1.0000	0.2379	0.0609

E[RD] 0.238

Var[RD] 0.004

s[RD] 0.066

Beta **3.62**

Table 20 Summary of the Results of Reliability Analysis for Pavement Performance
(a) Section 1

	MVFOSM	PEM	FORM
$E[SM_{rut}]$	0.162	0.160	-
$\sigma[SM_{rut}]$	0.075	0.076	-
$COV[SM_{rut}]$	0.463	0.475	-
Reliability Index	2.17	2.11	2.01
Number of Runs	15	128	90

(b) Section 2

	MVFOSM	PEM	FORM
$E[SM_{rut}]$	0.240	0.238	-
$\sigma[SM_{rut}]$	0.065	0.066	-
$COV[SM_{rut}]$	0.271	0.277	-
Reliability Index	3.71	3.62	3.07
Number of Runs	15	128	90

CHAPTER VI

DEVELOPMENT OF PRACTICAL RELIABILITY-BASED M-E FLEXIBLE PAVEMENT DESIGN ALGORITHMS

General

In Chapter V, engineering reliability techniques that can be applied to pavement structural analysis were presented. In this chapter, illustrative examples will be presented demonstrating the application of reliability algorithms to M-E flexible pavement design.

Method 1: Reliability Factor Design (RFD) Approach

The basic concept in the reliability-based design is that the reliability associated with an appropriate design equation should equal a target value representing a certain degree of structural safety. Using the rut prediction model, this study suggests a main pavement design equation with a target reliability, R^* :

$$RD_{max} = S_o * \beta_{target} + RD_{predicted} \quad (51)$$

where :

β_{target} = target reliability index defined as $\phi^{-1}(R^*)$, in which ϕ is the cumulative distribution function of a standard normal variate.

Based on equation 51, the pavement is designed to accommodate a cumulative traffic volume that is expected during its intended service life, there is a probability R^* that the pavement will not fail before total rut-depth caused by the cumulative traffic volume reaches a maximum allowable level. In this equation, the product of the overall standard deviation and target reliability index is defined as the reliability factor (RF) to represent a specified level of structural safety. Thus, the pavement design procedure using this equation can be called as the M-E flexible pavement design procedure using the

reliability factor design (RFD) approach. Table 21 shows a relationship between the target reliability index and its corresponding reliability. In principle, an optimum target reliability index can be determined by performing a life cycle cost analysis (LCCA) as shown in Figure 19 [16]. It is theoretically possible to reach the most economical target reliability by estimating initial cost and future cost including maintenance and rehabilitation costs, and establishing an optimal strategy. At the present time, however, it is reported by Brown et, al. that such an approach is impractical because the inference space over which a pavement design guide is being applied is much too large that the formulation of LCCA is difficult in practice [47]. This means that for the time being, the most practical way to assign the optimal target reliability of the pavement is to depend on reasonable engineering judgement of experienced pavement designers [48]. The basic objective of the reliability-based design of the pavement is to guarantee that the probability of unsatisfactory performance of a pavement lies below an intended target level. If this probability is located far below the target level, the objective is explicitly achieved. However, that design is uneconomical and the reliability concept in the design is misapplied.

Modeling and Analysis of the Uncertainties in RFD Approach

As described in the previous sections, the uncertainties associated with predicting the pavement performance can be quantified with five steps by considering their sources and types.

Table 21 Relationship between Target Reliability Level and its Corresponding Reliability Index

Target Reliability (R^*)	Target Reliability Index $\left(\beta_{target} = \phi^{-1}\left(R^*\right)\right)$
50%	0
60%	0.253
70%	0.524
75%	0.674
80%	0.841
85%	1.037
90%	1.282
95%	1.645
99%	2.054

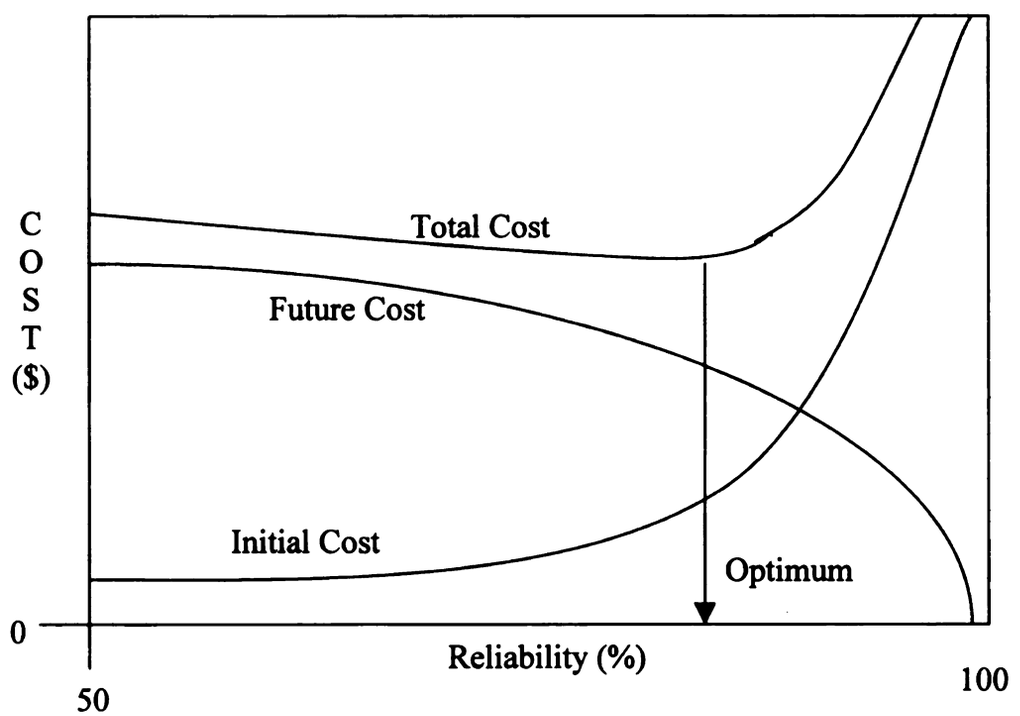

Figure 19 Approach to Identifying the Optimum Reliability Level for a Given Pavement [16]

1. Integrate uncertainties due to spatial variation ($V_{Spatial}$) and uncertainties due to imprecision in quantifying parameters ($V_{\text{Im precision in Quantifying Parameter}}$) into parameter uncertainties ($V_{Parameter\ Uncertainty}$).

2. Using FOSM or PEM, quantify $V_{Parameter\ Uncertainty}$ in terms of a standard deviation (S_p) of pavement performance predicted by M-E design procedure.

3. Integrate model bias in pavement structural analysis ($V_{Model\ Bias}$) and statistical error due to the lack of fit of the transfer function ($V_{Statistical\ Error}$) into systematic error of the M-E design procedure ($V_{Systematic\ Error}$)

4. Quantify $V_{Systematic\ Error}$ in terms of a standard deviation (S_m) of pavement performance predicted by M-E design procedure. The technique for quantifying $V_{Systematic\ Error}$ will be introduced later.

5. Determine overall standard deviation (S_o) of a pavement performance predicted by M-E design procedure as:

$$S_o = \sqrt{S_p^2 + S_m^2} \tag{52}$$

These steps are summarized in equation 53.

$$V_{Total} = \begin{cases} V_{Parameter\ Uncertainty} \begin{cases} V_{Spatial} \\ +V_{\text{Im precision in quantifying parameter}} \end{cases} \\ +V_{Systematic\ Error} \begin{cases} V_{Model\ Bias} \\ +V_{Statistical\ Error} \end{cases} \end{cases} \tag{53}$$

where:

V_{Total} = total uncertainty in an prediction of the pavement performance, expressed as a variance.

Even if the variations of design parameters are adequately quantified and their effects on pavement performance function are considered in a reasonable probabilistic manner, a predictive value by the pavement performance function still has a possibility to deviate from the actual value because of systematic error. It is very difficult to estimate the variations of predicted values due to this error [38]. The most precise approach to handle this error is to independently treat agents (modeling bias and statistical error) of the error and quantify each of them. However, this approach could yield an excessively sophisticated analysis procedure to pavement engineers and requires elaborate experiments and investigations in order to obtain adequate values. Thus, in this study, an integrated quantification of these agents of the systematic error is used as shown in equation 53. The variance caused by the systematic error in a prediction of pavement performance was estimated by the following equation [39]:

$$S_m^{\,2} \approx MSE + \underline{X}'_m s^2\{g\}\underline{X}_m \tag{54}$$

where :

MSE	=	error mean square of the performance function,
$\underline{X}_m$	=	gradient vector of the coefficients of the performance function, which is evaluated at the mean values of the independent variables of the function, and
$s^2\{g\}$	=	variance-covariance matrix of the coefficients of the performance function.

Using the revised rut prediction model in this study as the performance function, $\underline{X}_m$ is derived as follows:

$$\underline{X}_m = \frac{\partial RD}{\partial \underline{a}} = \begin{Bmatrix} \partial RD/\partial a_1 \\ \partial RD/\partial a_2 \\ \vdots \\ \vdots \\ \partial RD/\partial a_n \end{Bmatrix} \tag{55}$$

where :

RD	=	rutting prediction model developed in this study, and
$\underline{a}$	=	vector of the coefficients of the rutting prediction model.

$s^2\{g\}$ can be approximately estimated by :

$$s^2\{g\} = MSE(D'D)^{-1} \tag{56}$$

where :

D	=	the matrix of partial derivatives of the coefficients evaluated at all data points as follows:

$$D = \begin{bmatrix} \frac{\partial RD}{\partial a_1}\Big|_{\underline{X}_1} & \frac{\partial RD}{\partial a_2}\Big|_{\underline{X}_1} & \frac{\partial RD}{\partial a_3}\Big|_{\underline{X}_1} & \frac{\partial RD}{\partial a_4}\Big|_{\underline{X}_1} & \frac{\partial RD}{\partial a_5}\Big|_{\underline{X}_1} & \frac{\partial RD}{\partial a_6}\Big|_{\underline{X}_1} & \frac{\partial RD}{\partial a_7}\Big|_{\underline{X}_1} & \frac{\partial RD}{\partial a_8}\Big|_{\underline{X}_1} & \frac{\partial RD}{\partial a_9}\Big|_{\underline{X}_1} & \frac{\partial RD}{\partial a_{10}}\Big|_{\underline{X}_1} & \frac{\partial RD}{\partial a_{11}}\Big|_{\underline{X}_1} \\ \frac{\partial RD}{\partial a_1}\Big|_{\underline{X}_2} & \frac{\partial RD}{\partial a_2}\Big|_{\underline{X}_2} & \frac{\partial RD}{\partial a_3}\Big|_{\underline{X}_2} & \frac{\partial RD}{\partial a_4}\Big|_{\underline{X}_2} & \frac{\partial RD}{\partial a_5}\Big|_{\underline{X}_2} & \frac{\partial RD}{\partial a_6}\Big|_{\underline{X}_2} & \frac{\partial RD}{\partial a_7}\Big|_{\underline{X}_2} & \frac{\partial RD}{\partial a_8}\Big|_{\underline{X}_2} & \frac{\partial RD}{\partial a_9}\Big|_{\underline{X}_2} & \frac{\partial RD}{\partial a_{10}}\Big|_{\underline{X}_2} & \frac{\partial RD}{\partial a_{11}}\Big|_{\underline{X}_2} \\ \vdots & \vdots & \vdots & \vdots & \vdots & \vdots & \vdots & \vdots & \vdots & \vdots & \vdots \\ \vdots & \vdots & \vdots & \vdots & \vdots & \vdots & \vdots & \vdots & \vdots & \vdots & \vdots \\ \frac{\partial RD}{\partial a_1}\Big|_{\underline{X}_n} & \frac{\partial RD}{\partial a_2}\Big|_{\underline{X}_n} & \frac{\partial RD}{\partial a_3}\Big|_{\underline{X}_n} & \frac{\partial RD}{\partial a_4}\Big|_{\underline{X}_n} & \frac{\partial RD}{\partial a_5}\Big|_{\underline{X}_n} & \frac{\partial RD}{\partial a_6}\Big|_{\underline{X}_n} & \frac{\partial RD}{\partial a_7}\Big|_{\underline{X}_n} & \frac{\partial RD}{\partial a_8}\Big|_{\underline{X}_n} & \frac{\partial RD}{\partial a_9}\Big|_{\underline{X}_n} & \frac{\partial RD}{\partial a_{10}}\Big|_{\underline{X}_n} & \frac{\partial RD}{\partial a_{11}}\Big|_{\underline{X}_n} \end{bmatrix} \tag{57}$$

M-E Flexible Pavement Design Procedure Using RFD Approach

In light of the principles mentioned in the above section and using equation 52, a detailed reliability-based M-E flexible pavement design procedure called the Reliability Factor Based Design (RFD), is suggested:

Step 1: Prepare input data

- Input Data : Cross Sectional Data
  Layers' Moduli
  Target Reliability Level
  Overall Standard Deviation (based on S_p and S_{input})
  Maximum Allowable Rut-Depth (RD_{max})
  Environmental Information
  Expected Cumulative Traffic Volume (N)

Step 2: Calculate primary structural responses (e.g. deflection, stress, and strain) and predicted rut-depth ($RD_{predicted}$)

Step 3: Until the difference between RD_{max} and $RD_{predicted}$ converges to a specified tolerance level, iterate through steps 1 and 2 with changing cross sectional data or layer moduli.

Step 4: Produce final cross-section design of the pavement structure.

A flowchart illustrating this procedure is shown in Figure 20. In an effort to be compatible with current MDOT design practices that utilizes specified thickness for aggregate base and subbase layers, the pavement designer is asked to consider changing the bituminous layer's properties.

Sample Experimental Design Matrix

In order to determine a rational value for the standard deviation (S_p) associated with the uncertainties of design parameters in RFD, a factorial experiment matrix with thirty-six cells was designed and is summarized in Table 22. Each cell represents a specific design feature. The factorial matrix provides a simple but effective way to relate design features to site conditions. Three major design variables of traffic volume, AC thickness, and resilient modulus of subgrade were selected and included in the matrix. High, moderate, and low values for each variable were determined based on the findings reported in NCHRP 1-32 project and MDOT pavement design practice [26].

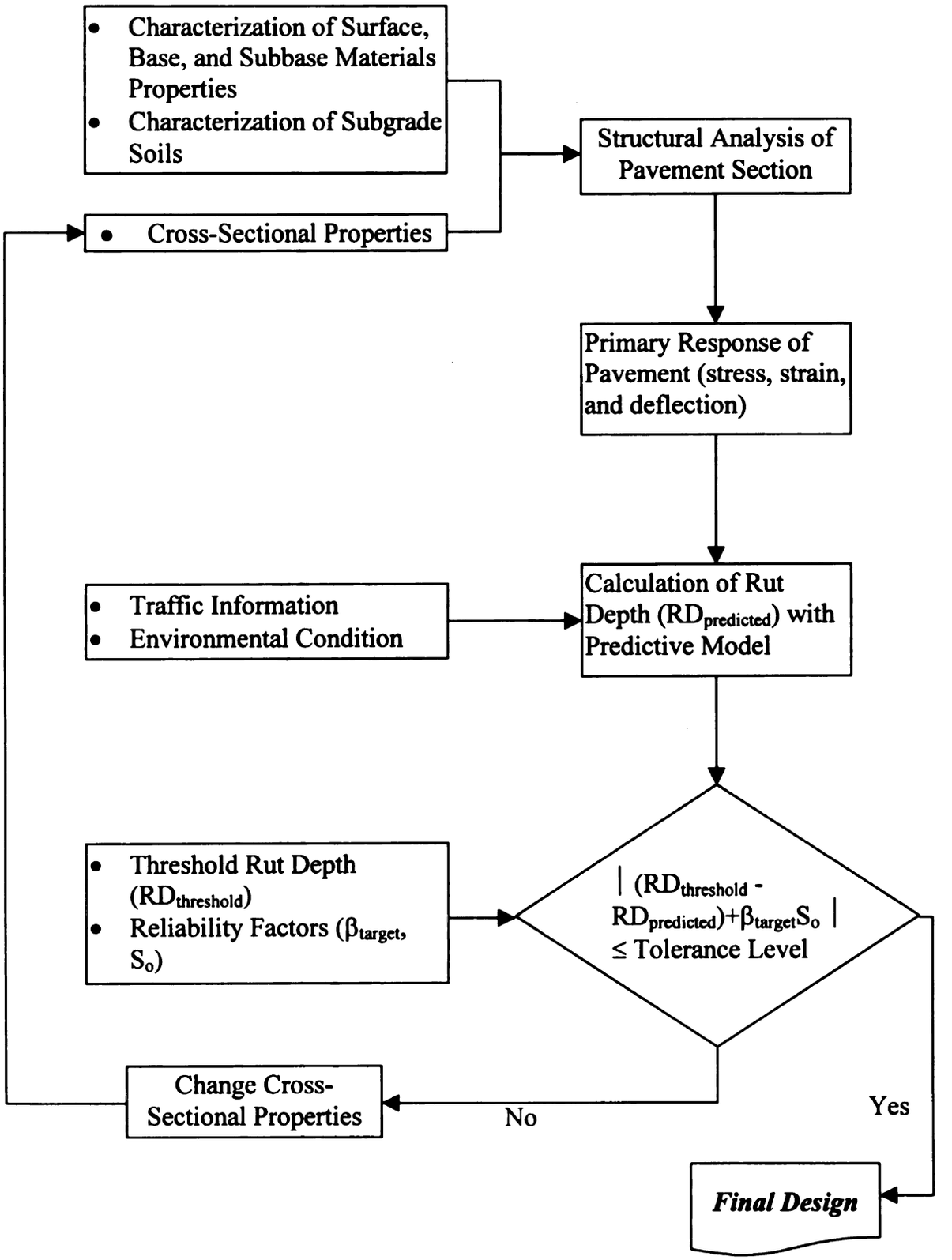

Figure 20 Flowchart for M-E Flexible Pavement Design Procedure Using RFD Approach

Table 22 Factorial Experiment Matrix with Major Design Variables (AC Thickness, Subgrade Modulus, and Traffic)

Traffic Volume (ESAL)		1.0.E+06			5.0E+06			1.5E+07		
Subgrade Modulus (ksi)		4	8	14	4	8	14	4	8	14
AC Thickness (inch)										
	3	1	2	3	4	5	6	7	8	9
	5	10	11	12	13	14	15	16	17	18
	7	19	20	21	22	23	24	25	26	27
	10	28	29	30	31	32	33	34	35	36

Table 23 Standard Deviations Associated with Parameter Uncertainties

Traffic Volume (ESAL)		1.0.E+06			5.0E+06			1.5E+07		
Subgrade Modulus (ksi)		4	8	14	4	8	14	4	8	14
AC Thickness (inch)										
	3	0.034	0.033	0.036	0.036	0.035	0.034			
	5				0.036	0.034	0.034			
	7				0.036	0.035	0.034	0.039	0.039	0.038
	10							0.044	0.043	0.043

The eighteen shaded cells in Table 22 were considered and the individual S_p's were computed by the MVFOSM with 0.5 inches of rut depth as a threshold value. The same statistical conditions as those in the illustrative example of Chapter V were used in the computations. The results are shown in Table 23. As can be seen in Table 23, the pavements that are subjected to heavier traffic volume and designed with a thicker AC layer have a larger standard deviation. With this finding, one can explain why the pavement of the interstate or urban freeway that always accommodates heavy traffic volume should be designed with a higher level of design reliability. It is necessary in heavy-duty pavements to reduce the possibility of underestimating traffic volume with higher variance. The design S_p was determined as 0.036 from those in Table 23, while the design S_m was calculated as 0.066 from an analysis of the data collected in this study using equation 54 to 57. Then S_o for the design was calculated as 0.076.

Illustration of RFD Approach

Figure 21 shows an example of the design outputs computed by selected design input parameters in the spreadsheet. As mentioned in the above section, the design procedure uses an iterative process to produce an optimal pavement cross-section whose structural resistance allows total permanent deformation to closely reach a threshold amount at the end of design life. A tolerance level of 0.01 inch was used in this study. The explanations of the design steps shown in Figure 21 are as follow:

(a) Initial Stage

1.Site Condition and Design Criterion

Traffic Volume (N)	4.0.E+06	EASL
Reliability Level	0.8	
$RD_{threshold}$	0.5	in
Annual Temperature	45	(^{o}F)
Subgrade Resilient Moduli	8000	psi

2.Material and Cross-Sectional Inputs

	AC	Base	Subbase
Thickness (in)	2.2	8.0	16.0
cm	5.6	20.3	40.6
Moduli (psi)	450000	30000	15000
Moduli (kPa)	3100500	206700	103350
Asphalt Type		AC 10	
Kinematic Viscosity		273	centistoke

3.Degree of Uncertainty

S_m	0.066	**S_p**	0.036
S_o	0.076		

4.Intermediate Variables from Structural Analysis

Surface Deflection	Strain_Base	Strain-Subgrade
3.400E-02	1.627E-03	4.255E-04

5.Design Outputs

$RD_{predicted}$	0.54
β_{target}	0.84

6. Decision

Tolerance Level		**$RD_{threshold}$-($RD_{predicted}+S_o*\beta_{target}$)**
0.01	<	0.108

Adjust 2.Material and Cross-section Inputs

Figure 21 Illustration of M-E Flexible Pavement Design Using RFD Approach

(b) Final Stage (End of the Iteration)

1.Site Condition and Design Criterion

Traffic Volume (N)	4.0.E+06	EASL
Reliability Level	0.8	
$RD_{threshold}$	0.5	in
Annual Temperature	45	(°F)
Subgrade Resilient Moduli	8000	psi

2.Material and Cross-Sectional Inputs

	AC	**Base**	**Subbase**
Thickness (in)	4.5	8.0	16.0
cm	11.4	20.3	40.6
Moduli (psi)	450000	30000	15000
Moduli (kPa)	3100500	206700	103350
Asphalt Type		AC 10	
Kinematic Viscosity		273	centistoke

3.Degree of Uncertainty

S_m	0.066	**S_p**	0.036
S_o	0.076		

4.Intermediate Variables from Structural Analysis

Surface Deflection	**Strain_Base**	**Strain-Subgrade**
2.435E-02	8.804E-04	3.117E-04

5.Design Outputs

$RD_{predicted}$	0.44
β_{target}	0.84

6. Decision

Tolerance Level		**$RD_{threshold}$ - ($RD_{predicted}$+S_o*β_{target})**
0.01	>	0.000

O.K.

Figure 21 (cont'd)

1. The user is required to input expected traffic volume during pavement service life, a desired reliability level, a threshold rut-depth as failure criterion ($RD_{threshold}$), ambient annual temperature around the site, and effective resilient modulus of the subgrade soil of the site.
2. The user needs to set up initial pavement cross-sectional and material properties.
3. The user needs to determine a certain degree of uncertainty accompanied with the design procedure in terms of an overall standard deviation of the design model (S_o): The S_m, S_p, and S_o of 0.066, 0.036 and 0.076 are considered as default values.
4. The pavement analysis computer program computes the surface deflection and compressive vertical strains at the top of the base layer and subgrade.
5. A predictive pavement rut-depth ($RD_{predicted}$) is computed using the developed rutting prediction model, and the desired reliability level set up in step 1 is converted to the target reliability index (β), which is a standard normal variate of the desired reliability.
6. If $RD_{threshold} - (RD_{predicted}+S_o*\beta) >$ a specified tolerance level, the pavement cross-section should be modified and step 2 through 6 repeated until $RD_{threshold} - (RD_{predicted}+S_o*\beta) \leq$ the tolerance level. When the iteration is stopped, the cross-section at the final iteration becomes the design pavement cross-section.

Method 2: Load and Resistance Factor Design (LRFD) Approach

In this section, a reliability-based M-E flexible pavement design procedure adopting the LRFD format is presented. The basic concept of the LRFD approach applied to this study can be expressed as follows:

$$D_{threshold} \geq \gamma_{overall} f_R(q_1, q_2, \ldots\ldots q_n) \quad (58)$$

where:

$D_{threshold}$	=	Threshold amount of pavement distress,
$\gamma_{overall}$	=	Overall safety factor reflecting a specified target reliability,
f_R	=	Procedure for predicting pavement performance in terms of pavement distress, and
q_i	=	Parameters in a pavement design procedure.

The specific form of the model for this study where pavement rutting is considered as a major pavement distress can be written as follows:

$$RD_{threshold} \geq \gamma_{overall} f_R(H_{AC}, E_{AC}, E_{Base}, E_{SB}, E_{SG}, N) \quad (59)$$

where :

H_{AC}	=	AC thickness,
E_{AC}	=	Modulus of AC,
E_{Base}	=	Modulus of Base,
E_{SB}	=	Modulus of Subbase,
E_{SG}	=	Modulus of Subgrade, and
N	=	Traffic Volume.

The $\gamma_{overall}$ required to obtain a target reliability index, β_{target} can be determined by following partial safety factor approach using FORM, for which an iterative evaluation procedure was described previously.

$$\gamma_{overall} = \frac{f_R\left(\phi_{H_{AC}} H_{AC}, \phi_{E_{AC}} E_{AC}, \phi_{E_{Base}} E_{Base}, \phi_{E_{SG}}, \phi_{E_{SB}} E_{SB}, E_{SG}, \gamma_N N\right)}{f_R(T_{AC}, E_{AC}, E_{Base}, E_{SG}, N)} \quad (60)$$

where :

ϕ_i or γ_j is a partial safety factor of each variable for reduction or amplification of its amount.

For a specified β_{target}, ϕ_i and γ_j can be calculated by the following equations [49].

$$\phi_i = \left(\frac{m_i}{n_i}\right)\left(1 + \alpha_i \beta_{target} COV_i\right) \quad (61)$$

$$\gamma_j = \left(\frac{m_j}{n_j}\right)\left(1 + \alpha_j \beta_{target} COV_j\right) \tag{62}$$

where:

n	=	Nominal values of design variables,
α	=	Unit vectors associated with the design point, and
COV	=	Coefficients of variations of variables of design variables.

The selection of the nominal values of design variables is typically performed on the basis of the judgement of the pavement engineer. In this study, the nominal values of design variables were assumed to be their mean values.

If r_j is a lognormally distributed loading variable, then [49]

$$\gamma_j = \frac{m_j}{n_j}\exp\left(-0.5\ln\left(COV_j^2 + 1\right) + \alpha_j \beta_{target}\left(\ln\left(COV_j^2 + 1\right)\right)^{0.5}\right) \cong \frac{m_j}{n_j}\exp\left(\alpha_j \beta_{target} COV_j\right) \tag{63}$$

Modeling and Analysis of the Uncertainties in the LRFD Approach

In order to successfully implement the LRFD format in a practical pavement design procedure, the uncertainties caused by the systematic errors including model bias and statistical error as well as those of model parameters must be quantified and reflected in the format as they were in the RFD approach. In other words, the quantification of the systematic errors is a prerequisite to computing the overall safety factor in the LRFD format. The most common way to quantify systematic errors is to employ the professional factor, P that is defined as a ratio of the measured to predicted value [46] :

$$P = \frac{RD_{measured}}{RD_{predicted}} = \frac{RD_{measured}}{f_R(T_{AC}, E_{AC}, E_{Base}, E_{SB}, E_{SG}, N)} \tag{65}$$

Enough data is not available to assess the parameters E[P] and COV_p in all situations but, where available, comparisons between design predictions and measured results could be used to estimate them. Based on the analysis of observed and predicted rut-depths in the test sites of this study and 24 LTPP-GPS sites, E[P] and COV_p of 0.89 and 0.2 were used in this study.

M-E Flexible Pavement Design Procedure Using LRFD Approach

Incorporating the professional factor, the LRFD format in equation 58 can be rewritten as;

$$RD_{threshold} \geq \gamma'_{overall} \cdot [P \cdot f_R(T_{AC}, E_{AC}, E_{base}, E_{SG}, N)] \quad (64)$$

where:

$$\gamma'_{overall} = \frac{\gamma_P P \cdot f_R(\phi_{H_{AC}} H_{AC}, \phi_{E_{AC}} E_{AC}, \phi_{E_{Base}} E_{Base}, \phi_{E_{SB}} E_{SB}, \phi_{E_{SG}} E_{SG}, \gamma_N N)}{P \cdot f_R(H_{AC}, E_{AC}, E_{Base}, E_{SB}, E_{SG}, N)} \quad (65)$$

A detailed M-E flexible pavement design procedure employing equation 64 is illustrated in Figure 22. In this design procedure, the cross-section of a pavement is optimally determined by an iterative algorithm where the computation is continued until the difference between predicted and threshold rut-depth has converged to a specified tolerance level as it was done in the design procedure adopting the RFD approach. In order to determine reasonable values of overall safety factors corresponding to target reliability indices, a factorial experiment matrix was used as summarized in Table 21. First, the reliability index, failure points of design variables, and unit vectors associated with the design points in each cell were determined by FORM with 0.5 inches of rut depth as the limit state. Then, partial safety factors and overall safety factors corresponding to specified target reliability indices were calculated.

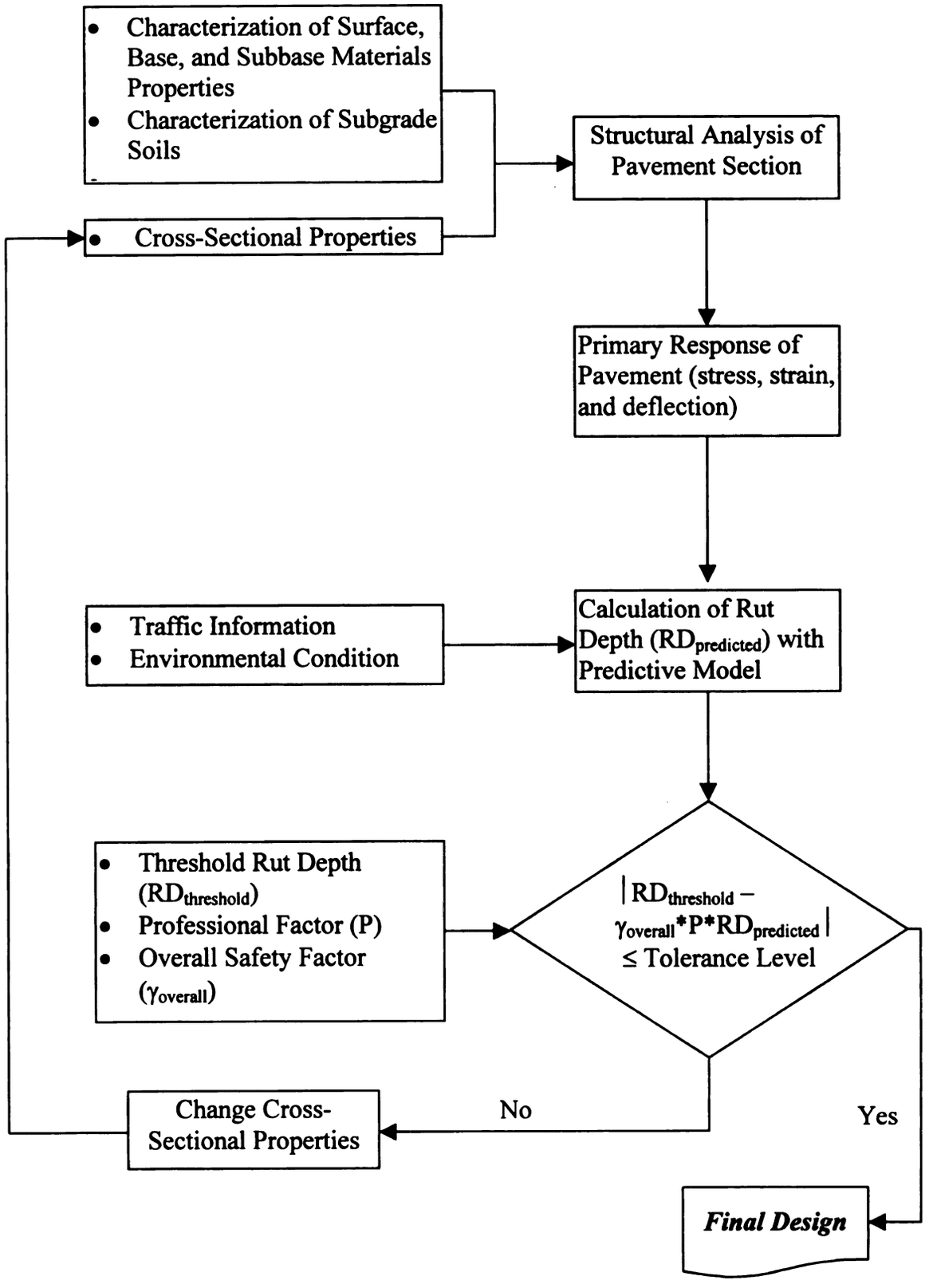

Figure 22 Flowchart for M-E Flexible Pavement Design Procedure Using LRFD Approach

As an illustrative example for this procedure, cell No. 35, which is equivalent to pavement section 2 in the illustrative examples of Chapter V, was selected. As can be seen in Table 16, failure points for design variables were evaluated at the end of the iteration in FORM. Using unit vectors at the failure points and the target reliability index of 1.65 for 95% reliability, partial safety factors and overall safety factors were computed using equations 61,62,63, and 65. Table 24 summarizes these computations. From the results of partial and overall safety factors computed in selected 18 cells, the design partial and overall safety factors for various target reliabilities were determined and summarized in Table 25.

Illustration of LRFD Approach

An illustration of a M-E flexible pavement design procedure using LRFD approach is made in this section. An example of the design outputs computed by selected design input parameters using the spreadsheet is shown in Figure 23.

The explanations of the design steps shown in Figure 23 are as follow:

1. The user is required to input expected traffic volume during pavement service life, a desired reliability level, a threshold rut-depth as failure criterion ($RD_{threshold}$), ambient annual temperature around the site, and effective resilient modulus of the subgrade soil of the site.
2. The user needs to set up initial pavement cross-sectional and material properties.

Table 24 Summary of Computations for Partial and Overall Safety Factors at Cell No.35

	Initial Input	Unit Vector (Alpha)	Target Reliability Index	Partial Safety Factor	Initial Input * Partial Safety Factor
Eac (psi)	450,000	-0.135	1.65	0.94	424,999
Tac (in)	10	-0.601	1.65	0.90	9.01
Ebase (psi)	30000	-0.042	1.65	0.99	29,584
Esubbase (psi)	15000	-0.034	1.65	0.99	14,833
Esg (psi)	8000	-0.096	1.65	0.97	7,745
Traffic Volume (ESAL)	15,000,000	0.257	1.65	1.18	17,676,307
Professional Factor	0.89	0.736	1.65	1.24	1.11
Predicted Rut-Depth	0.29				0.34

$$\therefore \text{Overall Safety Factor} = 1.24 * \frac{0.34}{0.29} \approx 1.454$$

Table 25 Summary of Partial and Overall Safety Factors with Various Target Reliabilities

Reliability (%)	**75**	**80**	**90**	**95**	**99**
Reliability Index (Normal Variate)	0.68	0.84	1.28	1.65	2.33
$\gamma_{Overall}$	*1.15*	*1.19*	*1.30*	*1.39*	*1.55*
γ_P	1.12	1.15	1.22	1.29	1.40
γ_N	1.08	1.11	1.16	1.21	1.29
$\phi_{E_{AC}}$	0.98	0.98	0.97	0.96	0.94
$\phi_{E_{Base}}$	0.99	0.99	0.98	0.98	0.97
$\phi_{E_{Subbase}}$	0.99	0.99	0.99	0.99	0.98
$\phi_{E_{SG}}$	0.99	0.99	0.98	0.98	0.97
$\phi_{T_{AC}}$	0.98	0.97	0.96	0.95	0.92

(a) Initial Stage

1.Site Condition and Design Criterion

Traffic Volume (N)	4.0.E+06	EASL
Reliability Level	0.8	
$RD_{threshold}$	0.5	in
Annual Temperature	45	(°F)
Subgrade Resilient Moduli	8000	psi

2.Material and Cross-Sectional Inputs

	AC	**Base**	**Subbase**
Thickness (in)	5.2	8.0	16.0
cm	13.2	20.3	40.6
Moduli (psi)	450000	30000	15000
Moduli (kPa)	3100500	206700	103350
Asphalt Type		AC 10	
Kinematic Viscosity		273	centistoke

3.Degree of Uncertainty

Professional Factor	0.890

4.Intermediate Variables from Structural Analysis

Surface Deflection	**Strain_Base**	**Strain-Subgrade**
2.267E-02	7.620E-04	2.871E-04

5.Design Outputs

$RD_{predicted}$	0.43
$\gamma_{overall}$	1.19

6. Decision

Tolerance Level		**$RD_{threshold}$- ($P*\gamma_{overall}*RD_{predicted}$)**
0.01	<	0.049

Adjust 2.Material and Cross-section Inputs

Figure 23 Illustration of M-E Flexible Pavement Design Using LRFD Approach

(b) Final Stage (End of the Iteration)

1.Site Condition and Design Criterion

Traffic Volume (N)	4.0.E+06	EASL
Reliability Level	0.8	
$RD_{threshold}$	0.5	in
Annual Temperature	45	(°F)
Subgrade Resilient Moduli	8000	psi

2.Material and Cross-Sectional Inputs

	AC	**Base**	**Subbase**
Thickness (in)	4.2	8.0	16.0
cm	10.7	20.3	40.6
Moduli (psi)	450000	30000	15000
Moduli (kPa)	3100500	206700	103350
Asphalt Type		AC 10	
Kinematic Viscosity		273	centistoke

3.Degree of Uncertainty

Professional Factor	0.890

4.Intermediate Variables from Structural Analysis

Surface Deflection	**Strain_Base**	**Strain-Subgrade**
2.529E-02	9.494E-04	3.248E-04

5.Design Outputs

$RD_{predicted}$	0.47
$\gamma_{overall}$	1.19

6. Decision

Tolerance Level		**$RD_{threshold}$- ($P^*\gamma_{overall}^*RD_{predicted}$)**
0.01	>	0.004

O.K.

Figure 23 (cont'd)

3. The user needs to determine a certain degree of uncertainty accompanied with the design procedure in terms of an overall safety factor ($\gamma'_{overall}$) of the design model: From Table 25, select a value in accordance with the desired reliability level set up in step 1.
4. The pavement analysis computer program computes the surface deflection and compressive vertical strains at the top of the base layer and subgrade.
5. A predictive pavement rut-depth ($RD_{predicted}$) is computed using the developed rutting prediction model.
6. If $RD_{threshold} - (\gamma'_{overall} * P * RD_{predicted}) >$ a specified tolerance level, the pavement cross-section should be modified and repeat step 2 through 6 until $RD_{threshold} - (\gamma'_{overall} * P * RD_{predicted}) \leq$ the tolerance level. When the repetition is stopped, the cross-section at the final iteration becomes the design pavement cross-section.

Sensitivity Analysis of RFD and LRFD Approaches

In order to evaluate the effects of the level of reliability, amount of traffic volume, and resilient moduli of subgrade on design pavement thickness with suggested M-E flexible pavement design procedure using the RFD and LRFD approaches, a sensitivity analysis was performed. Table 26 summarizes the set of design parameters held to be constant in the sensitivity analysis. Figures 24 and 25 summarize the results of the sensitivity analysis. Figure 24 shows the relationships between the traffic volume and AC thickness at different reliability levels, while Figure 25 illustrates the relationship between the reliability level or overall safety factor and the AC thickness at different traffic volumes. These illustrations can assist designers in selecting the appropriate

pavement cross section based on the expected traffic volume and desired reliability level. The slopes of the curves in the figures correspond to the rate of change of AC thickness corresponding to change of traffic volume or reliability level. The slopes of the curves from RFD and LRFD approaches appear to have similar trends with change of traffic volume and reliability level. This fact can lead to two interpretations:

1. Faced with a specified pavement design situation that is subject to a given traffic volume, two design approaches with a specified failure criterion and reliability level would produce similar results implying that generally, design outputs from the two are comparable to each other.

2. The outputs from two design approaches have similar sensitivities to the reliability level.

Table 26 Constant Design Parameters in the Sensitivity Analysis

Parameter	Magnitude
Annual Ambient Temperature	45°F
Kinematic Viscosity	273 centistroke
Thickness of Base	8in
Thickness of Subbase	16in
Modulus of Bituminous Layer	450ksi
Modulus of Base Layer	30ksi
Modulus of Subbase Layer	15ksi
Modulus of Subgrade Soil	8ksi

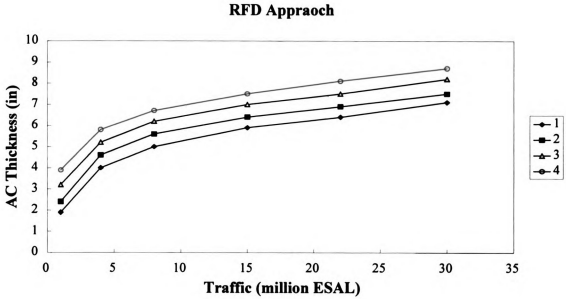

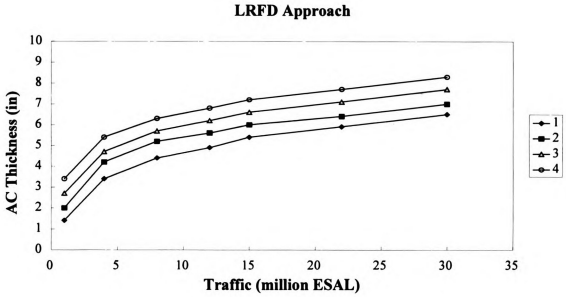

	Target Reliability (%)	$\gamma_{overall}$
1	75	1.15
2	80	1.19
3	90	1.30
4	95	1.39

Figure 24 Variation of AC Thickness with Various Traffic Levels

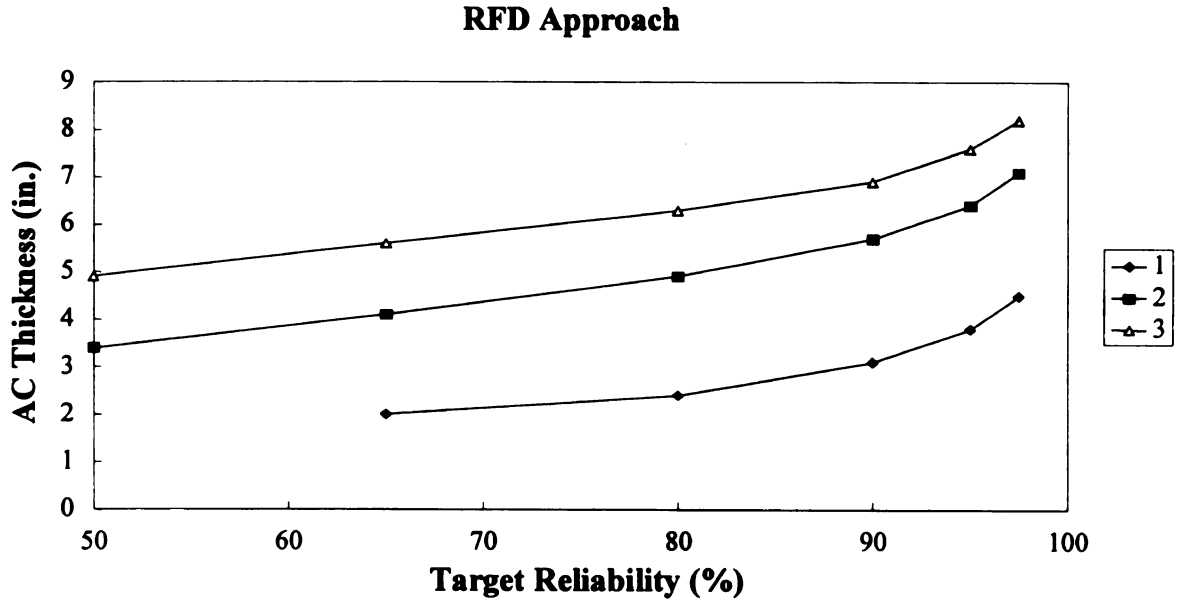

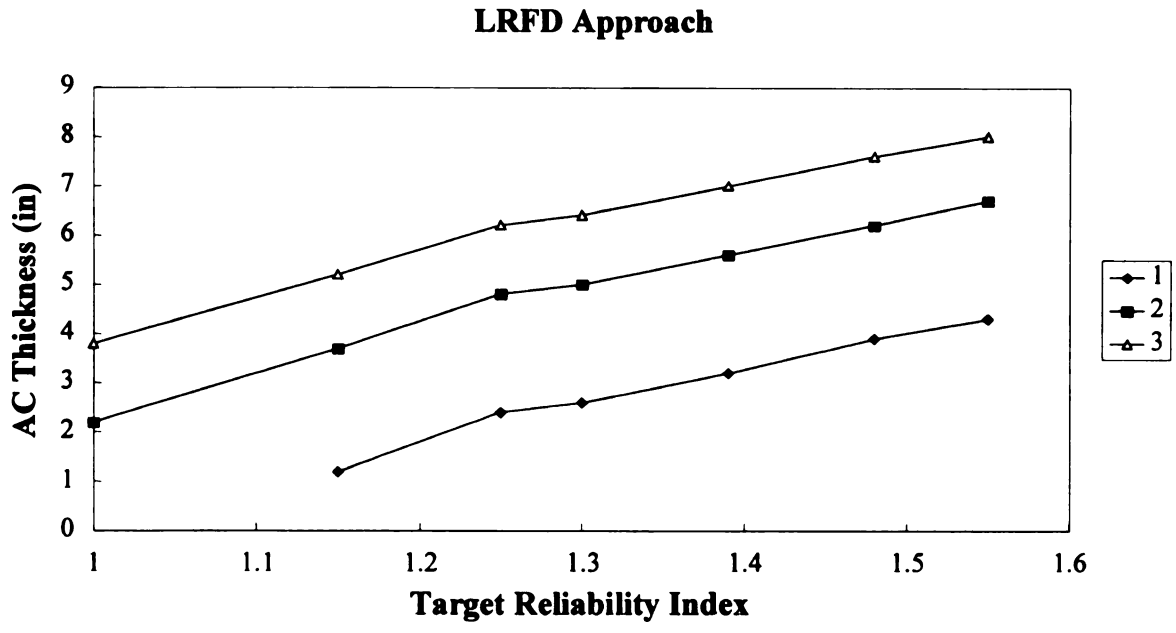

	Traffic Level
1	1,000,000
2	5,000,000
3	15,000,000

Figure 26 Variation of AC Thickness with Various Target Reliability Levels

CHAPTER VII

SUMMARY, CONCLUSIONS, AND RECOMMENDATIONS

Summary

The objectives of this study were to:

- Revise a rutting prediction model based on field data and present its application to M-E flexible pavement design.
- Develop a reliability analysis procedure for the pavement performance
- Develop a reliability-based M-E flexible pavement design procedure by extending the developed reliability analysis procedure.

A comprehensive literature review regarding the state-of-the-art rutting prediction models based on mechanistic and mechanistic-empirical approaches was presented. Based on the field data collected from in-service flexible pavements in Michigan, a M-E rut prediction model was developed. The robustness of this model was tested against the field data collected in 1998 and LTPP data from 24 GPS sites.

So that the new model systematically combines non-mechanistic factors with primary mechanistic factors, the model was developed through nonlinear regression using SYSTAT [30], a statistical computer program, was developed. The model consists of two parts: one containing observational variables and the other containing mechanistic parameters. This was done in an effort to separately explain the effects of load-related mechanistic and non-mechanistic factors including environmental, asphaltic, and cross-sectional properties on pavement rutting. The attributes of the nonlinear regression model are as it follows:

- More than 760 data locations from 39 test sections were analyzed and then they were grouped into 51 statistical samples.

- The R^2 of the model was 90.5%.
- The p-value of 2.044E-18 for the regression relation between predicted rut-depth and independent variables leads to the conclusion that the regression relation is useful for making predictions of rut-depths.

Because of a certain amount of bias associated with the measurement of rut, estimation of traffic and determination of material and cross-sectional properties, this study set up a tolerance level of ±0.1 inch within which the difference between observed and predicted rut-depth was considered not to be significant.

The developed model can account for rate-hardening (load applications vs. rut-depth) in the progression of rutting with increased load applications. This model simulated a rapid pavement rutting-rate in the early life of the pavement and a slower rutting development in the middle of the pavement age. This trend of the pavement rutting development corresponds well with the typical field rutting behavior that was reported from several field investigations [19,50,51,52]. The developed model also considers the rut-depth as a performance function and hence can easily handle various threshold rut-depths. This means that pavements can be designed with various terminal service levels using this model.

The developed model characterizes traffic in terms of the ESAL without considering the actual axle load spectrum in light of field practices in pavement engineering.

In the sensitivity analysis, no violation of mechanistic rules of pavement performance were found implying that the model can successfully explain the relationship between the pavement rutting behavior and material/cross-sectional properties.

The literature review regarding general M-E flexible pavement design procedures suggest that M-E procedures do not accurately address the variabilities associated with design parameters and model bias. This results in a failure to adequately predict pavement performance with a degree of confidence.

The performance reliability in a given pavement section can be expressed as the reliability index, β_c, the number of standard deviations by which the expected value of the performance function exceeds the limit state or β_{HL}, the invariant minimum distance between the origin and the failure surface [34,35].

A reliability analysis model for evaluating uncertainties in the M-E flexible pavement design procedure was developed. This model consists of two subsystems: an analytically derived mechanistic subsystem for predicting pavement performance and a reliability subsystem for analyzing the limit state function that is defined as the difference between maximum allowable (or threshold) and predicted rut-depth in this study. In order to analyze the limit state function and calculate its reliability index, the FOSM, PEM and FORM were used. The results from these methods were compared through illustrative examples.

The probabilistic methodologies applied to the development of the reliability analysis model for pavement performance was also used to improve currently suggested M-E flexible design procedures by providing comprehensive reliability handling tools. Within a framework of the improvement of existing design methods, not intending the replacement of new design method, two practical reliability-based M-E flexible pavement procedures: RFD and LRFD approaches were introduced and explained in detail.

In RFD approach,

- The overall standard deviation of the design procedure is determined by the first order combination of the standard deviations due to uncertainties of design parameters and systematic errors in the design model.
- Incorporating the reliability factor (RF) that is the product of the overall standard deviation and target reliability index, an iterative process was developed to produce an optimal pavement cross-section whose structural resistance allows its total permanent deformation to closely reach a threshold amount at the end of design life.

In LRFD approach,

- The professional factor, P that can be defined as a ratio of measured rut-depth to predicted rut-depth was employed to quantify systematic errors in the design model [46].
- A overall safety factor based on the partial safety factors of all design variables was applied to the limit-state function, which, in this study, was defined as the safety margin reflecting the difference of maximum allowable (threshold) and predicted rut-depth
- The cross-section of a pavement is optimally computed by an iterative algorithm where the computation is continued until the limit-state function including an overall safety factor converges to zero.

Conclusions

Revision of Rutting Prediction Model

One of the biggest issues in the pavement design is how a transfer/pavement performance function can reasonably combine non-mechanistic factors such as geometric, material, and environmental properties with purely mechanistic factors such as load-related distress mechanisms. The performance functions with only mechanistic factors that were based on laboratory and field testing results have not been successful in getting their applicability to a variety of regional site conditions revealing the lack of consideration of non-mechanistic factors.

In the validation study of revised rutting prediction model with field data collected most recently in Michigan and from 24 LTPP-GPS database, the plot of observed versus predicted rut-depth indicates good agreement between them. This fact implies that revised rutting prediction model shows some potential to be nation-wide applied.

Development of Reliability Analysis Model for the Pavement Performance

Reliability of the pavement performance can be expressed as the probability that the pavement will not exceed distress criterion during its service life. This study showed that the conventional reliability index, β_c, is a best representative for the reliability of the pavement performance because it provides a convenient and valid comparative measure for an engineering system not requiring the assumption of any particular distribution for the performance function. However, for design application, β_{HL} should be used to accurately evaluate failure points of design variables and determine exact minimum

distance to the failure surface that is approximated to a tangent hyperplane at the failure point. By calculating the reliability index of a given limit state function, the study evaluated both advantages and disadvantages of FOSM, PEM and FORM. Comparisons of the accuracy of calculated reliability indices and the computation time leads to the conclusion that FOSM and PEM are preferred for characterizing the effects of parameter uncertainties on the pavement performance in the pavement reliability analysis, while FORM is the best choice to quantify the uncertainties of design parameters and model bias for establishing reliability-based M-E pavement design procedure.

Development of Practical Reliability-Based M-E Flexible Pavement Design Procedures

Basically, most of pavement design procedures including AASHTO guide, M-E procedure from NCHRP 1-26, and Corps of Engineers' method [53] have employed the concept of limit state design that is a logical formalization of the traditional design approach that would help to expedite the explicit recognition and treatment of engineering risks. The reliability methodology can make this limit state design concept robust, accounting for the critical uncertainties around the limit state.

It is demonstrated that the two suggested practical reliability-based M-E flexible pavement design procedures, RFD and LRFD approaches, successfully handle design uncertainties and produce design outputs warranting desired reliability level.

It should be emphasized again that suggested reliability-based design procedures do not intend to replace existing M-E design procedures but improve on them by providing conventional reliability handling capability. They could partly help the M-E design procedure overcome the obstacles in its more advance implementation.

The biggest difference between two approaches is that LRFD approach employs partial safety and overall safety factors whose values are varying with target reliability indices, whereas the RFD directly uses target reliability indices with the overall standard deviation that is independently estimated by a first order probabilistic approach. Despite of this difference, this study showed that the two approaches were likely to produce similar design pavement thickness for a specified design condition (Figures 24 and 25).

Recommendations for Future Research

- In order to achieve higher suitability for various site conditions, the calibration work for the revised rutting prediction model should be continued with updated version of the LTPP database.
- An attempt needs to be made to apply traffic characterized in terms of actual loading groups rather than ESALs to this rutting prediction model.
- The proposed reliability analysis model for the pavement performance in this study assumes that all variables are normally or log-normally distributed, which is not entirely accurate. The attempt should be made to enable the reliability analysis model to rationally handle non-normal random variables using advanced probabilistic technique such as normal tail approximation [54].
- The system reliability techniques to handle simultaneously more than one pavement distress should be considered in the future reliability analysis model for the pavement performance.
- The key requirements to implement reliability-based M-E flexible pavement design procedures are (1) the capability of reflecting the reliabilities of major load-related

pavement distresses to a pavement design algorithm and (2) the determination of unified overall standard deviations in RFD and overall safety factors in LRFD.

REFERENCES

1. Buch, N., Baladi, G.Y., Harchandran, R.S., *Calibration of MICHPAVE's Rut and Fatigue Distress Models Development of An Overlay Design Procedure in MICHBACK.* A Research Proposal to the Michigan Department of Transportation, Department of Civil and Environmental Engineering, Michigan State University, East Lansing, Michigan, 1996.

2. Thompson, M.R. *Mechanistic-Empirical Flexible Pavement Design: An Overview.* Transportation Research Record 1539, TRB, National Research Council, Washington, D.C., 1995, pp. 1-5.

3. Harichandran, R. S., Yeh, M-S., and Baladi, G. Y. *MICH-PAVE: A nonlinear finite element program for the analysis of flexible pavements.* Transportation Research Record 1286, TRB, National Research Council, Washington, D.C., 1990, pp 123-131.

4. Harichandran, R. S., Mahmood, T., Raab, A., and Baladi, G. Y. *Backcalculation of pavement layer moduli, thicknesses and bedrock depth using a modified Newton method.* In Nondestructive Testing of Pavements and Backcalculation of Moduli (Second Volume), ASTM STP 1198, H. L. Von Quintas, A. J. Bush and G. Y. Baladi (eds.) American Society for Testing and Materials, Philadelphia, PA, 1994, pp 68-82.

5. Shumann, E., *Instrumentation of Comparative Bituminous Pavement Sections on I-96.* A Research Report submitted to Department of Civil and Environmental Engineering, Michigan State University, for the Degree of M.S., 1996.

6. Baladi, G.Y., Harichandran, R.S.,Mukthar, H., and Mahmood, T. *Reduction of Rutting and Fatigue Cracking Under Vehicle Loads and Backcalculation of Layer Moduli.* Department of Civil and Environmental Engineering, Michigan State University, East Lansing, Michigan, 1994.

7. *Report 5, The AASHO Road Test*, Highway Research Board Special Report 61E, 1962.

8. Hughes C.S. and Maupin, Jr G.W. *Experimental bituminous Mixes to Minimize Pavement Rutting,* AAPT Vol. 56, 1987.

9. Smith, H.A. *Truck Tire Characteristics and Asphalt Concrete Pavement Rutting,* Paper No. 910035, Transportation Research Board (TRB) 70th Annual Meeting, 1991.

10. Mukhtar, H. *Reduction of Pavement Rutting and Fatigue Cracking.* Ph.D Dissertation, Michigan State University, 1993.

11. Kenis, W.J., *Predictive Design Procedures, a Design Method for Flexible Pavemens Using the VESYS Structural Subsystem.* Proceedings, 4th International Conference on the Structural Design of Asphalt Pavements, Vol. 1, 1977, pp 101-147.

12. Huang, Y., *Pavement and Analysis Design,* Prentice-Hall. Englewood Cliffs, N.J. 1993

13. Owusu-Antwi, E.B., Titus-Glover, L. and Khazanovich, L., *A Rutting Model for Implementation in Mechanistic Base Design Procedure.* Presented at 77th Annual Meeting, TRB, National Research Council, Washington, D.C., 1998.

14. Leahy, R.B. and Witczak, M.W. *The Influence of Test Conditions and Asphalt Concrete Mix Parameters on Permanent Deformation Coefficient Alpha and Mu.* AAPT, Vol 60, 1991.

15. Ali, H., Tayabji, S., and La Torre, F., *Calibration of A Mechanistic-Empirical Rutting Model for In-Service Pavements.* Presented at 77th Annual Meeting, TRB, National Research Council, Washington, D.C., 1998.

16. *1993 AASHTO Guide for Design of Pavement Structures.* American Association of State Highway and Transportation Officials, Washington, D.C., 1993.

17. Allen, D.L., and Deen, R.C., *A Computerized Analysis of Rutting Behavior of Flexible Pavement.* Transportation Research Record 1095, TRB, National Research Council, Washington, D.C., 1986, pp. 1-10.

18. Baladi G.Y. *Fatigue Life and Permanent Deformation Characteristics of Asphalt Concrete Mixes.* Transportation Research Record 1227, TRB, National Research Council, Washington, D.C., 1989, pp 75-87.

19. Carpenter, S.H. *Permanent Deformation: Field Evaluation.* Transportation Research Record 1417, TRB, National Research Council, Washington, D.C., 1993, pp. 135-143.

20. *Calibrated Mechanistic Structural Analysis Procedure for Pavements*, Volume 1. NCHRP Project 1-26, Final Report, Phase 2. TRB, National Research Council, Washington, D.C., 1992.

21. Timm, D., Brigsson, B., and Newcomb, D. *Development of Mechanistic-Empirical Pavement Design in Minnesota.* Presented at 77th Annual Meeting, TRB, National Research Council, Washington, D.C., 1998.

22. *DATAPVE,* a Software Package for Long Term Pavement Performance Information Management System (LTPP-IMS), FHWA, 1997.

23. Harichandran, R.S., Ramon, C.M., and Baladi, G.Y., *MICHBACK User's Manual.* Department of Civil and Environmental Engineering, Michigan State University, East Lansing, Michigan, 1994.

24. Killingsworth, B. and Von Quintus, H. *Backcalculation of Layer Moduli of LTPP General Pavement Study.* Final Report, FHWA-RD-97-086, Federal Highway Administration, Washington, D.C., 1997.

25. Elliot, R.P. *Selection of Subgrade Modulus for AASHTO Flexible Pavement Design.* Transportation Research Record 1354, TRB, National Research Council, Washington, D.C., 1992, pp. 39-44.

26. Von Quintus, H., Killingsworth, B.M, Darter, M.I., Owusu-Antwi, E., and Jiang, J. *Catalog of Recommended Pavement Design Features.* Final Report, NCHRP 1-32, TRB, National Research Council, Washington, D.C., 1997.

27. Park, D.Y., and Buch, N., Personal communications; Temperature Correction for Backcalculated Asphalt Moduli, Department of Civil and Environmental Engineering, Michigan State University, East Lansing, Michigan, 1998.

28. Warren, H., and Dieckmann, W.L., *Numerical Computation of Stresses and Strains in a Multiple-Layer Asphalt Pavement System,* Internal Report, Chevron Research Corporation, Richmond, CA., 1963.

29. *SPSS User's Guide.* 3rd edition SPSS Inc., Chicago, IL., 1995.

30. Leland, W., Hill, M., Welna, J.P., and Birkenbeuel, G.K., *SYSTAT for Windows: Statistics.* Version 5 edition, SYSTAT, Inc., Evanston, IL., 1992.

31. Ditlevesen, O, and Madsen, H.O., *Structural Reliability Methods.* John Wiley and Sons Ltd., West Sussex, England, 1996.

32. Kim, H.B., Harichandran, R.S., and Buch, N. *Development of Load Resistance Factor Design Format for Flexible Pavenemts.* Canadian Journal of Civil Engineering, Vol. 25, 1998, pp.880-885.

33. Wolff, T.F., Hassan, A., Khan, R., Ur-Rasul, I., and Miller, M. *Geotechnical Reliability of Dam and Levee Embankments.* A Technical Report prepared to U.S. Army Engineer Waterways Experiment Station, Geotechnical Laboratory, Vicksburg, MS, Sep. 1995.

34. Wolff, T.F. *Analysis and Design of Embankment Dam Slopes: A Probabilistic Approach.* Ph.D. Thesis, Purdue University, May, 1985.

35. Hasofer, A.M., and Lind, N.C., *Exact and Invariant Second-Moment Code Format.* Journal of the Engineering Mechanics, (ASCE), Vol. 100, pp 111-121.

36. Ang, A. and Tang, W. *Probability Concept in Engineering Planning and Design Volume- I and II.* John Wiley and Sons, Inc., 1975 and 1984.

37. Wolff, T.F. *Probabilistic Slope Stability in Theory and Practice.* Proceeding of the ASCE Speciality Conference on Uncertainty in the Geologic Environment, ASCE, New York, pp. 419-433.

38. Christian, J.T., Ladd, C.C., and Baecher, G.B. *Reliability Applied to Slope Stability Analysis.* Journal of Geotechnical Engineering (ASCE), Vol. 120, Dec. 1994, pp.2180-2207.

39. Neter, J., Kutner, M.H, Nachtsheim, C.J., and Wasserman, W., *Applied Linear Statistical Models.* Times Mirror Higher Education Group, Inc., 1996.

40. Harr, M.E., *Reliability-Based Design in Civil Engineering.* Mcgraw-Hill, New York, 1987.

41. Wolff, T.F., *Evaluating the Reliability of Existing Levees.* A Technical Report prepared to U.S. Army Engineer Waterways Experiment Station, Geotechnical Laboratory, Vicksburg, MS, Sep. 1994.

42. Rusenblueth, E. *Point Estimates for Probability Moments.* Proceedings, National Academy of Science, USA, Vol. 72, 1975, pp. 3812-3814.

43. Thoft-Christensen, P., and Murotsu, Y., *Application of Structural Syetems Reliability Theory.* Springer-Verlag, Berlin, 1986.

44. Rackwitz, R., and Fiessler, B., *Structural Reliability under Combined Random Load Sequences.* Computers & Structures, Vol. 9, 1978, pp. 489-494.

45. Madsen, H.O., Krenk, S., and Lind, N.C. *Methods of Structural Safety.* Prentice-Hall, Inc., Englewood Cliffs, N.J. 1986.

46. Ravindra, M.K., and Galambos, T., *Load and Resistance Factor Design for Steel.* Journal of Structural Division (ASCE), Vol. 104, Sept. 1978, pp.1337-1353.

47. Brown, J.L. *Reliability in Pavement Design? Who's Kidding Whom?* Transportation Research Record 1449, TRB, National Research Council, Washington, D.C., 1994, pp. 26-29.

48. Kulhawy, F., and Phoon, K.K., *Engineering Judgement in the Evolution From Deterministic to Reliability-Based Foundation Design.* Proceeding of the ASCE Speciality Conference on Uncertainty in the Geologic Environment, ASCE, New York, pp. 29-48.

49. Thoft-Christensen, P. and Baker, M.J., *Structural Reliability Theory and Its Applications.* Springer-Verlag, Berlin. 1982.

50. Lister, N.W. and Addis, P.R., *Field Observations of Rutting and Their Implications.* Transportation Research Record 1015, TRB, National Research Council, Washington, D.C., 1985, pp. 28-34.

51. Thompson, M.R., and Nauman, D., *Rutting Rate Analyses of the AASHO Road Test Flexible Pavements.* Transportation Research Record 1384, TRB, National Research Council, Washington, D.C., 1993, pp. 36-48.

52. Carpenter, S.H. *Load Equivalency Factors and Rutting Rates: The AASHO Road Test.* Transportation Research Record 1354, TRB, National Research Council, Washington, D.C., 1992, pp. 31-38.

53. U.S. Army. Pavement Design for Roads, Streets, and Open Storage Areas, Elastic Layer Method. Technical Manual TM 5-800-09, Department of Army, Washington, D.C., 1988.

54. Ditlevsen, O. *Principle of Normal Tail Approximation.* Journal of Engineering Mechanics, (ASCE), Vol. 107, Dec. 1981, pp.1191-1208.

55. Ayyub, B.M., and White, G.J., *Reliability-Conditioned Partial Safety Factors.* Journal of Structural Division (ASCE), Vol. 113, Feb. 1987, pp.279-294.

56. Elingwood, B., Galambos, T., McGregor, J., and Cornell, C.A., *Development of Probability-Based Load Criterion for American National Standard A58.* Special Publication 577, National Bureau Standards, Washington, D.C. 1980.

57. Monismith C.L. and Tayebali, A.A. *Permanent Deformation (Rutting) Consideration in Asphalt Concrete Pavement Sections.* AAPT Vol. 57, 1988.

58. Brown E.R. and Cross, A.S.*A Study of In-Place Rutting of Asphalt Pavements.* AAPT Vol 58, 1989.

59. Noureldin, A.S., Sharaf, E., Arafah, A., and Al-sugair, F. *Estimation of Standard Deviation of Predicted Performance of Flexible Pavement Using AASHTO Model.* Transportation Research Record 1449, TRB, National Research Council, Washington, D.C., 1994, pp. 46-56.

60. Johnson, A.M. and Baus, R.L. *Alternative Method for Temperature Correction of Backcalculated Equivalent Pavement Moduli.* Transportation Research Record 1335, TRB, National Research Council, Washington, D.C., 1992, pp. 75-81.

61. Vanmarcke, E.H. *Reliability of Earth Slope.* Journal of Geotechnical Engineering, (ASCE), Vol. 103, Nov. 1977, pp.1247-1265.

62. Yoder, E.J. and Witczak, M.W. *Principles of Pavement Design,* A Wiley-Interscience Publication, John Wiley and Sons, Inc., 1975.

63. Ditlevesen, O., *Model Uncertainty in Structural Reliability.* Structural Safety, Vol. 1, 1982, pp. 73-86.

64. Kulkarni, R.B. *Rational Approach in Applying Reliability Theory to Pavement Structural Design.* Transportation Research Record 1449, TRB, National Research Council, Washington, D.C., 1994, pp. 13-17.

65. Yoon, G.L., and O'Neill, M.W., *Resistance Factors for Single Driven Piles from Experiments.* Transportation Research Record 1569, TRB, National Research Council, Washington, D.C., 1997, pp. 47-54.

66. Alsherri, A., and George, K.P., *Reliability Model for Pavement Performance.* Journal of Transportation Engineering (ASCE), Vol. 114, May. 1988, pp.294-306.

67. Bates, M.S., and Watts, D.G., *Nonlinear Regression Analysis and Its Applications.* John Wiley and Sons, New York, 1988.

68. Chou, Y.T., *Reliability Design Procedures for Flexible Pavements.* Journal of Transportation Engineering (ASCE), Vol. 116, Sept./Oct.. 1990, pp.603-614.

69. Kim, Y,R., Hibbs, B.O., and Lee, Y-C., *Temperature Correction of Deflections and Backcalculated Asphalt Concrete Moduli.* Transportation Research Record 1473, TRB, National Research Council, Washington, D.C., 1994, pp. 55-62.

70. Phoon, K.K. and Kulhawy, F.H. *Practical Reliability-Based Design Approach for Foundation Engineering.* Transportation Research Record 1546, TRB, National Research Council, Washington, D.C., 1994, pp. 94-99.

71. Baecher, G.B., *Parameter and Approximations in Geotechnical Reliability.* in the Uncertainty Modeling and Analysis in Civil Engineering, CRC Press, LLC.,1998.

72. Chua, K.H., Der Kiureghian, A., and Monismith, C.L. *Stochastic Model for Pavement Design* Journal of Transportation Engineering (ASCE), Vol. 118, NOV/DEC. 1992, pp.769-786.

73. Ali. H, and Tayabji, S.D., *Evaluation of Mechanistic –Empirical Performance Prediction Models for Flexible Pavement.* Presented at 77th Annual Meeting, TRB, National Research Council, Washington, D.C., 1998.

74. Monismith, C.L. *Analytically Based Asphalt Pavement Design and Rehabilitation: Theory to Practice, 1962-1992.* Transportation Research Record 1354, TRB, National Research Council, Washington, D.C., 1992.

75. Cornell, C.A. *A Probability-Based Structural Code.* Journal of ACI, 66(12), 974-985.